Max-Planck-Institut für molekulare Pflanzenphysiologie
Arbeitsgruppe Stitt

Subcellular compartmentation of primary carbon metabolism in mesophyll cells of *Arabidopsis thaliana*

Dissertation
zur Erlangung des akademischen Grades "doctor rerum naturalium"
(Dr. rer. nat.)
in der Wissenschaftsdisziplin "Pflanzenphysiologie"

eingereicht an der

Mathematisch-Naturwissenschaftlichen Fakultät

der Universität Potsdam

von
Daniel Vosloh
Potsdam, den 16.05.2011

Published online at the
Institutional Repository of the University of Potsdam:
URL http://opus.kobv.de/ubp/volltexte/2011/5553/
URN urn:nbn:de:kobv:517-opus-55534
http://nbn-resolving.de/urn:nbn:de:kobv:517-opus-55534

Eidesstattliche Erklärung

Die vorliegende Dissertationsschrift ist das Ergebnis meiner eigenen praktischen Arbeit. Sie wurde von Juni 2007 bis Mai 2011, am Max-Planck-Institut für molekulare Pflanzenphysiologie in Potsdam-Golm, in der Arbeitsgruppe von Prof. Dr. Mark Stitt durchgeführt. Ich erkläre, dass ich die vorliegende Arbeit selbständig und ohne unerlaubte Hilfe angefertigt habe. Es wurden keine anderen als die angegebenen Quellen und Hilfsmittel benutzt. Die verwendeten Quellen sind als solche im Text kenntlich gemacht. Die Arbeit wurde zuvor noch an keiner anderen Stelle eingereicht.

Potsdam, den 16.05.2011

Daniel Vosloh

Table of Contents

Table of Figures

Table of Tables

Chapter 1: General Introduction

1.1 Subcellular compartmention in plant cells and the importance of primary carbon metabolism

A defining feature of eukaryotic cells is the presence of multiple subcellular compartments, each having its own specialised functions within the cell. Apart from a few unusual cell types, e.g. mammalian erythrocytes, all eukaryotic cells contain a nucleus, mitochondria, endoplasmic reticulum, Golgi apparatus, ribosomes, peroxisomes and cytosol. Plant cells have even more compartments, including plastids (e.g. chloroplasts, amyloplasts and chromoplasts), vacuoles and cell walls, making them arguably the most complex of all eukaryotic cells (ap Rees, 1987). Most of the subcellular compartments are physically separated from each other by single or double membranes, which restrict the free movement of most small molecules as well as mRNAs and proteins. Thus the cell requires a whole host of membrane transporters and channels to allow movement of metabolites and macromolecules between compartments. The physical separation of metabolic pathways allows incompatible reactions to occur simultaneously within one cell, and the resulting division of labour can improve metabolic efficiency. Compartmentation also allows a certain degree of independence in the control of different parts of metabolism, providing flexibility to adapt to changes in environmental conditions. Nevertheless, coordination of pathways in different compartments is also essential to prevent metabolic imbalances, and eukaryotic organisms have evolved complex networks for intracellular communication and metabolic control.

Photosynthesis is not only one of the most important processes in plants, but also one of the most highly compartmented metabolic networks, with branches located in chloroplasts, mitochondria, peroxisomes and the cytosol. Photosynthetic carbon fixation by plants, including green algae, is the basis for most life on Earth, and provides mankind with food, fuel, fibres and many other valuable products. With the global human population predicted to increase to 9 billion this century (United Nations, 2004), there is an urgent need to increase the yield of crop plants, and improving photosynthetic performance is a major goal for plant breeders. To reach this goal we

need a comprehensive understanding of photosynthesis at the molecular, cellular and whole-organism levels, to underpin both conventional and transgenic plant breeding efforts. Research over many years has provided us with a reasonably complete picture of the distribution of enzymes and transport proteins involved in photosynthetic metabolism. This thesis investigates the compartmentation of the metabolites involved in photosynthesis, either directly as pathway intermediates or as components of intracellular signalling networks. Such information could not only help resolve some of the remaining uncertainties in our map of photosynthetic metabolism, but also provide new insights into the control and coordination of photosynthesis in plants. The work will focus on two photosynthetic systems – the unicellular green alga *Chlamydomonas reinhardtii* and mesophyll cells from leaves of the model plant *Arabidopsis thaliana*.

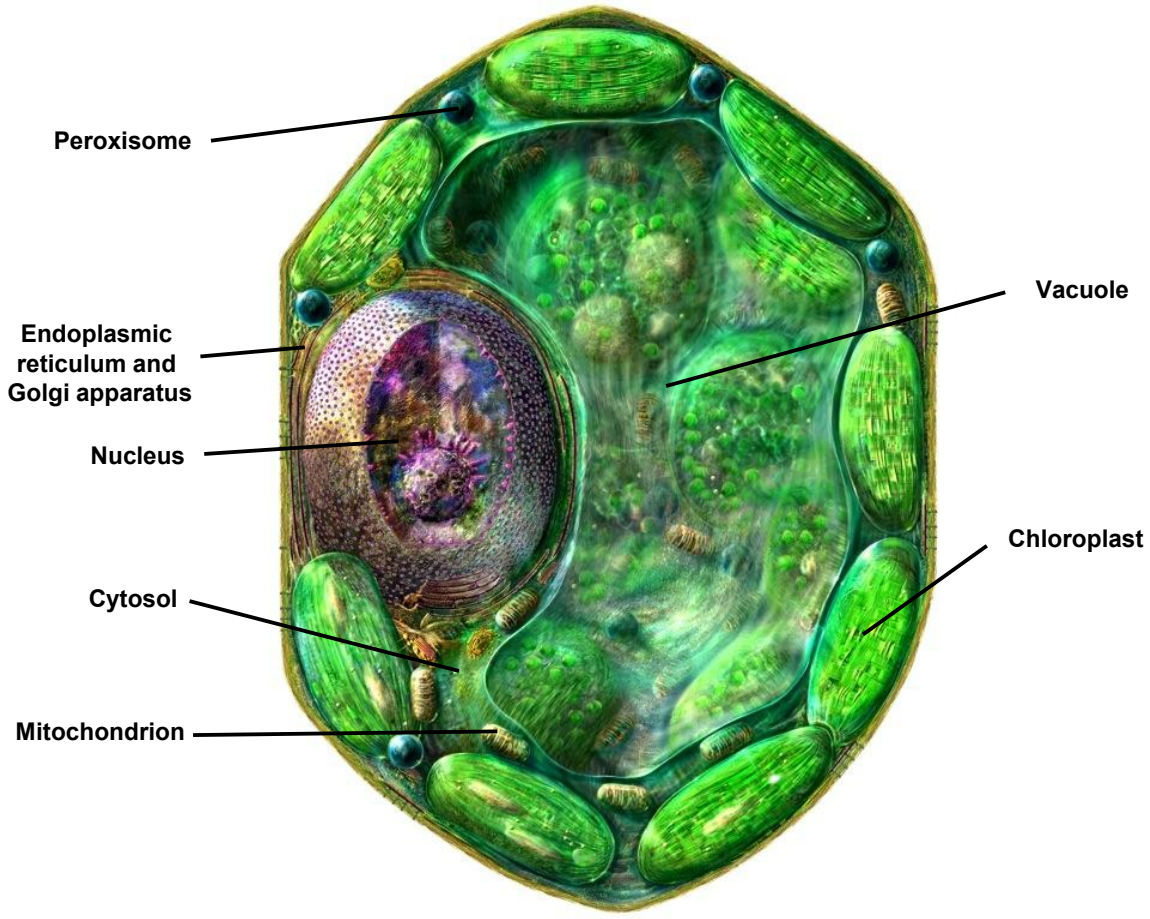

Figure 1-1: Cross-section of a higher plant mesophyll cell

This drawing shows the main subcellular structures in a typical leaf mesophyll cell: nucleus, cytosol, mitochondria, chloroplasts, peroxisomes, Golgi apparatus and endoplasmic reticulum, each drawn to the same scale and in a realistic arrangement within the cell. © Russel Knightey Media. Modified with permission of the copyright holder

1.2 Origins of compartmentation

Cellular organisms are divided into three domains: Bacteria, Archaea and Eukaryota. The first two are historically known as prokaryotes and have simple, mostly non-compartmented cells. Therefore, cell structure, metabolism and its regulation are much simpler in prokaryotes compared to eukaryotes (see Fig. 1-2).

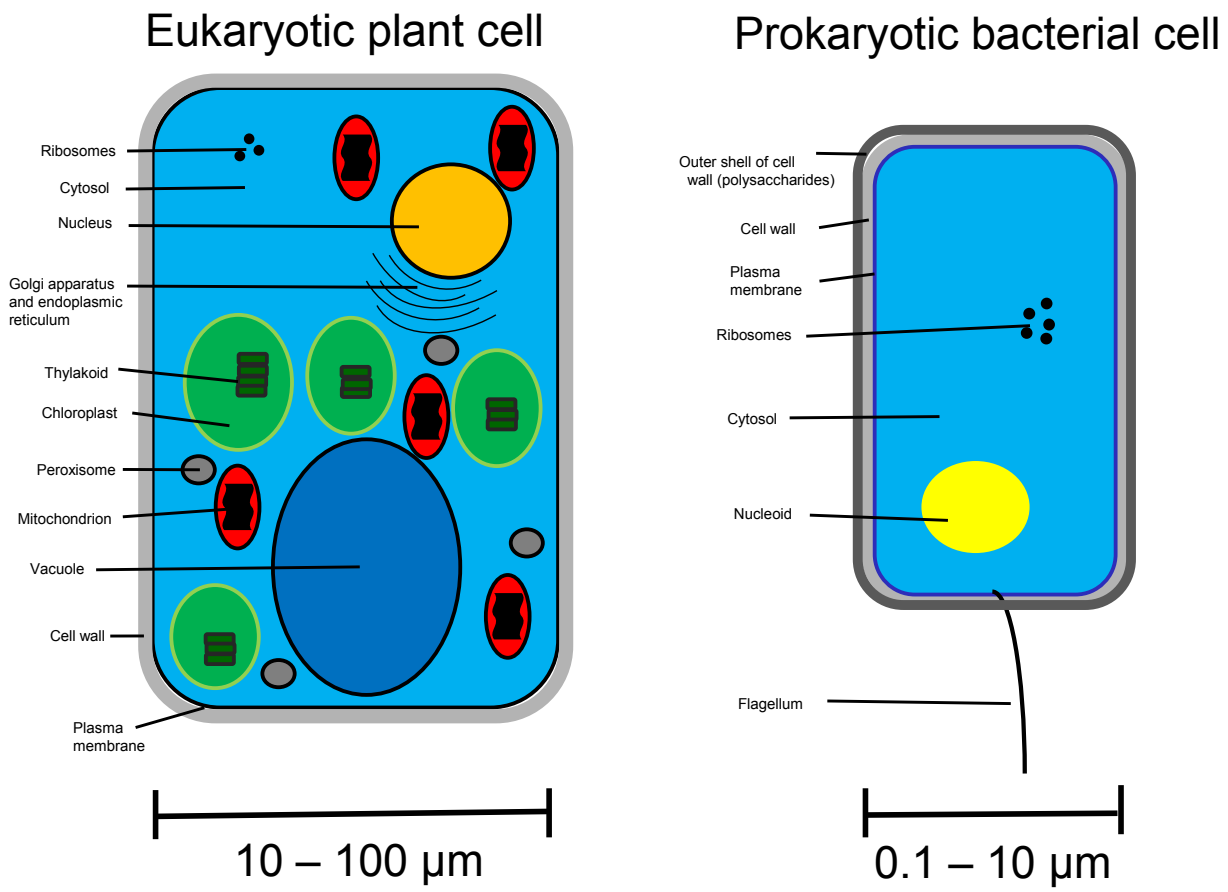

Figure 1-2: Comparison of the cell structure of a eukaryotic mesophyll plant cell and a typical prokaryotic cell
Eukaryotic plant cells possess multiple subcellular structures: the nucleus, cytosol, mitochondria, chloroplasts, peroxisomes and the vacuole. Additionally they contain the Golgi apparatus and the endoplasmic reticulum (both involved in protein folding and sorting). Prokaryotic cells generally do not have any membrane-bound organelles, although the circular DNA is often organized in a nucleoid structure. Both cell types have ribosomes for translation of mRNA into proteins, and these are present in three compartments in plant cells: cytosol, chloroplasts and mitochondria.

The differences between the cell structures of prokaryotes and eukaryotes are best understood in the light of evolution. The endosymbiont theory explains the stepwise development from a primitive prokaryotic like cell to a full eukaryote (Fig. 1-3). The bacterial cell possesses all of the necessary features for independent life, its own genetic information and the machinery needed to duplicate this information for reproduction. It also has sensory mechanisms to interact with its surroundings, and a complement of enzymes to catalyze the basic biochemical reactions needed for growth and reproduction, and to help the cell react to a changing environment.

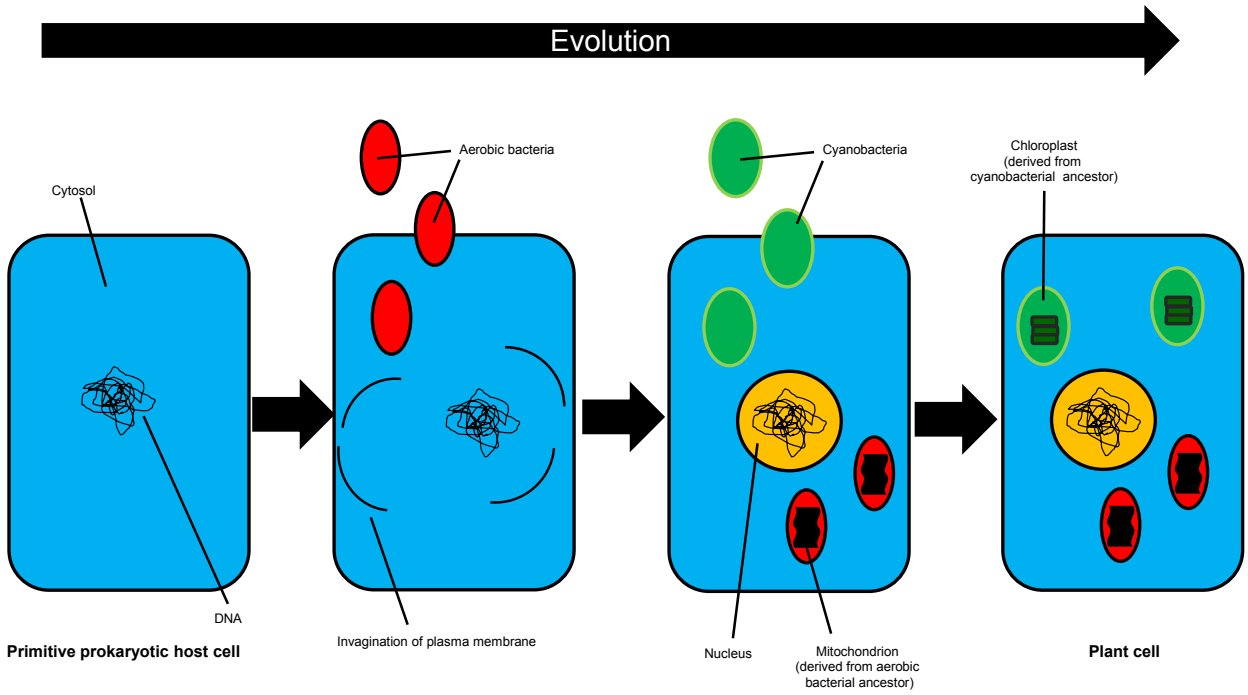

Figure 1-3: Schematic overview of the likely evolutionary development of the eukaryotic plant cell

During evolution a primitive prokaryotic cell captured first an aerobic proteobacterium that became the mitochondrion. Additionally parts of the plasmembrane became invaginated and coated the DNA to form a true nucleus. In a second endosymbiotic event this non-photosynthetic eukaryote captured a cyanobacterium-like cell that eventually became the chloroplast. Extensive exchange of genetic information between the host cell and the two symbionts took place. Most of the DNA from the bacterial and cyanobacterial ancestors was lost or transferred to the nucleus, although both mitochondria and chloroplast retain residual genomes containing 30 – 150 genes.

1.2.1 Evolutionary origins of eukaryotes

About 850 billion years ago an event took place where a host cell of unknown type assimilated a free living proteobacterium, but did not destroy it. Instead the host cell incorporated it into its

cellular environment. The endosymbiont gave most of its genetic information to its host, which together with its original genome finally led to the formation of the nucleus. The endosymbiont eventually became what are known today as the mitochondria. The transfer of the DNA from the bacterial ancestor to the nucleus is called endosymbiotic gene transfer. Strong evidence for the bacterial ancestry of mitochondria and chloroplasts comes from their general similarity of structure with free-living bacteria. Their genomes consist of circular DNA molecules, as are bacteria genomes, and their membrane composition resembles that of bacterial cells. It is still a matter of debate what the original host cell that incorporated the proteobacterium looked like. The traditional view is that the original host was already a eukaryotic cell with a nucleus, endoplasmic reticulum and most of the other traits that characterize a eukaryotic cell, except the presence of mitochondria (Cavalier-Smith, 2009). In contrast, an alternative theory claims that the original host was a prokaryote, possibly an archaeal cell, and that all eukaryotic traits evolved after the endosymbiosis of the proteobacterium. New molecular studies that investigate the similarity of essential genes for replication, transcription and translation show a greater similarity of the eukaryotic genes to their archaeal counterparts than to those from bacteria. The finding favors the prokaryote-host theory (Cox et al., 2008), but the scientific community is still far from a consensus. There is yet another theory for the origin of the nucleus, which proposes that the nucleus arose from viruses that initially attacked the cell but did not kill it, and eventually amalgamated with the cell's genome in a kind of hostile takeover (Pennisi, 2004).

1.2.2 Evolution of photosynthetic eukaryotes

A very similar event to the endosmybiosis of the proteobacterium took place several million years later in evolution, when this eukaryote engulfed a cyanobacterium-like cell that possessed the capacity for oxygenic photosynthesis (Margulis, 1971). It also gave most of its genetic information to the host cell and finally evolved to become the chloroplast. Several lineages of photosynthetic eukaryotes are derived from this ancestral plastid-containing cell (see Fig. 1-4). There is strong molecular evidence that all eukaryotic organisms that can perform oxygenic photosynthesis form a monophyletic group; in other words they are all derived from one common ancestor (Smith et al., 2010). The glaucophytes (Glaucophyta) separated earliest from this common ancestor. They are a small group of freshwater algae containing unique chloroplasts,

known as cyanelles that retain several primitive features such as a peptidoglycan envelope that resembles the bacterial cell wall. The rhodophytes (Rhodophyta) or red algae represent a larger group of mainly marine algae. The third, and most diverse, group is the green plants (Viridiplantae). This is divided into two major lineages: the chlorophytes (true green algae) and the streptophytes, which include both land plants and some aquatic algal types, e.g. charophytes. *C. reinhardtii* belongs to the division of the chlorophytes. The bryophytes (e.g. mosses and liverworts) are land living multicellular organisms that lack vascular tissue, and represent the most primitive type of land plants. The development of vascular tissue allowed plants to transport water from the soil via their roots to the aerial parts and so become larger, eventually forming the huge diversity of ferns and seed plants, i.e. the gymnosperms and angiosperms such as *A. thaliana* (Smith et al., 2010).

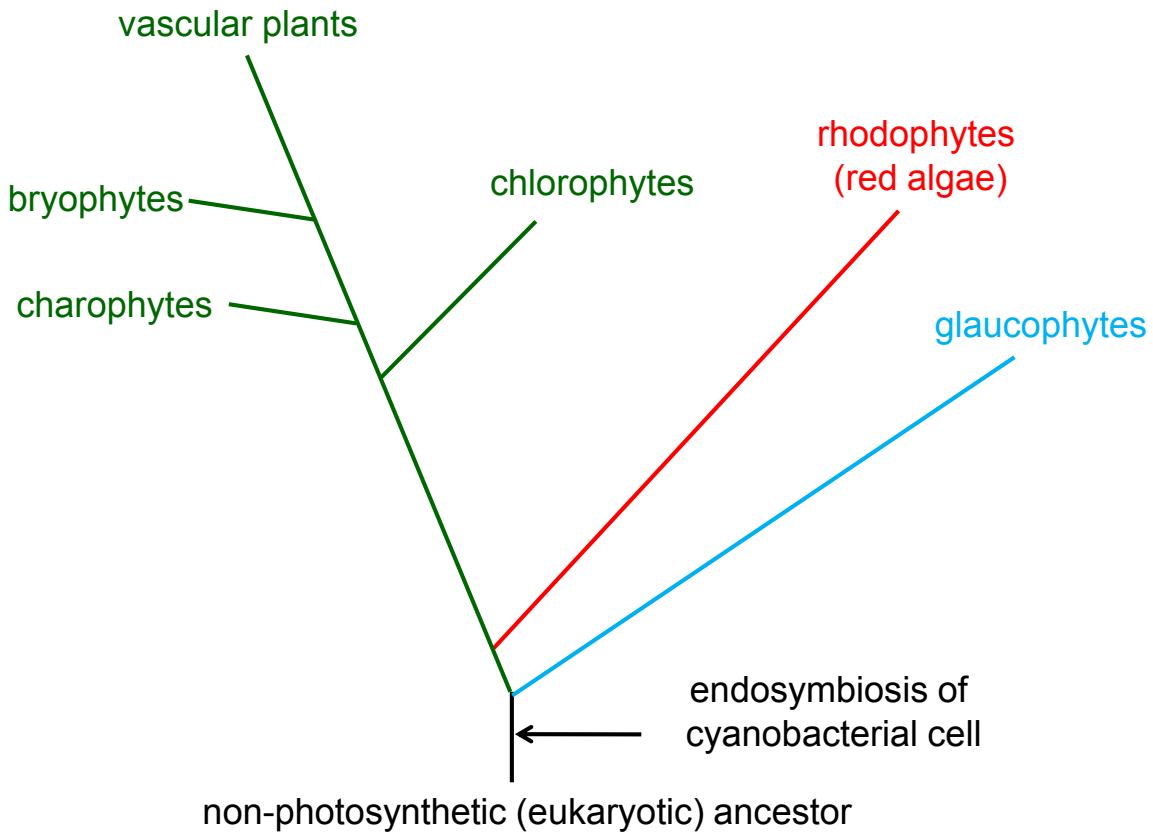

Figure 1-4: Evolutionary tree of photosynthetic eukaryotes

After the endosymbiosis of a cyanobacteria-like prokaryote, photosynthetic eukaryotes diverged to form three main lineages. One is the glaucophytes, a small group of fresh water algae. A second lineage is the rhodophytes, the red algae. The third lineage divides into chlorophytes (green algae including *C. reinhardtii*), charophytes (different class of green algae), bryophytes (mosses, hornworts and liverworts) and the vascular plants such as *A. thaliana*.

Although similar to land plants in many respects, including general cell structure and composition, and the function of the photosynthetic machinery, *C. reinhardtii* and other chlorophyte algae possess some unique characteristics. They developed the same biochemical machinery for photosynthesis as the streptophytes (including land plants), but the latter diverged from the chlorophyte algae in evolution about 500 million years ago (Wellman and Gray, 2000), which explains their differences in cell structure and interaction with the environment. Chlorophyte algae are not sessile but have a flagellum which enables them to be mobile in aquatic environments (Fig. 1-5).

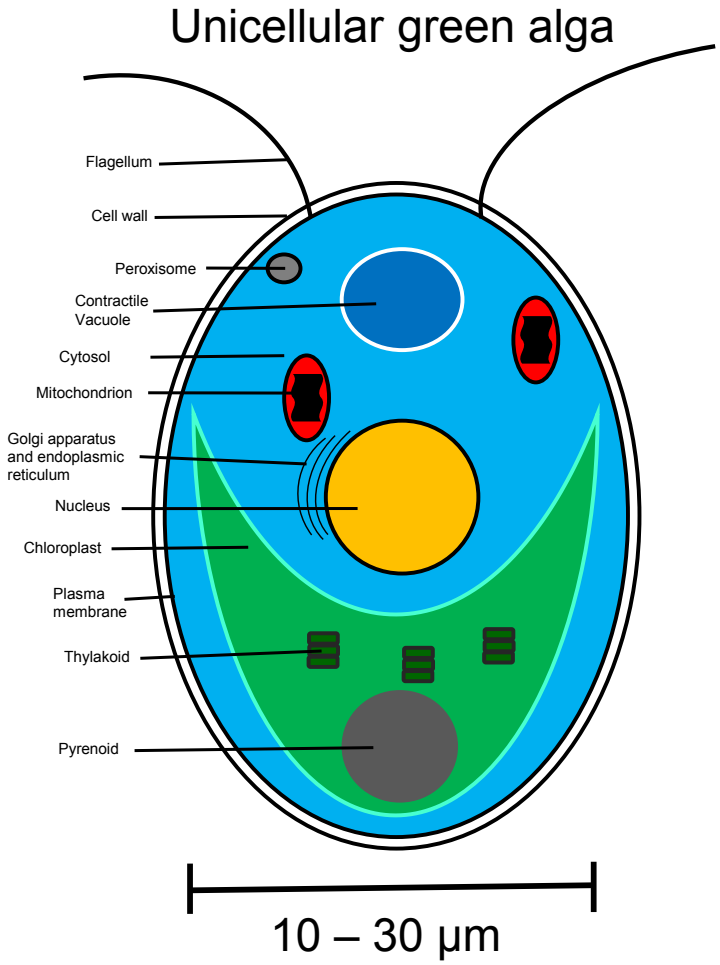

Figure 1-5: Overview of the cell structure of a unicellular alga such as *Chlamydomonas reinhardtii*

Unicellular algal cells contain all of the subcellular structures typical of a eukaryotic plant cell: cytosol, mitochondria, vacuole, nucleus, chloroplast, peroxisomes, endoplasmic reticulum and Golgi apparatus. Unlike plant cells they are mobile aquatic organisms that have flagella to move actively. Their vacuole is not a storage place but is responsible for active osmotic balance. Unlike land plants, the cells contain only a single large chloroplast that contains an ultrastructure called the pyrenoid. This is a semicrystalline structure built from starch and Rubisco.

This also leads to some major changes in their cell architecture; they possess only a single, large chloroplast and their vacuole is rather small compared to the rest of the cell volume, and its main function is not storage but osmotic regulation. In the chloroplast they have a structure called a pyrenoid, which is a starch-containing semi-crystalline structure in which most of the Rubisco enzyme is embedded (Suss et al., 1995). In the pyrenoid the concentration of carbon dioxide is enriched to suppress the oxygenation reaction of Rubisco. Higher plants do not form pyrenoids. These differences in cell architecture have been elucidated mainly by electron microscopy.

1.2.3 Protein targeting mechanisms

The bacterial ancestors of the chloroplast and the mitochondrion either lost or transferred most of their DNA to the nucleus of the host cell, so only a few organellar proteins are encoded by their respective organellar genomes. Other proteins in mitochondria and chloroplasts have a non-organellar origin and were acquired from multiple sources. Phylogenetic studies suggest that duplication of the host's genes gave rise to multiple isoforms of the same protein, some of which evolved to become located in the organelles (Martin, 2010). As a consequence of these evolutionary processes, only a few proteins are encoded by the mitochondrial or plastidial genomes and synthesised by their respective organellar ribosomes. Most organellar proteins are now encoded by nuclear genes and synthesised by cytosolic ribosomes. This means that the cell must ensure that newly synthesized proteins are guided properly to their destination. Therefore, many of the proteins are expressed as a pre-protein that has a specific transit peptide at the N-terminus, which is recognized by specialised machinery for import into the corresponding organelle.

About 95 % of all proteins in the chloroplast are encoded in the nucleus, synthesized in the cytosol and then guided to the chloroplast. The most common way for import of proteins is via two translocases. These translocases are called Toc (Translocon at the outer chloroplast envelope) and Tic (Translocon at the inner chloroplast envelope). These bind the transit peptide of the pre-protein and deliver it to the stroma, where the transit peptide is cleaved off and the protein is folded and assembled into its functional conformation. The thylakoid cpSRP (chloroplast Signal Recognition Particle), cpSec (chloroplast Secratory pathway), and cpTat (Twin arginine translocation) pathways are translocases for transport within the chloroplast into the thylakoid

membrane or into the thylakoid lumen (Cline and Dabney-Smith, 2008). The import of proteins into the mitochondria occurs by a similar mechanism. It consists of an outer translocase Tom (Translocon at the outer mitochondrion envelope) that binds the transit peptide and Tim (Translocon at the inner mitochondrion envelope) that translocates the protein into the mitochondrial matrix (Macasev et al., 2000).

The endomembrane system is responsible for transport of proteins to the apoplast or the vacuole. First the N-terminal signal peptide of the partially translated protein is recognized by a signal recognition particle, which guides the ribosome/mRNA/protein complex to the translocation apparatus of the endoplasmic reticulum (ER). A protease at the inner site of the ER cleaves off the signal peptide, and this allows protein synthesis to proceed with the protein being released into the ER lumen. There the protein is processed further, usually glycosylated and folded into the correct conformation. After this step the proteins are passed from the ER to the Golgi apparatus, where the glycosylation is finalized. Then proteins reach their native conformation state and their final destination is determined by secondary structural motifs, such as the C-terminal KDEL motif that acts as an ER retention signal. Proteins destined for the vacuole or apoplast are packed into vesicles that fuse with the tonoplast or plasmalemma, releasing their contents into the vacuole or apoplast. Often these vesicles are coated with the protein clathrin (Rojo and Denecke, 2008). Peroxisomal proteins are translated in the cytosol and are then imported into the peroxisomes. The peroxisomal targeting signal can be at either the N- or C-terminus of the protein. They are transported into the peroxisome via specific receptor systems without being unfolded (Brown and Baker, 2008).

1.3 Compartmentation of metabolism

As the compartmented architecture of eukaryotic cells evolved, the complexity of their metabolism also increased greatly in comparison to prokaryotic cells. The present day compartmentation of metabolic pathways partly reflects the evolutionary origins of these pathways, but other factors have played an equally important role in determining where a pathway is located within a cell. Looking at it only from the evolutionary point of view, the organelles derived from endosymbiotic events, have essentially retained their major biological functions; the chloroplasts carry out photosynthetic carbon fixation and the mitochondria respire sugars to provide energy in the form of ATP. Interestingly many of the genes for the enzymes

that catalyze these processes are encoded in the nucleus. This is due to the transfer of most of the DNA from the bacterial ancestors to the nucleus of the host. Many pathways resemble each other and have several enzymes in common, for example, the sucrose biosynthesis pathway in the cytosol and starch synthesis in the chloroplast. As a consequence different isoforms of the enzymes exist, which most likely evolved via gene duplication events. It is more probable that whole pathways were duplicated and transferred to a new destination rather than single enzyme events. Such a process can explain the similarity of certain reactions in the cell (Martin, 2010).

Compartmention brings many advantages for a eukaryotic cell, enabling it to develop extremely complex metabolic networks to cope with constantly changing environmental conditions. Compartmentation also allows biochemical reactions that generate harmful products to be sequestered out of the way. For example, by restricting the H_2O_2-producing reactions of photorespiration to the peroxisome, which contains high catalase activity to destroy H_2O_2, the rest of the cell is protected from this harmful compound. The vacuole is also used as a kind of waste storage bin, because very few metabolic reactions are occurring there, so harmful metabolites are less likely to cause any damage compared to other parts of the cell (Martinoia et al., 2007). Even non-toxic metabolites can interfere with other reactions. For example, some pathways involve both oxidative and reductive reactions coupled to reduction of $NAD(P)^+$ or oxidation of NAD(P)H, respectively. For readily reversible reactions the $NAD(P)^+$: NAD(P)H ratio is a major factor in determining the direction and net flux of the reaction. In eukaryotic cells, different $NAD(P)^+$: NAD(P)H ratios can be maintained in different compartments to allow some reactions to proceed in the oxidative direction while similar, or even the same, reactions go in the reductive direction elsewhere in the cell (Pracharoenwattana et al., 2007).

One of the downsides of complex cell architecture is that all of the different compartments need to be osmotically balanced against each other. The chloroplasts, the cytosol, peroxisomes, mitochondria and the vacuole all possess very different solute compositions. While the cytosol, the chloroplasts and the mitochondria contain most of the phosphorylated intermediates and nucleotides, the vacuole is the main storage site for sugars and organic acids. The vacuole also has the biggest volume of all compartments, so the majority of solutes, including inorganic ions, are present in this part of the cell to maintain the osmotic balance within the cell.

These and other factors help to explain why photosynthesis and related pathways of primary carbon metabolism are so highly compartmented in plants. In the next sections I will describe these pathways and their intracellular location in more detail.

1.3.1 Compartmentation of metabolism in higher plants

Animal and plant cells share many biochemical pathways, such as glycolysis and the TCA cycle. Additionally plant cells have the ability to photosynthesize and possess pathways like the Calvin-Benson-cycle, and starch and sucrose synthesis. From the perspective of primary metabolism, the main function of the chloroplast is to supply the rest of the cell with energy in the form of redox equivalents and ATP, and sugars derived from photosynthetic carbon fixation. Many of the most energy intensive pathways take place in the chloroplast, for example, carbon fixation itself (Calvin and Benson, 1948), starch metabolism (Zeeman et al., 2007), nitrogen and sulphur assimilation (Bowsher and Tobin, 2001) and amino acid metabolism (Neuhaus and Emes, 2000). In contrast the vacuole mainly acts as a storage compartment, not only for energy-rich molecules such as free sugars, but also for ions and toxic compounds, e.g. heavy metals (Martinoia et al., 2007). One of the main photosynthesis-related functions of the cytosol is the synthesis of the transport sugar sucrose (Lunn and MacRae, 2003). The mitochondria provide energy donor molecules, such as ATP, in the night when photosynthesis is inactive, via the TCA cycle and the respiratory chain (Fernie et al., 2004). In combination with peroxisomes and chloroplasts, the mitochondria are also involved in the process of photorespiration (Bauwe et al., 2010). Additionally peroxisomes are involved in the breakdown of long-chain fatty acid chains in a process called beta-oxidation, which is especially important during the germination of oil-containing seeds (Baker et al., 2006).

Table 1-1: Distribution of primary metabolic pathways in plant cells

Compartment	Biochemical pathways
Chloroplast	CO_2 fixation
	Starch metabolism
	Nitrogen assimilation
	Sulphur assimilation
	Amino acid metabolism
	Photorespiration
	Fatty acid synthesis
Cytosol	Sucrose metabolism
	Glycolysis
	Amino acid metabolism
	Nitrate reduction
Mitochondrion	TCA cycle
	Oxidative phosphorylation
	Photorespiration
Peroxisome	Beta-oxidation
	Photorespiration
Vacuole	Sugar storage
Endoplasmic Reticulum	Lipid synthesis/modification
	Synthesis of cell wall precursors

The nucleus contains the majority of the DNA, the genetic information of the cell. The information carried within the genes is transcribed by RNA polymerases to messenger RNA (mRNA), which is then exported from the nucleus. The process of translation is the production of proteins on the basis of the information stored in the mRNA. This process is accomplished by ribosomes that can either be free in the cytosol or bound to the endoplasmic reticulum. The smooth endoplasmic reticulum does not bind ribosomes, but is involved in lipid synthesis. The Golgi apparatus modifies proteins and lipids and prepares them for export or for specific destinations in the cell (Smith et al., 2010). It must be stressed that this summary is a very simplified overview of the metabolic functions of these compartments, and a complete description of all the pathways is beyond the scope of this thesis. Such information is readily available from plant physiology textbooks (Heldt et al., 2010; Smith et al., 2010). The following discussion will focus on the central pathways of CO_2 fixation and carbohydrate metabolism. The main reactions and their compartmentation in a typical leaf mesophyll cell are shown in two

figures; Fig. 1-6 shows the main pathways operating during the day, while Fig. 1-7 shows night-time metabolism.

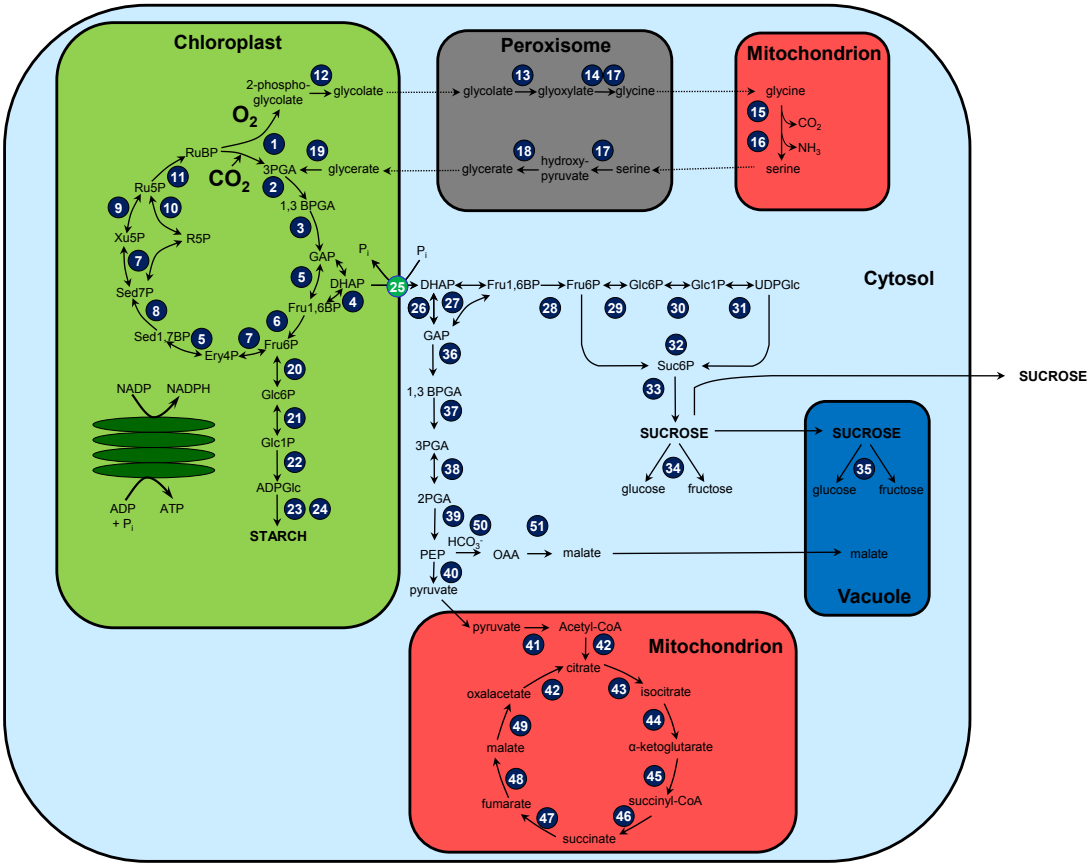

Figure 1-6: Primary carbon metabolism during the day in an *A. thaliana* leaf mesophyll cell

The carbon fixation in the chloroplast is integrated with photorespiration in the peroxisome and the mitochondrion, as well as the synthesis of starch in the chloroplast and sucrose in the cytosol, and the TCA-cycle in the mitochondrion. The reactions are catalyzed by the following enzymes: (1) RubiscCO; (2) phosphoglycerate kinase; (3) NADP-glyceraldehyde-phosphate dehydrogenase; (4) plastidic triose-phosphate isomerase; (5) plastidic aldolase; (6) plastidic fructose-1,6-bisphosphatase; (7) transketolase; (8) sedoheptulose-1,7-bisphosphatase; (9) ribulose-5-phosphate epimerase; (10) ribose-5-phosphate isomerase; (11) phosphoribulokinase; (12) phosphoglycolate phosphatase; (13) glycolate oxidase; (14) glutamate:glyoxylate aminotransferase; (15) glycine decarboxylase; (16) serine hydroxymethyl transferase, (17) serine:glyoxylate aminotransferase; (18) hydroxypyruvate reductase; (19) glycerate kinase; (20) plastidic phosphoglucoisomerase; (21) plastidic phosphoglucomutase; (22) ADPglucose pyrophosphorylase; (23) starch synthase; (24) starch branching enzyme; (25) triose-phosphate translocator; (26) cytosolic triose-phosphate isomerase; (27) cytosolic aldolase; (28) cytosolic fructose-1,6-bisphosphatase; (29) cytosolic phosphoglucoisomerase; (30) cytosolic phosphoglucomutase; (31) UDP-glucose pyrophosphorylase; (32) sucrose-phosphate synthase; (33) sucrose phosphatase; (34) cytosolic invertase; (35) vacuolar invertase, (36) NAD-glyceraldehyde-phosphate dehydrogenase; (37) phosphoglycerate kinase; (38) phosphoglycerate mutase; (39) enolase; (40) pyruvate kinase; (41) pyruvate dehydrogenase; (42) citrate synthase; (43) aconitase; (44) isocitrate dehydrogenase; (45) α-ketoglutarate dehydrogenase; (46) succinyl-CoA synthetase; (47) succiniate dehydrogenase; (48) fumarase; (49) mitochondrial malate dehydrogenase; (50) phosphoenolpyruvate carboxylase; (51) cytosolic malate dehydrogenase. For clarity the involvement of GAP as a substrate in the two transketolase reactions and of DHAP in the second aldolase reaction that forms Sed1,7BP is not shown.

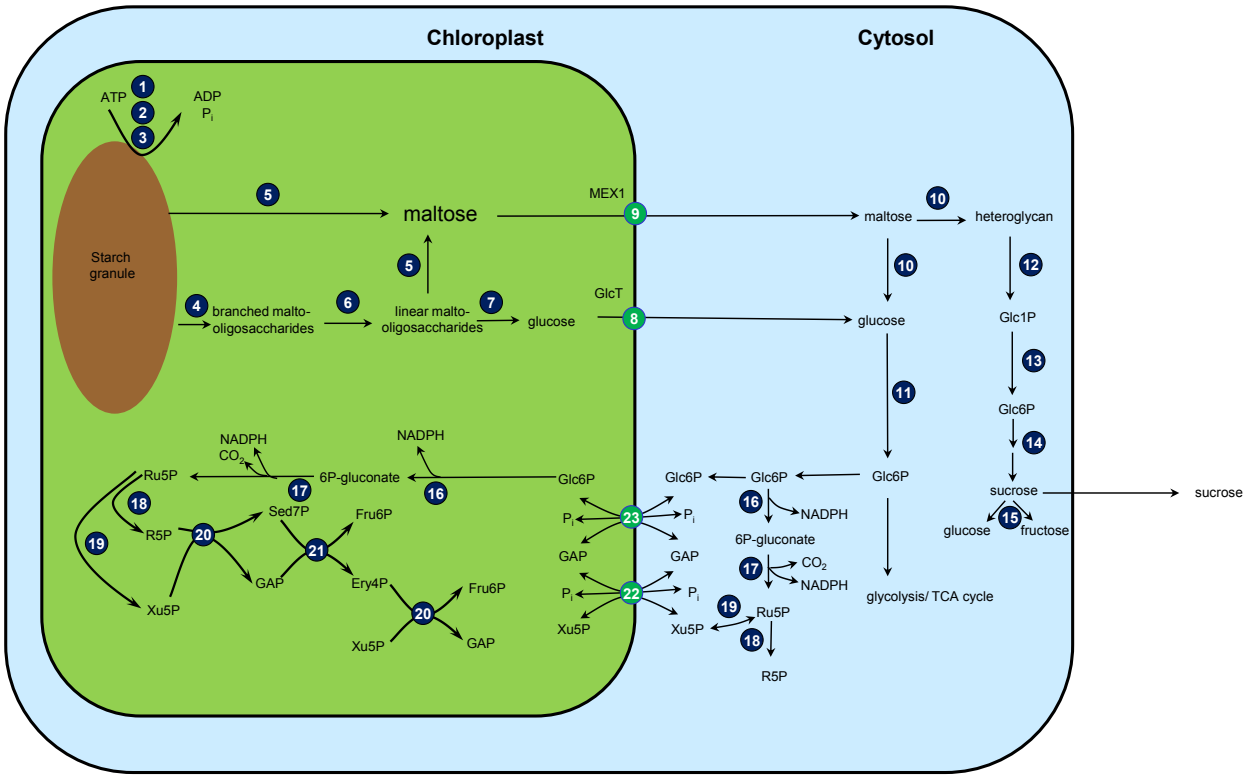

Figure 1-7: Primary carbon metabolism during the night in an *A. thaliana* leaf mesophyll cell

Starch degradation occurs in the chloroplast and its main breakdown products, maltose and a small amount of glucose, are exported to the cytosol, where they can be used for the synthesis and export of sucrose. The complete oxidative pentose phosphate pathway operates in the chloroplast and some reactions also occur in the cytosol, except for those dependent on transketolase, which is absent from the cytosol. The reactions are catalyzed by the following enzymes: (1) glucan water dikinase; (2) phosphoglucan water dikinase; (3) phosphoglucan phosphatase; (4) α-amylase; (5) β-amylase; (6) limit dextrinase; (7) disproportionating enzyme; (8) glucose transporter, (9) maltose transporter; (10) transglucosidase; (11) hexokinase; (12) α-glucan phosphorylase; (13) cytosolic phosphoglucomutase; (14) sucrose synthesizing enzymes (compare Fig. 1-6); (15) cytosolic invertase; (16) glucose-6-phosphate dehydrogenase; (17) 6-phosphogluconate dehydrogenase; (18) ribose-5-phosphate isomerase; (19) ribulose-5-phosphate epimerase; (20) transketolase; (21) aldolase; (22) Xu5P/phosphate translocators (XPT); (23) Glc6-P/phosphate translocator (GPT).

Furthermore plants possess hundreds, if not thousands of reactions of secondary metabolism that produce metabolites that are not strictly essential for the plant to survive, but are important for fitness in natural environments. These include glucosinolates for insect and fungal defense in the Brassicacea (e.g. *A. thaliana*) and alkaloids such as nicotine in tobacco, which is a neurotoxin that protects against herbivores. Secondary metabolites can be beneficial in the human diet, for example, polyphenols such as resveratsol can function as antioxidants and protect cells against free radicals (Acamovic and Brooker, 2005), and glucosinolates are thought to protect against some forms of cancer (Verkerk et al., 2009). The initial synthesis of the precursors for secondary metabolites is well established but in many cases the later steps are still unknown or poorly

described, and the intracellular compartmentation of much of secondary metabolism is unexplored (Lunn, 2007).

1.3.2 Compartmentation of metabolism in unicellular alga

Unicellular algae have some advantages as subjects for research into plant metabolism, because only one cell type needs to be considered, compared with higher plants that have many different cell types and where interactions between cells within a tissue or whole organism also need to be taken into account. Although a few studies have taken advantage of the relative simplicity of algal cells to look more deeply into the issue of metabolic compartmentation and biochemistry, most of the research that has been done on *C. reinhardtii* deals with flagellar motion or phototaxis. The primary carbon fixation by the Calvin-Benson cycle is essentially the same in chlorophytes and vascular plants. In contrast, the first steps of glycolysis from fructose-6-phosphate to triose-phosphates are restricted to the plastids in chlorophyte algae, while the remaining steps from glycerate-3-phosphate to pyruvate take place in the cytosol (Klein, 1986). In higher plants there is almost complete duplication of glycolysis in the plastids and cytosol. There is very little, if any, sucrose synthesis in *C. reinhardtii*, which makes sense in light of its main function as a transport sugar in higher plants, which is not needed in a unicellular organism (Klein, 1987). Besides these general differences in cell structure and biochemistry, *C. reinhardtii* has some unique properties that do not exist in higher plants. When faced with low CO_2, or rather HCO_3^- in the aquatic environments this species usually inhabits, they can establish a carbon concentrating mechanism. This includes carbon transporting mechanisms at the plasma membrane and the plastidial membrane, as well as synthesis of carbonic anhydrases (Yamano and Fukuzawa, 2009). Another feature of *C. reinhardtii* is its ability to produce molecular hydrogen under sulphur deprivation conditions (Hemschemeier et al., 2008). This makes it a very interesting system for studying the potential of green algae for commercial production of biofuels.

1.4 The physiological significance of metabolic compartmentation

Some of the benefits of compartmentation in eukaryotic cells were outlined in section 1.3, but here I shall discuss the physiological significance of compartmentation for plants and their metabolism in more detail. A very important factor that varies between organelles and within organelles is pH. The gradient of protons across a membrane is often used as a power source for producing energy-carrying metabolites such as ATP. ATP is produced by the ATP synthases, which are embedded in the inner membranes of the mitochondria, or in the thylakoid membranes of the chloroplasts. These ATP synthases use the chemical and electrical potential that is stored in the form of charge separation across the membrane to drive the phosphorylation of ADP to produce ATP. In the light the thylakoid lumen becomes acidified down to about pH 4, whereas the stroma becomes more alkaline, up to about pH 8 (Smith et al., 2010). This corresponds to a difference in proton concentration of four orders of magnitude. The flow of protons, also called proton motive force (pmf), drives a rotary mechanism that forces the formation of ATP (Nakamoto et al., 2008).

Membrane transport in general is often driven by the charge separation of protons across membranes. Here, ATP-dependent proton pumps use ATP to transport protons across the membranes to generate a proton motive force. The backflow of these protons is then used to drive transport of other ions or metabolites across the membrane against an electrical or concentration gradient (Nelson, 1994; Martinoia et al., 2007).

Another example of the physiological significance of charge separation across membranes is Ca^{2+} signalling. The Ca^{2+} concentration in the cytosol is very low compared to the concentrations in organelles such as the ER. This is brought about by the action of several Ca^{2+} transporters and channels in the membranes of the organelles. Environmental stimuli often lead to release of Ca^{2+} from organelles into the cytosol, where it can bind to specific proteins that stimulate downstream processes, for example, transcription factor activation (Kudla et al., 2010). The Ca^{2+} response in stomatal guard cells, and its role in control of stomatal aperture, has been studied extensively. Abscisic acid is perceived by a specific guard cell receptor and functions as a signal of water stress. This signal triggers a release of Ca^{2+} into the cytosol, where it activates K^+ channels, which leads to release of K^+ from the guard cell, an osmotic driven decrease in cell turgor and closing of the stomata to prevent water loss (Roelfsema and Hedrich, 2010).

Variation in pH between compartments means that enzymes that are located in either acidic or alkaline environments are often adapted to have different pH optima. Interestingly, changes in pH can be used to regulate enzyme activity. Many of the enzymes in the Calvin-Benson cycle have a pH optimium that lies in the alkaline range around pH 8. When the light reactions of photosynthesis are operating during the day, protons are pumped from the stroma into the thylakoid lumen, causing the pH of the stroma to rise and thereby increasing the activity of enzymes that have an alkaline pH optimum. In the night the stromal pH decreases and so reverses this activation. Light/dark induced changes in Mg^{2+} concentration and in the redox state of several enzymes (phosphoribulokinase, Rubisco activase (and thereby Rubisco), NADP-glyceraldehyde-phosphate dehydrogenase, sedoheptulose-1,7-bisphosphatase and fructose-1,6-bisphosphatase) also play a major role in regulating activities, and prevent unnecessary or wasteful reactions from operating in the dark (Wolosiuk et al., 1993). This is just one example of the sophisticated mechanisms that plants have evolved to regulate their metabolism in response to changing environmental conditions.

Separation of enzymes that share substrates or products in common, but metabolise these in opposite ways, can help to prevent futile cycles. A futile cycle means that certain products are synthesized and consumed again without any benefit to the cell, and in the process wasting energy that is dissipated as heat. One example would be the presence of hexokinase and sugar-phosphatase in the same compartment. Phosphorylation of hexose sugars by hexokinase consumes ATP, and if there were a sugar-phosphatase activity in the same compartment this would dephosphorylate the hexose-phosphate and so effectively waste the ATP-energy used for its synthesis. Both of these reactions are individually necessary for the cell, phosphorylation of hexoses is needed to break them down via glycolysis whereas sugar-phosphates may need to be dephosphorylated to transport them from one compartment to the other or to release P_i for other reactions. One way to avoid such futile cycles is to restrict each enzyme to different compartments. In general, it is advantageous to avoid futile cycles, but there are situations where futile cycles can benefit the plant. For example, the cyclic degradation and resynthesis of sucrose allows sucrose to be taken up from the apoplast by sink cells, and so is sometimes an important process in the transport of sucrose from source to sink tissues via the phloem (Schwender et al., 2004).

Malate dehydrogenase (MDH) is a particularly interesting example because the enzyme is present in multiple compartments, and the isoforms in each of these have specific functions, operating in different directions in different places. The cytosolic and mitochondrial isoforms are involved in the malate-aspartate shuttle between cytosol and mitochondria. The peroxisomal MDH reduces oxaloacetate to malate, to provide NAD^+ for β-oxidation in the peroxisome (Pracharoenwattana et al., 2007). There is also MDH activity in the chloroplast, which is involved in transfer of reducing equivalents to other parts of the cell. This shows once more how important it is for the plant to tightly regulate reactions to allow potentially conflicting reactions to operate simultaneously.

The presence of multiple isoforms of the same enzyme located in different compartments allows essentially the same reactions to be regulated in different ways in each compartment. A good example is fructose-1,6-bisphosphatase, which is present in plastidial and cytosolic isoforms. Both catalyze the dephosphorylation of fructose-1,6-bisphophate to fructose-6-phosphate, but their regulatory properties differ substantially. The plastidial isoform is under the direct influence of redox regulation, while the cytosolic isoform is regulated by the levels of AMP and fructose-2,6-bisphophate. Both reactions are extremely important in plant metabolism as changes in either of these activities have a profound effect on photosynthesis and plant growth (Serrato et al., 2009). The different regulatory and kinetic properties (e.g. K_m and V_{max}) of the plastidial and cytosolic isoforms allow them to be regulated independently, so that their activities are aligned with the requirements of their respective pathways.

As noted previously, another advantage of compartmentation is the possibility to confine reactions that produce harmful compounds to a limited space, where these toxic compounds cannot damage the rest of the cell. Within the context of photosynthetic metabolism, a good example is the oxidation of glycolate to glyoxylate by glycolate oxidase during photorespiration. The oxidant in this reaction is O_2, which is reduced to the extremely reactive compound H_2O_2. This compound would cause severe damage to the cell, but because it is only produced in the peroxisome, where it is directly split into H_2O and O_2 by catalase, it is effectively neutralized (Bauwe et al., 2010). If this reaction were not separated from the rest of the cell it could cause damage to the DNA and change the genetic information of the cell (Konat, 2003).

Compartmentation in plant cells is even further complicated by the fact that different metabolic reactions take place at different times of the day. For example, during the day when photosynthesis and carbon fixation are operating, a certain part of the fixed carbon is partitioned between synthesis of starch in the chloroplast and sucrose in the cytosol. During the night starch is degraded in the chloroplast and maltose is exported to the cytosol where it can also be used to synthesize sucrose (see Fig. 1-6) (Zeeman et al., 2007). Another example of temporal compartmentation is the Crassulacean acid metabolism (CAM) in plants such as pineapple that are adapted to hot dry environments. They open their stomata in the night and fix CO_2 via phosphoenolpyruvate (PEP) carboxylase to form oxaloacetate, which is then converted to malate by malate dehydrogenase and stored in the vacuole. During the day malate is transported to the plastid stroma, where it is decarboxylated to pyruvate by malic enzyme or PEP carboxykinase. Then the released CO_2 can enter the Calvin-Benson cycle (Dodd et al., 2002). This mechanism is beneficial for the plant because it can close its stomata during the day to avoid water loss.

From the examples described above it is clear that compartmentation confers many advantages on the cell, and is a fundamental feature of photosynthesis in plants. In the following sections I will describe the main pathways of photosynthetic carbon metabolism in detail.

1.4.1 The reductive and oxidative pentose phosphate pathways

1.4.1.1 Discovery of the Calvin-Benson cycle

Photosynthetic carbon fixation is ultimately the basis for almost all life on earth. The biochemical pathway of CO_2 fixation was revealed in a groundbreaking series of studies led by Melvin Calvin (Calvin and Benson, 1948; Bassham et al., 1950; Calvin, 1950; Calvin et al., 1950). The basic approach the researchers took was to use the green alga *Chlorella pyrenoidosa* and grow it in a fermenter that could be opened from the bottom via a simple valve system. Then they exposed the algae to $^{14}CO_2$ in the light and sampled at intervals from seconds to minutes, to investigate the kinetics of labelling of different compounds by opening the valve and killing the cells in boiling ethanol. Using paper chromatography and autoradiography the intermediates and order of reactions in the pathway of carbon fixation and reduction were resolved. They also showed that

chlorophyll is the acceptor molecule of the energy in sunlight and not CO_2 as was believed previously.

1.4.1.2 The pathway of CO_2 fixation

In essence, the Calvin-Benson cycle can be separated into three parts. First CO_2 is fixed by the action of Rubisco using ribulose-1,5-bisphosphate (RuBP) as an acceptor molecule to produce two molecules of 3-phosphoglycerate (3PGA). In the second phase of the cycle, 3PGA is reduced to glyceraldehyde-3-phosphate (GAP) by the sequential action of phosphoglycerate kinase (PGK) and glyceraldehyde-3-phosphate dehydrogenase (NADP-GAPDH) using ATP and NADPH, respectively. Both coenzymes are produced by the action of the light reactions of photosynthesis. GAP is the first sugar compound in the cycle, being a triose-phosphate. In the third phase of the cycle the acceptor molecule RuBP is regenerated by the combined action of the enzymes triose-phosphate isomerase (TPI), aldolase, fructose-1,6-bisphosphatase (Fru1,6BPase), transketolase (TK), sedoheptulose-1,7-bisphosphatase (Sed1,7BPase) ribose-5-phosphate isomerase (R5P isomerase) and ribulose-5-phosphate epimerase (Ru5P epimerase) (see Fig. 1-6 and for a more detailed overview chapter 4). This consumes five-sixths of the total triose-phosphate, with the remaining one-sixth being available for end product synthesis. When the plant is first illuminated, even this net fixed carbon is often retained to generate even more RuBP and thereby increase flux through the cycle in an autocatalytic manner (Stryer, 2002). Besides the regeneration of RuBP for carbon fixation, the Calvin-Benson cycle produces substrates for other important biosynthetic reactions. Erythrose-4-phosphate (E4P) is the main substrate for the shikimate pathway for synthesis of aromatic amino acids and thousands of aromatic secondary metabolites (Smith et al., 2010), and ribose-5-phosphate (R5P) is used for synthesis of nucleotides (Stryer, 2002).

1.4.1.3 Photorespiration

Rubisco can also catalyze the oxygenation of RuBP using O_2, which as a consequence leads to a reaction series called photorespiration that also involves the peroxisomes and mitochondria (Fig. 1-6). The function of photorespiration is still under debate. The net outcome is a loss of organic carbon and from an energetic point of view it appears to be a wasteful process for the cell. It is most likely that it is an unavoidable side reaction of Rubisco. Rubisco evolved when the atmosphere on earth was different to the composition today. As most atmospheric oxygen is produced by the action of the water splitting complex in photosynthesis, it was not present in

substantial amounts during the early stages in the evolution of life, when Rubisco probably first appeared, and therefore it did not compete with CO_2 for binding to the enzyme's active centre (Smith et al., 2010). As the atmosphere changed over time, with more and more oxygen accumulating due to oxygenic photosynthesis by cyanobacteria, the oxygenation of RuBP by Rubisco would also increase. It is thought that photorespiration evolved to enable plants to recycle the unwanted by-product of oxygenation, 2-phosphoglycolate, into the Calvin-Benson cycle (see Fig. 1-6). After the oxygenation of RuBP by Rubisco the product 2-phosphoglycolate is dephosphorylated to glycolate in the chloroplast, which is then transported to the peroxisome. There it is converted to glyoxylate by glycolate oxidase and subsequently aminated into glycine by the combined action of glutamate:glyoxylate aminotransferase and serine:glyoxylate aminotransferase. Glycine moves into the mitochondrion where it is converted to serine by means of glycine decarboxylase and serine hydroxymethyl transferase. Serine moves back into the peroxisome where it is first converted to hydroxypyruvate by serine:glyoxylate aminotransferase and then to glycerate by hydroxypyruvate reductase. Glycerate can then enter the chloroplast, where it is phosphorylated by glycerate kinase to 3PGA, which re-enters the Calvin-Benson cycle (Bauwe et al., 2010).

1.4.1.4 The oxidative pentose phosphate pathway

The Calvin-Benson cycle is also known as the reductive pentose phosphate pathway, as it shares several reactions and intermediates with the oxidative pentose phosphate pathway (OPPP), which occurs in both plant and animal cells. The Calvin-Benson cycle consumes NADPH, whereas the main function of the OPPP is to produce NADPH, which is used in many biosynthetic reactions, e.g. fatty acid synthesis. In plants there is no need to produce NADPH via the OPPP during the day because it is a product of the light reactions in photosynthesis. Therefore, in plants glucose-6-phosphate dehydrogenase (G6PDH), the first committed enzyme in the OPPP, is inactive during the day. This is achieved by the action of thioredoxin that reduces a disulphide bridge in the active enzyme to the dithiol form and thereby inactivates the enzyme. When G6PDH is oxidized in the dark it becomes active and the OPPP starts to operate. After the first oxidation of G6PDH, 6-phosphogluconolactonase and 6-phosphogluconate dehydrogenase produce one more molecule of NADPH, plus CO_2 and Ru5P. The Ru5P is then metabolised via essentially the reverse reactions from the regenerative phase of the Calvin-Benson cycle, catalysed by transketolase, R5P isomerase and Ru5P epimerase plus aldolase, which converts the Ru5P to GAP and Fru6P

(see Fig. 1-7). In plants there is a complete OPPP in the chloroplast. The first part of the pathway is duplicated in the cytosol, but the pathways is incomplete due to lack of aldolase, transketolase, R5P isomerase and Ru5P epimerase in the cytosol (Schnarrenberger et al., 1995; Kruger and von Schaewen, 2003), so Ru5P produced in the cytosol must be transported into the plastid for further metabolism. This shows once more how important communication and regulation of metabolism between compartments are to ensure that the different parts of the cell are provided with the energy carrying molecules, and metabolic precursors needed for biosynthetic pathways.

1.4.1.5 Control of the Calvin-Benson cycle

The regulation of the Calvin-Benson cycle has been investigated by detailed biochemical analysis of individual components, e.g. by characterising the kinetic properties of purified enzymes (Buchanan and Schurmann, 1973; Wolosiuk and Buchanan, 1976, 1978b, a; Kruger and Schnarrenberger, 1983; Kopke-Secundo et al., 1990; Dunford et al., 1998). Such studies can reveal the individual mechanisms of regulation that operate in the cell, but a different approach is needed to investigate control of flux through the pathway as a whole. This can be done by studying the effects of changing environmental conditions on rates of photosynthesis, or by analysing mutants or transgenic plants with altered enzyme activities. Transgenic tobacco plants with decreased Rubisco content were used to determine the enzyme's flux control coefficient under different environmental conditions. It was shown that Rubisco has a strong control over net carbon fixation in limiting CO_2, but very little control in saturating CO_2 (Stitt et al., 1991). Transgenic plants that have lost the ability of Rubisco activase to carbamylate Rubisco, showed a strong decrease in carbon fixation, and normal growth was only achieved at high CO_2 levels (Mate et al., 1993). A more detailed analysis of the effect on varying amounts of Rubisco was carried out in tobacco (Quick, 1994). The findings of the effect of decreasing Rubisco activase activity in tobacco (Mate et al., 1993) were confirmed by similar experiments in *A. thaliana* (Eckardt et al., 1997). The effects of decreased Rubisco activity on nitrogen and amino acid metabolism have also been investigated, and showed a strong correlation between the effects on primary and secondary metabolites (Matt et al., 2002).

A decrease in the activity of plastidial GAPDH did not lead to any change in 3PGA levels, but did lower rates of CO_2-fixation (Price et al., 1995). These early studies used mutants with decreased enzyme activities to investigate metabolism and flux through pathways were discussed

in a review by Stitt and Sonnewald (1995), which also highlighted the potential for near-equilibrium reactions to contribute to control of flux through the pathways.

Other Calvin-Benson cycle enzymes were targeted in later studies. A decrease in activity of plastidial aldolase led to inhibition of photosynthesis, a drop in carbon fixation, and growth retardation (Haake et al., 1998). This is especially interesting because aldolase was always believed to have very little control over carbon fixation. A moderate decrease of transketolase activity had a strong effect on RuBP regeneration and photosynthesis, but also led to lower sugar content and strong effects on secondary metabolic pathways that use E4P as a precursor (Henkes et al., 2001). Plants with decreased Sed1,7BPase activity had lower sugar and starch levels (Olcer et al., 2001; Lawson et al., 2006). An investigation of the effects of decreased Rubisco activity in *Flaveria bidentis* revealed that this enzyme still makes an important contribution to control of carbon fixation even in this C_4 plant under ambient CO_2 conditions (Furbank et al., 1996).

Together, these studies with transgenic plants greatly improved our knowledge about the function and control of the Calvin-Benson cycle and end product synthesis, but in almost all cases no increase in rates of carbon fixation was observed (Raines, 2003). Other transgenic approaches have been attempted, with the specific aim of trying to improve carbon fixation, such as increasing the carboxylation: oxygenation ratio of Rubisco (Whitney and Andrews, 2001, 2003) or decreasing photorespiration (Kebeish et al., 2007), but so far only marginal improvements have been achieved (Raines, 2006). Overexpression of Sed1,7BPase and Fru1,6BPase from cyanobacteria in tobacco is one of the few examples were photosynthesis and growth were reported to be improved (Miyagawa et al., 2001). Overexpression of *A. thaliana* Sed1,7BPase in tobacco led to increased photosynthesis and growth (Lefebvre et al., 2005). The main conclusions from all these studies are that control is shared between enzymes, and that the distribution of control of flux between enzymes varies with the environmental conditions.

1.4.1.6 Mathematical modelling of photosynthesis

Our in-depth knowledge of the Calvin-Benson cycle has allowed the pathway to be mathematically modelled. The first models that combined experimental data and mathematical descriptions were published in 1983 (Woodrow et al., 1983; Woodrow et al., 1984). These mainly focussed on the regulation of the enzyme Sed1,7BPase. The first purely mathematical model describing the whole pathway was published in 1988. It was able to reconstruct metabolic

concentrations under different experimental conditions, and was used to estimate fluxes through the pathway (Pettersson and Ryde-Pettersson, 1988). Later, even more complex models were developed that described two different steady states, and showed that the enzymes Rubisco and Sed1,7BPase have the biggest influence on the flux through the cycle (Poolman et al., 2000; Poolman et al., 2001). Another model was developed to test the elasticity of the Calvin-Benson cycle enzymes and their impact on the network structure (Kreim and Giersch, 2007). To date most of these models have combined data from multiple species, and invariably include some assumptions about the subcellular distribution and concentrations of many of the pathway intermediates. Methodological advances and the application of omics technologies to certain model species is providing a wealth of data, which opens up possibilities to model photosynthesis in even greater detail, not only at the single cell level, but also at the tissue and whole organism levels.

1.4.2 Photosynthetic end product synthesis – sucrose and starch metabolism

The two main end products of photosynthetic carbon metabolism are starch, which is synthesized and stored in chloroplasts during the day and serves as an energy source during the night, and sucrose, which is synthesized in the cytosol and is the main transport sugar in higher plants (compare Fig. 1-6 and 1-7) (Zeeman et al., 2007). The partitioning of photoassimilates between sucrose and starch, and the relative amounts of starch and soluble sugars stored in the leaf vary enormously between species. Wheat and rice store very little starch in their leaves (Lunn and Hatch, 1995), but starch is the main leaf storage product in the model species *A. thaliana*. Mutants that lack the ability to synthesize starch show a severe retardation of growth except when grown under continuous light (Caspar et al., 1985). The reduction of plastidial phosphoglucomutase activity in potato led to decreased starch and increased sucrose content, revealing an important role for the enzyme in carbon partitioning (Fernie et al., 2001). Starch also serves as a storage reserve in non-green parts of the plant, for example in potato tubers. In the seeds of cereal crop plants it is stored and used as the main respiratory substrate during germination. This starch reserve is one of the main sources of carbohydrate in the human diet. Other plant species such as sugarcane and sugar beet use sucrose as their main carbohydrate storage reserve instead of starch. In most plants sucrose is the main transport form of sugar from leaves (source tissue) to sink tissue (e.g. roots) (Kuhn and Grof, 2010).

1.4.2.1 Starch synthesis during the day

The generally accepted pathway of starch synthesis in mesophyll cells proceeds as follows, using fructose-6-phosphate (Fru6P) derived from the Calvin-Benson cycle. Fru6P is converted to glucose-6-phosphate (Glc6P) by the action of the plastidial phosphoglucoisomerase (PGI). Glc6P is then converted to glucose-1-phosphate (Glc1P) by the plastidial phosphoglucomutase (PGM). Following these two reactions, Glc1P and adenosine triphosphate (ATP) are used to produce adenosine diphosphoglucose (ADPGlc) and pyrophosphate by means of ADPGlc-pyrophosphorylase (AGPase). Alkaline pyrophosphatase cleaves pyrophosphate to two orthophosphate molecules (Weiner et al., 1987). This step makes the synthesis of ADPGlc practically irreversible *in vivo*. Different starch synthase isoforms transfer the glucosyl moiety of ADPGlc to the non-reducing end of pre-existing amylose or amylopectin glucan chains and release adenosine diphosphate (ADP). The glucose molecules are mostly joined by α(1-4) linkages, with various degrees of branching via α(1-6) linkages, unlike in cellulose where the glucose molecules are connected via β(1-4) linkages. Amylose is a linear molecule with very few branches, while amylopectin is a larger polymer and is highly branched. Soluble starch synthases generate α(1-4)-glucans and branch points are introduced by several branching enzymes to produce amylopectin, while granule bound starch synthase isoforms are responsible for the formation of amylose. Starch-branching enzymes introduce the α(1-6) side chains by cleaving a linear α(1-4)-glucan and attaching it in the new conformation to an acceptor glucose residue in a different chain (Martin and Smith, 1995). A starch granule is a complex structure that consists of many glucan chains of differing length and degree of branching.

In recent years an alternative model to the generally accepted starch synthesis pathway has been put forward (see Fig. 1-8). This model proposes that the majority of the starch precursor ADPGlc is not synthesized by the AGPase reaction in the chloroplast, but by the reaction of sucrose synthase in the cytosol, and is then imported by an adenylate transporter into the plastid where it is used for starch synthesis (Pozueta-Romero et al., 1991a; Pozueta-Romero et al., 1991b; Baroja-Fernandez et al., 2001; Baroja-Fernandez et al., 2003; Baroja-Fernandez et al., 2004; Munoz et al., 2005; Baroja-Fernandez et al., 2009). This alternative model calls into question our fundamental understanding of starch synthesis, but critics have pointed out several inconsistencies with experimental data and the model remains highly controversial. The conflicting theories will be discussed in more detail in chapter 5.

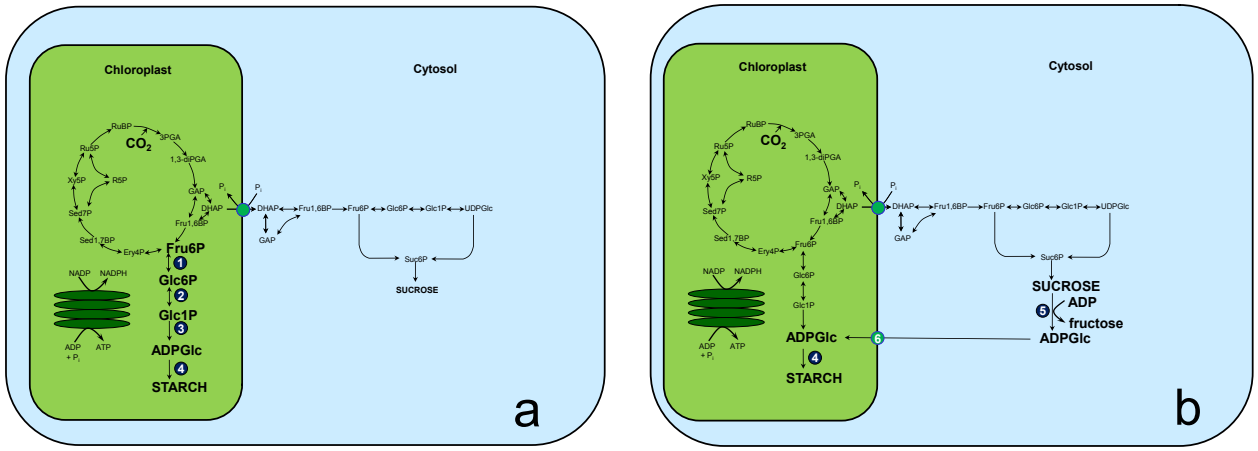

Figure 1-8: The two alternative models for starch synthesis in plant mesophyll cells

(a) The classical or textbook pathway. Fru6P derived from the Calvin-Benson cycle is converted to Glc6P, and then to Glc1P that is used to produce ADPGlc, the direct precursor for starch. (b) The alternative theory in which the synthesis of starch involves reactions outside the chloroplast. ADPGlc, the precursor of starch is proposed to be synthesized in the cytosol by the action of sucrose synthase, using ADP as a substrate for sucrose cleavage. The ADPGlc is then imported into the chloroplast via a putative adenylate transporter. The reactions are catalyzed by the following enzymes: (1) plastidic phosphoglucoisomerase; (2) plastidic phosphoglucomutase; (3) ADPglucose pyrophosphorylase; (4) starch synthase; (5) sucrose synthase; (6) BRITTLE1 like transporter.

1.4.2.2 Sucrose synthesis during the day

Sucrose is a non reducing disaccharide that consists of glucose and fructose moieties, which are linked via an α,β(1-2) glycosidic bond. During the day sucrose is synthesized in the cytosol from the triose-phosphates produced by carbon fixation via the Calvin-Benson cycle in the chloroplast. Triose-phosphates are exported from the chloroplast in exchange for orthophosphate via the triose-phosphate/phosphate translocator. In the cytosol the triose-phosphates, dihydroxyacetone phosphate (DHAP) and GAP, are kept close to equilibrium by the action of the cytosolic triose-phosphate isomerase (TPI). Aldolase uses DHAP and GAP to form fructose-1,6-bisphosphate (Fru1,6BP) via an aldol condensation. The cytosolic fructose-1,6-bisphosphatase (cFru1,6BPase) dephosphorylates Fru1,6BP to form Fru6P, which is first converted to Glc6P by cytosolic PGI and then to Glc1P by PGM. Following these reactions Glc1P and uridine triphosphate (UTP) are used to make uridine diphospho-glucose (UDPGlc) by the action of UDPGlc pyrophosphorylase (UGPase). In the cytosol Fru6P and UDPGlc are used as substrates by sucrose-phosphate synthase (SPS) to form sucrose 6´-phosphate (Suc6P). In a subsequent step Suc6P is dephosphorylated by sucrose-phosphatase (SPP) to make sucrose. The dephosphorylation step is

irreversible and pulls the reversible reaction of SPS in the direction of sucrose synthesis (Lunn and ap Rees, 1990).

As we can see from this outline of the pathway, the pathways of sucrose and starch synthesis have several reactions in common, although these are catalysed by different isoforms and located in separate compartments.

1.4.2.3 The conversion of starch to sucrose at night

The transitory starch reserves in leaves are broken down at night to provide carbon for leaf respiration, and for sucrose synthesis and export. In the night sucrose is synthesized from the glucose and maltose released by starch degradation. First the macromolecular starch molecule has to be made accessible to the degrading enzymes by the combined action of α-glucan, water dikinase (GWD), phosphoglucan, water dikinase (PWD) and phosphoglucan phosphatase to open up the structure by addition of phosphate groups on the C_6 or C_3 positions of some of the glucose moieties. One route to break the starch down uses α-amylase to produce malto-oligosaccharides, which are further broken down by limit dextrinase and the plastidial disproportionating enzyme to produce glucose. Glucose can be exported from the chloroplast for respiration or sucrose synthesis in the cytosol. However, the more important route of starch breakdown in *A. thaliana* is catalyzed by β-amylases, which produce maltose that leaves the chloroplast via the specific maltose transporter MEX1 (Niittyla et al., 2004). In the cytosol, one of the glucose moieties is transferred to a heteroglycan by a cytosolic transglucosidase (DPE2) releasing the other as free glucose. The glucose is cleaved from the heteroglycan by cytosolic glucan phosphorylase to release Glc1P (see Fig. 1-7). Turnover of starch reserves ensures that sugars are available to the whole plant throughout the daily light-dark cycle (Zeeman et al., 2002; Smith et al., 2003; Smith et al., 2005; Zeeman et al., 2007).

1.4.2.4 Regulation of the starch-sucrose metabolic network

The pathways of sucrose and starch synthesis compete with each other as they both use the fixed carbon from the Calvin-Benson cycle. Therefore fluxes through these pathways need to be tightly regulated and coordinated. The enzymes PRK, NADP-GAPDH, Fru1,6BPase and Sed1,7BPase from the Calvin-Benson cycle and AGPase from starch synthesis are activated by thioredoxin in the light, but are inactive in the dark. Therefore starch synthesis does not occur during the night. Sucrose synthesis is regulated by a feed forward mechanism (see Fig. 1-9). Triose-phosphates

produced by the Calvin-Benson cycle are exported in exchange for inorganic phosphate; this exchange increases triose-phosphate levels in the cytosol but decreases the concentration of orthophosphate. These reciprocal changes differentially regulate the two activities of the bifunctional enzyme fructose-6-phosphate, 2-kinase/ fructose 2,6-bisphosphatase (F2KP), thereby decreasing the level of the signal metabolite fructose 2,6-bisphosphate (Fru2,6BP), which is a potent inhibitor of the cytosolic Fru1,6BPase. Decline of Fru2,6BP and synthesis of Fru1,6BP from triose-phosphates increase flux through the cytosolic Fru1,6BPase into hexose-phosphates (Stitt and Heldt, 1985; Stitt, 1987). The resulting increases in hexose-phosphate and UDPGlc levels then lead to activation of SPS by increased availability of the substrates, and the higher concentration of its allosteric activator Glc6P. This feed forward mechanism results in sucrose synthesis being activated rapidly once the supply of triose-phosphate from the Calvin-Benson cycle is sufficient to support end product synthesis and maintain the regeneration of RuBP.

In addition to these mechanisms, SPS is also regulated by reversible protein phosphorylation. It can be activated by light and osmotic stress via reversible phosphorylation at different sites (Toroser and Huber, 1997; Toroser et al., 1999), and is also modulated by14-3-3 protein binding (Toroser et al., 1998). In spinach, phosphorylation at position Ser158 leads to inactivation of the enzyme, while phosphorylation of Ser424 promotes activity of the enzyme (Huber and Huber, 1996). Phosphorylation of SPS is catalysed by the SNF1-related protein kinase (SNRK1) and by calcium-dependent protein kinases (CDPK) (Winter and Huber, 2000). The dephosphorylation is performed by protein phosphatase 2A (PP2A) (Siegl et al., 1990). Phosphorylation of SPS is likely to be especially important in the regulation of night-time sucrose synthesis from starch, which bypasses the cytosolic Fru1,6BPase and so is not regulated by Fru2,6BP.

Accumulation of sucrose leads to a feedback inhibition of SPS and SPP via mechanisms that are not well characterized, but may include changes in the phosphorylation status of SPS. Inhibition of SPS will lead to accumulation of Fru6P, which allosterically activates the kinase activity of the F2KP, and inhibits the phosphatase activity, increasing Fru2,6BP levels and causing inhibition of cFru1,6BPase. The coordinated inhibition of enzymes in the pathway decreases the release of orthophosphate in the cytosol, which restricts the export of triose-phosphates from the chloroplast via the triose-phosphate/phosphate antiporter. This has the consequence of lowering orthophosphate levels in the stroma, which leads to less ATP production and rising 3PGA levels

in the chloroplast. Higher 3PGA and lower P_i together act to activate AGPase, increasing the flux of carbon into starch synthesis (Stitt and Quick, 1989).

In recent years the metabolite trehalose 6-phosphate (Tre6P) has become the focus of intense research interest and has been implicated in regulation of photoassimilate partitioning. It is synthesized by trehalose 6-phosphate synthase (TPS), using Glc6P and UDPGlc as substrates, and dephosphorylated to trehalose by trehalose 6-phosphate phosphatase (TPP). Tre6P is most likely synthesized exclusively in the cytosol (Paul, 2007; Paul et al., 2008). An elevated level of sucrose leads to an increase in Tre6P levels and so it has been proposed to act as a signal of the sucrose status in the cytosol (Lunn et al., 2006). It has been reported that Tre6P promotes the redox activation of AGPase, leading to the suggestion that high sucrose levels would lead to increased Tre6P, which enters the chloroplast and acts as a feed forward activator of starch synthesis (Kolbe et al., 2005).

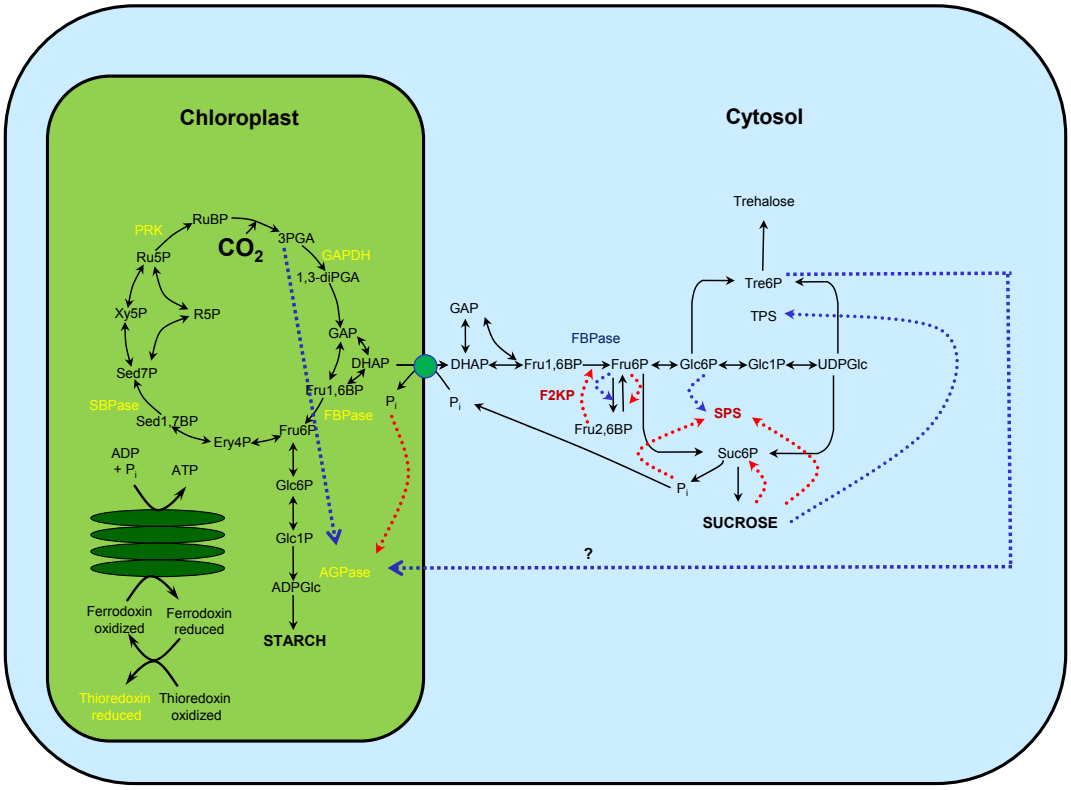

Figure 1-9: Coordinated regulation of photosynthetic CO_2 fixation and end product synthesis

The end products of carbon fixation are starch, which is stored in the chloroplast, and sucrose that is synthesized in the cytosol. The mechanisms that control this partitioning of carbon into the two main end products involve metabolites that work as regulators, and posttranslational modification of enzymes. Metabolite activation is shown with blue arrows, metabolite inhibition with red arrows. Proteins that are subjected to posttranslational redox modulation are shown in yellow and enzymes that are modified via protein phosphorylation are shown in red.

To study the networks and pathways I described above, it is necessary to elucidate the *in vivo* levels of metabolites and their compartmentation inside the cell, and relate these to enzyme activities in each compartment. To fully understand the interaction of metabolites with their respective enzymes it is not a suitable approach to isolate organelles from their cellular environment, because many metabolites of primary carbon metabolism have turnover times of less than a second (Arrivault et al., 2009). It is not possible to isolate organelles in such short time scales, and metabolite levels that are measured in organelles isolated by time consuming procedures are unlikely to reflect the *in vivo* situation. In the next section I will discuss some of the possible ways of measuring metabolites that reflect the *in vivo* situation.

1.5 Experimental systems to study compartmentation

Compartmentation has traditionally been studied by the use of sucrose or Percoll density gradients. These gradients enable the separation of different cell compartments. It is the most used system to determine the subcellular distribution of enzymes and pathways, and has been one of the foundations of plant biochemistry research. For this approach, cells are gently disrupted and the cell lysate is separated on density gradients of aqueous media. Then enzymes are measured in different fractions of the gradients and cross referenced against known marker enzymes for the various parts of the cell. If an enzyme co-localizes with a marker throughout the gradient it is considered to be localized in the same compartment. This system was used to separate plastids from spinach and pea leaves, and from castor bean endosperm (Miflin and Beevers, 1974). With different sucrose density gradients it was possible to separate Golgi apparatus, endoplasmic reticulum, mitochondria and microbodies from cell suspension cultures of soybean cells (Moore and Beevers, 1974), and to isolate amyloplasts from soybean suspension cultures (ap Rees and Macdonald, 1987). An improved isolation of plastids was achieved from protoplasts derived from castor bean endosperm (Nishimura and Beevers, 1978). This system was used to determine the cellular localisation of the sucrose synthesis pathway in the cytosol (Nishimura and Beevers, 1979). This finding was verified in wheat protoplasts (Robinson and Walker, 1979c). The disadvantage of sucrose density gradients and protoplast isolation from plant cells is that these are rather slow processes (1-3 h). Enzymatic reactions will continue during the separation procedure, and while this might not have a significant impact on the enzyme levels or their distribution, it will certainly lead to a very different picture at the

metabolite level, since the turnover times of many metabolites can be as short as fractions of a second (Arrivault et al., 2009).

Several other techniques have been used to determine the subcellular localization of enzymes. Immunohistochemistry uses specific antibodies that are labelled with specific markers (fluorescent, heavy atom, enzymatic) to visualize their binding to the protein of interest. Tissue sections are incubated with the antibodies, and their binding can be visualized by light or electron microscopes (Tobin and Yamaya, 2001). The main advantage of this method is the possibility to determine the localization of proteins that cannot be measured enzymatically, such as channels or structural proteins. The disadvantages of the method are potential cross reactions of the antibodies with other proteins, and antibodies are usually unable to distinguish between active and inactive forms of their target enzymes.

Cell compartmentation techniques such as sucrose density gradients have been combined with comprehensive proteomic analysis techniques using protein mass spectrometry. Although many proteins of the proteome of *A. thaliana* have been assigned to certain compartments by this technique, the intracellular locations of the majority of proteins, especially low abundance proteins, have still not been experimentally determined (Wienkoop et al., 2010). The power of this method lies in its broad coverage of proteins, which is independent of the availability of specific assays or antibodies that limit the other approaches. However, like immunohistochemical methods, this approach also has the disadvantage of not being able to discriminate between active and inactive forms of enzymes. Nonetheless it can help to assign functions to proteins of previously unknown function based on their localization. A good overview of the different subcellular proteome databases of *A. thaliana* has been published (Lilley and Dupree, 2007).

A more targeted approach is the labelling of a protein of interest with a fluorescent tag, e.g. green fluorescent protein (GFP). This enables the visualisation of the protein of interest *in vivo* with a fluorescence microscope (Tian et al., 2004). If the tagged protein is expressed under the control of its native promoter, this technique can provide information about both the inter- and intracellular distribution of the protein. A downside of the method is the potential mistargeting of the protein of interest inside the cell due to the attachment of the fluorescent protein, or artifactual compartmentation due to overloading of intracellular targeting mechanisms or disruption of

protein complexes that are necessary for correct targeting, especially if strong, constitutive promoters are used to drive expression of the tagged protein (Lunn, 2007).

Such techniques have provided much of our knowledge of enzyme compartmentation, but are not suitable for measurement of metabolites because of the long time it takes to prepare the samples compared to the relatively short turnover times of many metabolites. To overcome this limitation a number of different techniques have been developed for analysing compartmentation of metabolites, and these will be described in the following section.

1.5.1 Rapid fractionation of protoplasts

In 1979 a method was established to separate chloroplasts from the cytosol of protoplasts from wheat leaf cells in a very fast manner (Robinson and Walker, 1979b). Later the technique was extended to separate mitochondria as well (Lilley et al., 1982). The system was then used to measure adenine nucleotide levels in the cytosol, chloroplasts and mitochondria (Stitt et al., 1982). The method uses a syringe fitted with nylon nets of different mesh sizes to disrupt the protoplasts and differentially filter out smaller or larger organelles, all within about 0.1 second. Selective retention of chloroplasts alone or chloroplasts and mitochondria, depending on the pore size of the filters, yields extracts that are enriched in cytosol plus mitochondria or cytosol alone. Half of the filtrate is used to measure marker enzymes, while the other half is quenched immediately with $HClO_4$ to stop metabolism and allow measurement of metabolites. The amounts in each extract are compared with those in unfractionated protoplast extracts, to calculate the amounts of metabolites in each of the three major compartments – cytosol, mitochondria and chloroplasts.

Although the method has the advantage of very fast quenching of metabolism and therefore is suitable for measurement of *in vivo* levels of metabolites it has two big disadvantages. First the levels of metabolites in chloroplasts and mitochondria can only be calculated indirectly by subtraction from the cytosol, and are therefore rather sensitive to cross contamination, and the cytosolic fraction in reality contains the contents of other organelles, such as the vacuole. Secondly the method requires the preparation of protoplasts, which are disconnected from other cells, unlike the cells in their original tissue or organ, and this is likely to perturb their metabolism. Any results obtained from protoplasts must therefore be extrapolated to whole plants with caution.

1.5.2 *In vivo* Nuclear Magnetic Resonance Spectroscopy

Nuclear magnetic resonance (NMR) spectroscopy is a well established analytical technique for investigation of plant metabolism (Bligny and Douce, 2001; Ratcliffe and Shachar-Hill, 2005). Although it is usually applied to extracts of plant tissue (Krishnan et al., 2005), there are a few examples were NMR imaging has been used to investigate metabolism *in vivo*. For example, it has been used to detect the regulation of the pH and energy charge in the cytosol and vacuole of sycamore cells (Gout et al., 1992). It can also be used to detect metabolites such as sucrose or amino acids and to investigate their behaviour in living cells (Kockenberger, 2001). Using the combined analytical methods of GC-MS and NMR it was possible to measure *in vivo* activities of malic enzyme and pyruvate kinase in maize root tips during hypoxia (Edwards et al., 1998).

The relatively low sensitivity of *in vivo* NMR means that this method is only suitable for metabolites that have at least a millimolar concentration in plants, and therefore its application is restricted to very abundant metabolites. The air spaces in plant tissue can also disturb the measurements, and it can be difficult to maintain adequate oxygen supplies to the tissue under investigation. Due to these technical problems the method has so far had only limited application in plants.

1.5.3 Metabolite imaging

Förster resonance energy transfer (FRET) nanosensors, also commonly known as fluorescence resonance energy transfer nanosensors, are molecules containing two chromophores that display altered fluorescence properties upon binding of specific ligands. Several protein-based FRET nanosensors have been developed for *in vivo* visualisation of metabolites. One of the first applications was the Cameleon sensor used to monitor changes in Ca^{2+} levels in human Hela cells. The Cameleons consist of two different fluorescent proteins linked to the Ca^{2+}-binding protein calmodulin. When Ca^{2+} is bound to the calmodulin moiety, a conformational change brings the two fluorescent proteins closer together and so increases the FRET between them, which can be observed as a change in fluorescence output (Miyawaki et al., 1997). One of the most attractive features of this method is that it is possible to follow changes in metabolite concentrations at subcellular resolution in real time (Looger et al., 2005). The introduction of specific FRET nanosensors into living cells is achieved by transfection or transformation with DNA encoding the sensor protein so it is expressed within the cell. Specific cell signalling

sequences can be included to target the protein to the location of interest. Several other nanosensors, based on bacterial proteins, have now been developed to measure metabolites such as glucose or sucrose (Niittylae T, 2009). The method has also been successfully applied to monitor redox changes at subcellular levels (Yano et al., 2010). In plants FRET-based metabolite imaging has been used to measure the *in vivo* concentration of glucose in roots and leaves of *A. thaliana* (Deuschle et al., 2006).

Metabolite imaging with the help of FRET nanosensors is a very elegant method to measure metabolites because the measurement takes place in a living cell, and dynamics can be monitored directly. Nonetheless it can only monitor a very limited number of metabolites, as specific nanosensors need to be developed for each metabolite. Secondly transfection or transformation is required for their expression within the cell. Thirdly the behaviour of the nanosensor can change due to variation in the pH or ionic composition in different compartments, so it can be difficult to determine absolute rather than relative changes in metabolite concentrations. The sensitivity can also be an issue with this technique because no signal will be detectable if the nanosensor is expressed at too low levels, but if the nanosensor is too highly expressed it can lead to significant sequestration of the metabolite. At present it is only possible to visualize one metabolite at a time, which can be a powerful tool to address specific questions concerning a single metabolite, but provides only limited information insight into wider changes within complex metabolic networks.

An alternative to FRET nanosensors is Imaging Matrix Assisted Laser Desorption Ionization Mass Spectrometry, which has been applied to cryosections of tissues to visualize uneven distributions of amino acids, sugars and phosphorylated compounds. By recording the mass spectrum at each position of the tissue a two-dimensional image of the metabolic profile can be obtained. This has been successfully applied to developing wheat grains (Burrell et al., 2007). There is potential for this technique to resolve subcellular distribution of metabolites if technical advances improve the sensitivity and resolution of the mass spectrometers.

1.5.4 Non-aqueous fractionation

The first application of the separation of organelles in a non-aqueous medium was the determination of the ATP/ADP ratio in rat liver cells (Elbers et al., 1974). In this technique, the tissue is lyophilized to remove water and arrest metabolism, then fractionated in gradients of anhydrous organic solvents, where metabolism remains in stasis. Non-aqueous fractionation

(NAF) was first applied to plants in 1984, being used to elucidate the regulation of sucrose synthesis in spinach leaves (Gerhardt and Heldt, 1984; Gerhardt et al., 1987) and the role of pyrophosphate in plant metabolism (Weiner et al., 1987). Wider analyses of metabolite distributions including amino acids were later carried out in spinach (Riens et al., 1991) and maize leaves (Weiner and Heldt, 1992). The distribution of cell types and subcellular volumes in barley and spinach leaves has been estimated by electron microscopy of serial sections. This information was combined with NAF data to estimate the *in vivo* concentrations of metabolites in different compartments (Winter et al., 1993, 1994). The volumes of the different compartments have also been determined in wheat leaves (Bowsher and Tobin, 2001). The NAF method has also been applied to non-photosynthetic organs including potato tubers (Farre et al., 2001), and more recently to the model plant *A. thaliana* (Krueger et al., 2009). The NAF protocol is described in detail in chapters 2 (2.4 Non-aqueous fractionation) and 3 (3.1 Technical improvement of non-aqueous fractionation), and the basic workflow is shown in Fig. 1-10.

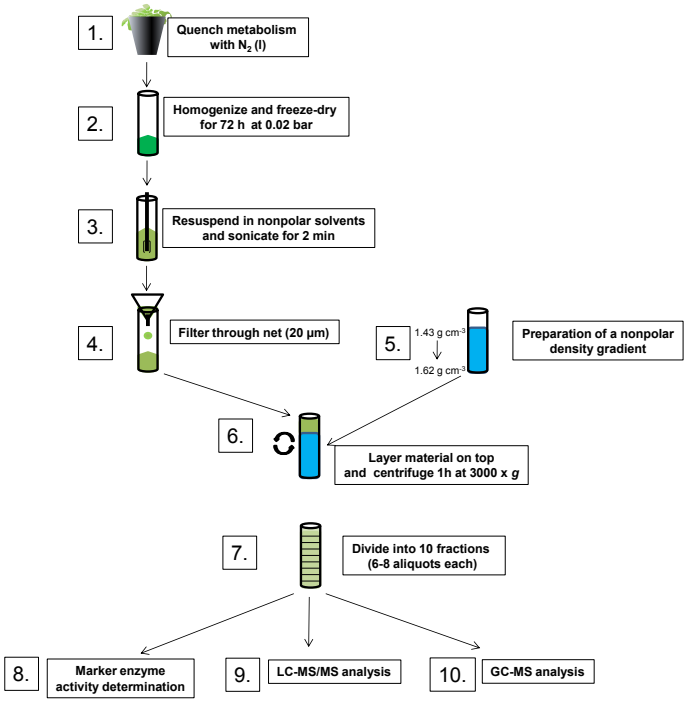

Figure 1-10: Overview of the workflow for non-aqueous fractionation

The plant tissue is quenched in liquid nitrogen to rapidly arrest metabolism. Afterwards the material is homogenized, freeze-dried, resuspended in nonpolar solvents and then the cells are broken up further by sonication. After filtration, any remaining intact cells and tissues are separated from the broken cells. The broken cell material is then layered on to a nonpolar density gradient, and after centrifugation ten fractions are taken starting from the top. These fractions are then used to measure the distribution of marker enzymes and the distribution of metabolites measured by several analytical platforms. On the basis of the marker enzyme distributions, the percentages of each metabolite in the chloroplast, cytosol and vacuole can be calculated.

NAF offers a number of advantages over the other methods for investigating metabolite compartmentation. It does not require preparation of protoplasts and can be used for whole plants or tissues harvested under normal growth conditions. The method can be applied to any genotype (wild type, mutants or transgenics) and many species, as there is no need for transformation. It has the potential to allow measurement of many metabolites, even low abundance metabolites, and so is more sensitive than some of the other methods, especially NMR. NAF also does not need expensive specialised equipment for the basic procedure. Table 1-2 summarises the advantages and disadvantages of these techniques, which will be discussed in more detail in chapter 3.1.

Table 1-2: Comparison of the methods used for metabolite compartmentation analysis

Method	**Applicability**	**Sensitivity**	**Requires specialised equipment**	**Metabolites analysed**
Protoplasts	non-physiological	high	no	many
In vivo NMR	limited to non-physiological conditions (dark)	low	yes[a]	few
FRET	transformable species only	high	yes[b]	one/few
Non-aqueous fractionation	general	high	no	many

[a] NMR spectrometer; [b] laser confocal microscope

1.6 Aim of the thesis

Photosynthetic CO_2 fixation is the basis for almost all life on earth. In plants, CO_2 fixation is tightly coordinated with sucrose and starch metabolism, and collectively these processes have a major influence on plant growth and productivity. These pathways form a very complex metabolic network that involves different compartments of the cell: chloroplasts, cytosol, mitochondria, peroxisomes and the vacuole. This network has been intensively studied, but many aspects are still poorly understood and even the basic pathway of starch synthesis has recently been called into question. Our knowledge of the compartmentation of the intermediate metabolites from these pathways is very limited. Improved knowledge of the interconnection and control of the reactions will help to advance our understanding of photosynthetic metabolism. Therefore, it is not only of general interest to understand plant photosynthetic metabolism in

greater depth but there is also potential to apply this knowledge in plant breeding to improve crop productivity.

The general aim of the work presented in this thesis is to achieve a detailed understanding of plant photosynthetic metabolism and how this metabolic network is controlled. More specifically this thesis addresses the following questions:

- What are the concentrations of primary carbon metabolites in the subcellular compartments in *A. thaliana*?
- How do the levels of metabolites compare with the kinetic properties of the enzymes in the pathway, and what does this tell us about regulation of individual steps and control of the network as a whole?
- What is the subcellular distribution of ADPGlc, and can this resolve the dispute about the source of ADPGlc in the pathway of starch synthesis?
- What is the subcellular distribution of Tre6P, and is this consistent with its proposed role as an intermediary in sugar signalling between cytosol and chloroplast?

The non-aqueous fractionation technique was applied to rosettes of *Arabidopsis thaliana* leaves to address these questions. The possibility of applying this technique to the unicellular alga *Chlamydomonas reinhardtii* was also investigated. The information obtained from these investigations gives us new insights into the regulation and control of the biochemical networks of photosynthetic CO_2 fixation and end product synthesis.

Chapter 2: Material and Methods

2.1 Plant material, growth and harvest

Arabidopsis thaliana [L.] Heyn. accession Columbia-0 (wild type Col-0) seeds were obtained from general stocks (MPIMP). The plastidial *pgm* and *adg1* mutants in the Col-0 background were derived from Caspar et al. (1985) and Lin et al. (1988).

Arabidopsis thaliana plants were grown in soil under the following conditions. Seeds were initially germinated on standard greenhouse soil (StenderAG, Schermbeck, Germany) in a 16 h/8 h day/night cycle (20 °C /6 °C) with 75 % relative humidity and 250 µmol quanta m^{-2} s^{-1} irradiance. After one week, plants were transferred into an 8 h/16 h day/night cycle (20 °C /18 °C), with 150 µmol quanta m^{-2} s^{-1} irradiance and a relative humidity of 60 %/75 % for day/night. After a further week (14 d post germination), individual plants were pricked out into individual 6-cm diameter pots (volume 100 cm^3) with the soil surface covered by a water-permeable black membrane. The pots were enclosed in a plastic tray covered with a transparent lid to maintain high humidity, and plants were grown for another 7 d in the short day conditions. At 21 d after germination, the lids were removed and the plants were transferred to a 12 h/12 h light/dark regime (with 150 µmol quanta m^{-2} s^{-1} irradiance and 80 % constant relative humidity and 22 °C). Plants (whole rosettes) were harvested 35- 40 d after germination, equivalent to 14 - 19 d after transfer to the 12 h/12 h light/dark regime. The harvest was performed by pouring liquid nitrogen directly over the plant rosette. For this 5 - 6 plants were placed in the front of the growth chamber, the door of the chamber was opened and liquid nitrogen was poured carefully from the top, trying to avoid any shading. After the leaves were completely frozen they were pooled and ground to a fine powder at liquid nitrogen temperature using a pestle and mortar. Frozen plant material was stored at -80 °C until analysis.

2.2 Algal material, growth and harvest

Chlamydomonas reinhardtii CC1690 cells were grown in a TAP-medium (May et al., 2008), without acetate to ensure photoautotrophic growth, in 5-L fermenters (Sartorius Stedim, Melsungen, Germany) in continuous light. The irradiance was 200 µmol quanta m^{-2} s^{-1} and the temperature was 24 °C. The cell cultures were constantly stirred and bubbled with air containing 5 % (v/v) CO_2. The culture was kept in mid logarithmic growth phase and with cell density set to

4 x 10^6 cells/ml. The cell density was kept constant in an automated way by using a turbidometer to measure the optical density between 840 and 910 nm ($OD_{840-910}$) of the culture. If the $OD_{840-910}$ increased due to cell division the system automatically pumped out culture and replaced it with fresh medium to maintain a constant $OD_{840-910}$. For the harvesting of the cells, 5-10 ml of cell culture were removed via a valve at the bottom of the fermenter, and the cells were collected by centrifugation at 4000 x *g* for 5 min at 22 °C. The supernatant was discarded and the pelleted cells were frozen in liquid nitrogen and stored at -80 °C until further use.

2.3 Reagents

Biochemicals, enzymes and other special reagents were obtained from Sigma (Taufkirchen, Germany), Roche (Mannheim, Germany), Merck (Darmstadt, Germany) and Carl Roth (Karlsruhe, Germany). All other chemicals were of analytical grade. All solutions were prepared with purified deionized water (PureLab plus, ELGA LabWater, Celle, Germany). Anhydrous solvents for non-aqueous fractionation were stored with molecular sieve (3 Å, Carl Roth).

2.4 Non-aqueous fractionation (NAF)

A. thaliana and *C. reinhardtii* cell components were separated by a modification of the non-aqueous-fractionation (NAF) technique described by Gerhardt and Heldt (1984) for analysis of spinach leaves. This technique allows fractionation of the plant material while metabolism is held in stasis. In brief, the plant tissue is freeze dried, suspended in an anhydrous organic solvent and fractionated by density gradient centrifugation in a mixture of anhydrous organic solvents. The gradient is separated into various fractions that are enriched in different subcellular compartments, and analysed for the distribution of compartment-specific marker enzymes and metabolites. Details of the protocols used for non-aqueous fractionation of *A. thaliana* and *C. reinhardtii* cells are described below.

2.4.1 Non-aqueous fractionation of *Arabidopsis thaliana leaves*

Frozen *A. thaliana* leaf powder (4-6 g of fresh weight) material was freeze dried in a Christ Alpha 2-4 lyophilizer at a negative pressure of 0.325 mbar for at least 96 h yielding 400-600 mg of dry weight. The lyophilized powder was suspended in 20 ml of anhydrous tetrachlorethylene:heptane (66:34 v/v, density 1.2 g cm^{-3}) and dispersed by 2 min sonication at 85 % power, in bursts of 5 s with a 5 s pause between each burst using a Bandelin Sonopuls HD2070 sonicator fitted with a Bandelin UW 2070 probe (Bandelin, Berlin). Afterwards the material was

filtered through a nylon net (HEIDLAND GmbH & Co. KG, Harsewinkel) with a mesh width of 20 µm to remove any remaining large tissue particles. The net was weighed before and after filtration (after drying) to determine the amount of plant material retained. The material was suspended in 30 ml of heptane and centrifuged at 4000 x *g* for 10 min at 25°C. The pellet was resuspended in 5 ml of solution A (66:34 v/v tetrachloroethylene/heptane, density 1.2 g cm^{-3}) and carefully layered onto a 27-ml gradient (density range: 1.43 g/cm^3 to 1.62 g/cm^3) in a 35 ml polyallomer tube (Eppendorf, Hamburg). The gradient was made by mixing 12 ml of solution A and 15 ml of tetrachlorethylene using an Econo gradient pump Kit 2 (Bio-Rad, Munich) at a flow rate of 1.15 ml min^{-1}. The density range was linear from 1.43 g cm^{-3} to 1.62 g cm^{-3}. The gradient was centrifuged at 2240 x *g* for 1 h at 25 °C in a Beckman SW 32-Ti spin-out rotor using a Beckman Coulter Optima L-80XP ultracentrifuge. After centrifugation 10 fractions of 3.1 ml were taken from the top of the gradients and diluted 3-fold with heptane. After centrifugation at 4000 x *g* for 10 min at 25°C the supernatant was discarded and the remaining pellet was resuspended in 4-8 ml of solution A (volume dependent on the amount of dry material applied to the gradient). The suspension was divided into 1-ml aliquots. The aliquots were centrifuged at 25,000 x *g* for 10 min at 25 °C in an Eppendorf 5417R table centrifuge with an Eppendorf FA45-24-11 rotor. The supernatant was discarded and the remaining pellet was dried in a vacuum dessicator for 12 h. The dried pellets were stored in a Bohlender STAR desiccating cabinet at a humidity of less than 20 % until further analysis. Aliquots of each fraction and of the unfractionated starting material were extracted for measurement of marker enzymes for chloroplasts (phosphoribulokinase, transketolase), cytosol (phosphoenolpyruvate carboxylase, UDP-glucose pyrophosphorylase) and vacuole (α-glucosidase, acid invertase), and metabolites as described below. The distribution of each metabolite between the three compartments was calculated using the BESTFIT ANALYSIS software developed by Dr. Dirk Steinhauser and Dr. Dirk Büssis (MPIMP). This software uses n-component regression analysis to fit the distribution to 2- (chloroplast and cytosol) or 3-compartment (chloroplast, cytosol and vacuole) models.

2.4.2 Non-aqueous fractionation of *Chlamydomonas reinhardtii*

Chlamydomonas reinhardtii cells were collected from 50 ml of cell culture (density: 3-5 x 10^6 cells ml^{-1}), and freeze dried in a Christ Alpha 2-4 lyophilizer at a negative pressure of 0.325 mbar for at least 120 h. The cells were fractionated under non-aqueous conditions as described above except for the following modifications. Sonication was applied for 2 and 10 min at 85 % power,

in 5 s bursts with a 5 s pause between bursts. After filtration through a 20 µm nylon net to remove unbroken cells, the cell suspension was diluted with 30 ml of anhydrous heptane and centrifuged at 4000 x *g* for 10 min. The supernatant was discarded and the pellet was resuspended in 5 ml of solution A (66:34 v/v tetrachloroethylene/heptane, density 1.2 g/cm^3) and carefully layered onto a 27-ml gradient (see results for details) in a 35-ml polyallomer tube (Eppendorf, Hamburg). Gradients were centrifuged at 2240 x *g* for 1 h at 25 °C and 8960 x *g* for 4 h at 25 °C. After centrifugation, the gradient was divided into ten 3.1-ml fractions, and the cell material was collected by centrifugation, dried under vacuum and stored in a desiccating chamber as described above.

2.5 Metabolite extraction and measurement

For the determination of soluble sugars, starch and protein, aliquots from the NAF procedure were extracted with first 250 µl and then 150 µl of 80 % (v/v) ethanol and once with 250 µl of 50 % (v/v) ethanol. The extracts were pooled to give a total volume of 650 µl, and used for sugar determination (Geigenberger et al., 1996). The remaining insoluble residue was used for protein and starch measurements.

Protein content was determined by a modification of the dye-binding method (Bradford, 1976). The insoluble residue from the ethanolic extraction was heated at 95 °C with 400 µl of 0.1 M NaOH for 30 min to solubilise the protein. The protein content was measured using the Bio-Rad Bradford reagent (Bio-Rad, Munich) according to the manufacturer's instructions. The standards were 0, 250, 500 and 1000 µg ml^{-1} bovum serum albumin in 0.1 M NaOH.

Starch content was measured in the NaOH treated residue from the protein measurement. Samples (390 µl) were acidified to pH 4.9 with 80 µl of 0.5 M HCl/0.1 M sodium-acetate (pH 4.9). Aliquots of the suspension (40 µl) were digested overnight with 70 units amyloglucosidase and 10 units α-amylase in 160 µl of 50 mM acetate/NaOH buffer pH 4.9 at 37 °C. After centrifugation the glucose content of the supernatant was measured enzymatically, and starch content was calculated as µmol glucose residues g^{-1} FW (Hendriks et al., 2003).

Sugar content (sucrose, glucose and fructose) was determined enzymatically in ethanolic extracts as described before (Geigenberger et al., 1996).

2.5.1 Sugar phosphates, nucleotides and organic acids

Samples were extracted with chloroform/methanol as described in Arrivault et al. (2009) except that after the first extraction step with chloroform/methanol two steel ball bearings (2 mm diameter) were added to the Eppendorf tube and resuspension of the dried pellet was enhanced by shaking at 30 Hz for 2 min in a ball mill (Retsch MM300). In addition, the chloroform phase was washed three times with 400 µl water to increase the extraction of the metabolites into the aqueous methanol phase.

Glutamate, aspartate, glycerate, Glc6P, Fru6P, Glc1P, malate, succinate, shikimate, citrate, isocitrate, aconitate, 2-oxoglutarate, R5P, Sed1,7BP, Sed7P, Xu5P + Ru5P, DHAP, NAD, AMP, UDPG, ADPG, Fru1,6BP, RuBP, NADP and ADP were measured by ion pair chromatography – triple quadrupole MS (IPC-MS/MS) using a Dionex HPLC system (Dionex GmbH, Idstein) coupled to a Finnigan TSQ Quantum Discovery MS-Q3 (Thermo Scientific, Dreieich) equipped with an electrospray (ESI) interface (Arrivault et al., 2009). The MS was operated in negative ion mode with selected reaction monitoring (SRM), using an ion spray voltage of 4000 V and a capillary temperature of -230 °C. The Finnigan XCALIBUR 1.4 software (Thermo Scientific) was used for both instrument control and data acquisition. The major MS/MS fragment patterns of each analyte were determined by direct infusion of the standards dissolved in water (final concentration 3 mM) at a flow rate of 5 µl min^{-1}. Aliquots of undiluted and 1/10 diluted extracts were analyzed to measure low- and high-abundance metabolites, in each sample. Chromatographic separation was performed by passing aliquots through a Gemini (C18) 4 x 2.00 mm pre-column (Phenomenex, Aschaffenburg), before separation on a Gemini (C18) 150 x 2.00 mm inner diameter, 5 µm 110 Å particle column (Phenomenex, Aschaffenburg) at 35 °C. Metabolites were quantified by comparison of the integrated MS-Q3 signal peak area with a calibration curve obtained using authentic standards.

Tre6P, Suc6P, fumarate, PEP, 3PGA and glycerol 3-P (G3P) were measured by anion exchange chromatography – triple quadrupole (Q3) MS (AEC-MS/MS) as described previously (Lunn et al., 2006), using a Dionex HPLC system (Sunnyvale, CA, U.S.A.), coupled to an Applied Biosystems Q-Trap 5500 apparatus (Applied Biosystems, Darmstadt). Aliquots (100 µl) of the extract were passed through a 2 × 50 mm AG11-HC pre-column (Dionex), before separation of anionic compounds on a 2 × 250 mm IonPac AS11-HC column (Dionex) at 25 °C.

2.5.2 Amino acids, trehalose, maltose and inositol

The dried pellet from the NAF samples was extracted with 1.4 ml of methanol by shaking in a ball mill (Retsch MM300) at 30 Hz for 2 min. GC-MS analysis was performed as described by Lisec et al. (2006) with online derivitization with methoxyaminhydro chloride and N-methyl-N-(trimethylsilyl)trifluoroacetamide using a 6890N gas chromatograph (Agilent, Böblingen) coupled to a Pegasus III time-of-flight mass spectrometer (Leco Instruments, Mönchengladbach).

2.6 Extraction of enzymes and activity determination

Extractions for enzyme measurements were performed as described by Gibon *et al* (2004b). To ensure efficient extraction, after addition of 500 µl extraction buffer to the dried pellet from the NAF samples, two or three steel ball bearings (2 mm diameter) were added and the sample tube was agitated at 30 Hz for 2 min in a ball mill (Retsch MM300). Preliminary experiments were performed to optimize the assay conditions for each marker enzyme. The marker enzymes were measured as follows.

Phosphoribulokinase activity was measured as the ribulose-5-phosphate (Ru5P) dependent production of ADP from ATP. ADP production was determined spectrophotometrically by coupling to oxidation of NADH using pyruvate kinase and lactate dehydogenase. The reaction contained: 200 mM Tricine-KOH pH 8.0, 5 mM PEP, 3 mM NADH, 1 mM ATP, 100 µM Ru5P, 7 unit mL^{-1} pyruvate kinase, 10 unit mL^{-1} lactate dehydrogenase, 21 mM $MgCl_2$, 1 mM DTT and 5 µl of extract (diluted 1:5 after first extraction) in a final volume of 100 µl. The reaction was started by addition of extract and NADH oxidation was monitored continuously at 340 nm. The activity was determined from the difference in rate of change of absorbance in reactions containing Ru5P compared to blank reactions without Ru5P.

Transketolase activity was measured as the production of GAP from E4P and Xu5P. GAP was measured spectrophotometrically after conversion to G3P via triosephosphate isomerase and glycerol-3P dehydrogenase. An aliquot (2 µl) of the undiluted extract was incubated in a reaction mixture containing: 50 mM Hepes/KOH, pH 7.7, 10 mM $MgCl_2$, 0.8 mM NADH, 1.25 mM thiamine pyrophosphate, 1 unit mL^{-1} TPI, and 1 unit mL^{-1} G3P dehydrogenase, in a total volume of 20 µl, for 20 min at 25 °C. The reaction was started by the addition of E4P and Xu5P to a final

concentration of 2.5 mM and 10 mM. Blank reactions contained no Xu5P or E4P. The reaction was stopped by addition of 20 µL of 0.5 M HCl. G3P was measured in the presence of 1.8 units mL^{-1} glycerol-3-P oxidase, 0.7 unit mL^{-1} glycerol-3-P dehydrogenase, 1 mM NADH, 1.5 mM $MgCl_2$, and 100 mM Tricine/KOH, pH 8.0. The absorbance was read at 340 nm (30 °C). The activity was determined by the difference in rate of absorbance between the reaction containing E4P and Xu5P and the blank reactions without substrates.

UDP-glucose pyrophosphorylase was assayed in the reverse direction by measuring the PP_i-dependent production of UTP from UDP-glucose. An aliquot (2 µl) of the undiluted extract was incubated in a reaction mixture containing: 50 mM Hepes/KOH, pH 8.0, 5 mM $MgCl_2$, 1 unit mL^{-1} glycerokinase, 0 (blank) or 5 mM (maximal activity) UDP-glucose, 1.5 mM sodium fluoride, and 120 mM glycerol, in a total volume of 20 µl, for 20 min at 25 °C. The reaction was started by the addition of 2 µl of 20 mM $Na_4P_2O_7$ to give a final concentration of 2 mM. The reaction was stopped by addition of 20 µL of 0.5 M HCl. G3P was measured as described above. The activity was determined by the difference in rate of absorbance between the reaction containing UDP-glucose and the blank reactions without substrates.

Phosphoenolpyruvate carboxylase activity was assayed as the production of oxalacetate from PEP and bicarbonate. An aliquot (2 µl) of the undiluted extract was incubated in a reaction mixture containing: 100 mM Tricine/KOH, pH 8.0, 20 mM $MgCl_2$, 1 unit mL^{-1} malate dehydrogenase, 10 mM $NaHCO_3$, and 0.1 mM NADH, in a total volume of 20 µl, for 20 min at 25 °C. Contaminating NAD^+ was previously removed by preparing a 20 mM NADH stock solution in 100 mM NaOH and heating for 10 min at 95 °C before addition of the NADH to the PEPcarboxylase assay mixture. The reaction was started by the addition of PEP to a final concentration of 0 (blank) or 2 mM (maximal activity). The reaction was stopped by addition of 20 µL of 0.5 M HCl, and then heated at 95 °C for 10 min to destroy NADH. After cooling, 10 µL 1 M NaOH, and 10 µL of 0.2 M Tricine/KOH, pH 9.0, were added to adjust the pH to 9.0. NAD^+ was measured in the presence of 6 units mL^{-1} alcohol dehydrogenase, 100 mM Tricine/KOH, pH 9.0, 4 mM EDTA, 0.1 mM phenazine ethosulfate, 0.6 mM methylthiazolyldiphenyl-tetrazolium bromide, and 500 mM ethanol. The absorbance was monitored at 570 nm (30 °C). The activity was determined by the difference in rate of absorbance between the reaction containing PEP and the blank reactions without substrates.

α-Glucosidase activity was measured as the production of 4-methylumbelliferone from cleavage of 4-methylumbelliferyl-α-D-glucopyranoside. An aliquot (5 µl) of the undiluted extract was incubated in a reaction mixture containing: 100 mM citrate/KOH pH 4.5 and 500 µM 4-methylumbelliferyl-α- D-glucopyranoside, in a total volume of 50 µl, at 25 °C. The reaction was stopped by addition of 100 µl of 200 mM Na_2CO_3 after 0 or 20 min. 4-Methylumbelliferone production was measured fluorometrically with excitation at 360 nm and emission at 450nm (30 °C). The activity was determined by the difference in fluorescence between the reactions incubated for 0 and 20 min.

Acid invertase was assayed by measuring glucose and fructose released upon incubation with sucrose. An aliquot (5 µl) of the undiluted extract was incubated in a reaction mixture containing: 50 mM acetate/KOH pH 5.0 and 20 mM sucrose, in a total volume of 50 µl, at 25 °C. The reaction was stopped after 20 or 40 minutes by addition of 20 µl of 0.5 M NaOH. Glucose content was measured in the presence of 200 mM Hepes/KOH, pH 7.0, 3 mM ATP, 1.5 mM $NADP^+$, 90 unit mL^{-1} hexokinase, 6 unit mL^{-1} phosphoglucoisomerase and 1 unit mL^{-1} glucose-6-P dehydrogenase. The absorbance was read at 340 nm (30 °C). The activity was determined by the difference in absorbance between timepoint 20 and 40 min.

2.7 Protein profiling by mass spectrometry and data analysis

The protein pellets of the different fractions were resuspended in 150 µL of 6 M urea / 2 M thiourea (pH 8) for in-solution protease digestion. After reduction with 0.5 mM DTT, and alkylation of cysteine groups with 2.5 mM iodoacetamide, proteins were digested with endoproteinase LysC for 3 h. Subsequently, the solution was diluted fourfold with 10 mM Tris-HCl (pH 8) before digestion of the proteins with trypsin (0.4 µg trypsin / 50 µg target protein; modified sequencing grade, Roche) at room temperature overnight (Kierszniowska et al., 2009). The digested peptides were desalted with C18 STAGE-tips before mass spectrometric analysis (Rappsilber et al., 2003). The desalted peptides were eluted from the C18 stage tips with 50 µl 80 % (v/v) acetonitrile, 0.5 % (v/v) glacial acetic acid solution. These tryptic peptide mixtures were analyzed exactly as described in Kierszniowska et al. (2009) by LC-MS/MS using a nanoflow HPLC (Proxeon Biosystems, Denmark) and an Orbitrap hybrid mass spectrometer (LTQ-Orbitrap, Thermo Electron, USA), except that the linear gradient of 4 to 64 % acetonitrile was run in 40 min instead of 90 min.

Peptide fragments were identified by comparison against a non-redundant *A. thaliana* protein database (TAIR8, version 2008-04; 31921 entries; www.arabidopsis.org) using the MASCOT algorithm (version 2.2.0; Matrix Science, UK, www.matrixscience.com) as described by Kierszniowska et al. (2009). Abundance of proteins in the different fraction was normalized on total protein content in each fraction.

Chapter 3: Optimisation of non-aqueous fractionation of *Arabidopsis thaliana* leaves and *Chlamydomonas reinhardtii* cells

3.1 Introduction

In order to fully understand the control and regulation of a metabolic network it is necessary to have knowledge about the subcellular compartmentation of the intermediate metabolites within the network. This is especially important because these intermediates often strongly influence the activity of enzymes and thus fluxes through metabolic networks. *A. thaliana* is the model organism of choice for most basic research in plant science in the early 21st century, and therefore it is desirable to increase our knowledge about its biochemistry and not rely on extrapolation from earlier studies on other species.

Surprisingly little is known about the compartmentation of primary metabolism in *A. thaliana*. Until now most analyses in this species only described a very limited number of metabolites from photosynthetic carbon fixation. We have a more detailed understanding of the metabolic networks of carbon fixation and end product synthesis in other species that were previously used as model plants, for example, studies on isolated chloroplasts or protoplasts from spinach, wheat and maize (Lilley et al., 1977; Fliege et al., 1978; Flugge et al., 1980; Giersch et al., 1980; Heldt et al., 1980; Robinson and Walker, 1980; Wirtz et al., 1980; Stitt et al., 1982). However, preparation of protoplasts and isolation of chloroplasts disturbs the photosynthetic metabolism of the cell. Recently a paper was published that combines protoplast preparation (see chapter 1.5.1) and mass spectrometry to analyze the compartmentation of primary carbon metabolism in barley (Keerberg et al., 2011). Although this method has the advantage of using a homogeneous cell type, as with previous protoplast studies the metabolism of the cells is strongly altered in comparison to intact plant leaf tissue. Most other non-invasive methods such as NMR-analysis or metabolite imaging also have major drawbacks, such as low sensitivity or poor coverage of metabolites. Comparison of the various techniques that can be used to investigate the subcellular compartmentation of metabolites highlighted several advantages of the non-aqueous fractionation

(NAF) technique (see section 1.5 for details). In particular, it can be applied to whole leaves or other tissues from a wide range of species (Table 3-1) and the plant material can be harvested under ambient growth conditions. Therefore, this technique was adopted to investigate photosynthetic carbon metabolism in *A. thaliana* leaves and *C. reinhardtii* cells.

Table 3-1: Published applications of non-aqueous fractionation in different species and organs

Species	**Metabolites analysed**	**Comments**	**Reference**
Spinach leaves	sucrose, malate	Diurnal behaviour	(Gerhardt and Heldt, 1984)
Spinach leaves	Fru1,6BP, PGA, RuBP, DHAP, Glc6P, Fru6P, UDPGlc	Control of SPS	(Gerhardt et al., 1987)
Spinach leaves	pyrophosphate	Energy donor in cytosol	(Weiner et al., 1987)
Bean leaves	phosphate	Role in regulation of photosynthesis	(Sharkey and Vanderveer, 1989)
Spinach leaves	uridine nucleotides	partitioning pattern	(Dancer et al., 1990)
Maize leaves	triose-phosphates, amino acids, 3PGA, malate		(Weiner and Heldt, 1992)
Barley leaves	amino acids, sucrose		(Winter et al., 1992)
Pea leaves	amino acids	Concentrations calculated	(Winter et al., 1993)
Spinach leaves	amino acids, sucrose, malate, phosphorylated compounds	Concentrations calculated	(Winter et al., 1994)
Tobacco, snapdragon and parsley leaves	glucose, fructose, mannitol		(Moore et al., 1997)
Potato tubers	sugars, sugar alcohols, organic acids, ATP, amino acids, hexose phosphates	First example of non-photosynthetic tissue	(Farre et al., 2001)
Bean leaves	maltose	Major breakdown product of starch is maltose	(Weise et al., 2004)
Soybean leaves	sugars, amino acids, organic acids, fatty acids		(Benkeblia et al., 2007)
A. thaliana leaves	cysteine	Subcellular localisation of cysteine biosynthesis	(Krueger et al., 2009)
A. thaliana leaves	primary metabolites, lipids, secondary metabolites	Broad range of polar and lipophilic compounds	(Krueger et al., 2011)

The main goal of the work described in this chapter was to optimise and validate the NAF method for *A. thaliana*. Until now NAF has only been used with higher plants. Studies on unicellular organisms circumvent the problem of having different cell types and vascular tissue in higher plant leaves. Therefore the NAF protocol was also tested for its potential to investigate subcellular compartmentation in the unicellular alga *C. reinhardtii*.

3.2 Non-aqueous fractionation in *Chlamydomonas reinhardtii*

Preliminary experiments with *C. reinhardtii* cells revealed that the algal cells have a much lower density than leaf tissue (see Fig. 3-1). Sonicated *C. reinhardtii* cells were layered on top of a gradient with a density range between 1.42 and 1.63 g cm^{-3}. The fragmented cell particles appeared to be very light in comparison to higher plant material, as all of the algal cell material stayed on top of the gradient during the centrifugation. To evaluate whether this was due to insufficient centrifugation, the centrifugation step was extended from 1 h to 4 h and the centrifugal force was increased from 2240 x *g* to 8960 x *g*, but neither of these modifications led to any greater entry of cell material into the gradient. Therefore, it appeared that the centrifugation conditions were not limiting, and centrifugation at 2240 x *g* for 1 h was used for all further experiments. Since the *C. reinhardtii* material seemed to be lighter than the material from higher plants, the density range of the gradient was decreased from 1.42-1.63 g cm^{-3} to 1.11-1.32 g cm^{-3}, which led to accumulation of all the material in a pellet at the bottom of the gradient. From these two observations it can be concluded that the density of the *C. reinhardtii* material is between 1.32 and 1.42 g cm^{-3}. In order to test this hypothesis, gradients with a density range of 1.20 to 1.40 g cm^{-3} were used. This led to an enrichment of the material in the last three fractions at the bottom of the gradient (Fig. 3-1), which verified that the density of the algal material lies within this range. The Calvin-Benson cycle enzymes phosphoribulokinase (PRK) and transketolase (TK) were used as marker enzymes for the chloroplast, while UDPgluccose pyrophosphorylase (UGPase) and phosphoenolpyruvate carboxylase (PEPC) were used for the cytosol. The specific location of these enzymes in the respective compartments was supported by bioinformatic prediction (May et al., 2009). The vacuolar compartment was not taken into account because it is thought that *C. reinhardtii* uses its vacuole primarily for osmotic regulation, and that it has only limited metabolic activity. The vacuole is not used for storage of sugars, and *C. reinhardtii* appears to produce very little, if any, sucrose (Klein, 1987). Gradients with a density range between 1.30 and 1.40 g cm^{-3} were prepared and tested with lyophilized *C.*

reinhardtii material, but did not improve the separation of cell fragments. Attempts to decrease the density rage even further (1.35-1.40 g cm^{-3}) failed, because with such small density differences the gradients became unstable and the layers of different density became intermixed. To test if the sonication step was sufficient to break up the cells into particles of different density the sonication time was extended from 2 min to 10 min. Longer sonication times (20 min) led to a massive decrease in enzyme activity, most likely due to denaturation of protein structure because of heating during the sonication. *C. reinhardtii* material that was sonicated for either 2 or 10 min was centrifuged in gradients with a density range of 1.20-1.40 or 1.30-1.40 g cm^{-3} and marker enzyme activities were determined (see Fig. 3-1).

Figure 3-1 Marker enzyme distribution after non-aqueous fractionation of *C. reinhardtii* cells at different density ranges and sonication treatments *C. reinhardtii* cells were lyophilised, sonicated for 2 min (A + B) or 10 min (C), filtered and applied to gradients of tetrachlorethylene:heptane mixtures of different density (A) 1.2-1.4 g cm^{-3}; (B) 1.3-1.4 g cm^{-3}; (C) 1.3-1.4 g cm^{-3}. The plastidial markers phosphoribulokinase (PRK) and transketolase (TK) are shown in green; the cytosolic markers UDPglucose pyrophosphorylase (UGPase) and phosphoenolpyruvate carboxylase (PEPC) are shown in blue. No data are shown for fractions 1-5 from the upper half of the gradients as these did not contain any detectable cell material. Data are mean ± SD (n=3).

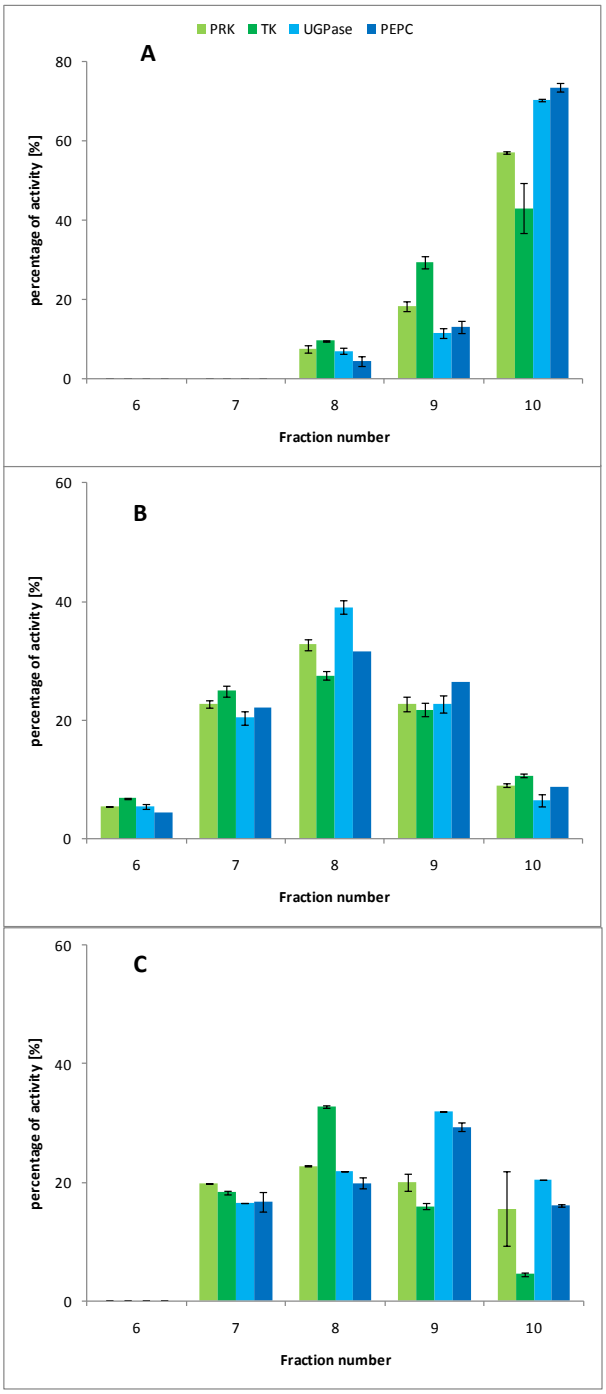

As can be seen from the different distribution profiles in figure 3-1, all of the *C. reinhardtii* cell material accumulated in the density region of approximately 1.35 to 1.40 g cm^{-3} at the bottom of the gradient, irrespective of the sonication treatment. Distribution profiles of the markers for chloroplast and cytosol did not show any distinct difference and thus were not separated from each other.

With the different tests applied to *C. reinhardtii* cells, I came to the conclusion that the general cell architecture of this unicellular alga is too different from higher plant cells to establish the NAF methodology for cell fractionation of this species. With the treatments performed it became apparent that the particles that are produced do not show enough differences in their density to separate them in the gradients, and so achieve enrichment of chloroplast and cytosol in different fractions. A test for improved separation by decreasing the difference in the density range of the gradient failed due to the instability of the gradients with such narrow density ranges.

3.3 Non-aqueous fractionation in *Arabidopsis thaliana*

The major goal for optimisation of the non-aqueous fractionation procedure with *A. thaliana* was to improve the separation of the three cell compartments, chloroplast, cytosol and vacuole, whose spatial separation was achieved in other species, and if possible to also resolve the mitochondria. A second major aim was to validate the procedure by systematically testing the stability of enzymes and different metabolite classes during the NAF treatment. Two main criteria were chosen to assess the success of the fractionation. First the chosen marker enzymes had to retain their activity after the fractionation procedure, and secondly the separation of these markers needed to be reproducible and large enough for mathematical analysis to be able to distinguish between the compartments. In order to improve the separation the volume of the gradient was increased and the density range was slightly extended compared to the experimental procedure used for analysis of spinach leaves (Gerhardt and Heldt, 1984). In earlier studies usually six fractions were analysed, while in this study 10 fractions were taken from the gradient to increase the resolution. Robotized enzyme assays were developed for all the marker enzymes, which increased the throughput and sensitivity of the measurements. Different marker enzymes were tested for loss of activity during the procedure by measuring recoveries of activity at each of the major steps. The chloroplast marker that was used in most previous studies, the $NADP^+$

dependent glyceraldehydes-3-phosphate dehydrogenase (NADP-GAPDH), showed more than 80 % loss of activity after the lyophilisation of leaf material and a further 60 % loss of activity after the NAF treatment. In contrast all of the other marker enzymes for chloroplasts (PRK and TK), cytosol (UGPase and PEPC) and vacuole (α-glucosidase and acid invertase) showed no or only moderate losses in activity during lyophilisation and NAF treatment. Recoveries of plastidial, cytosolic and vacuolar marker enzymes from the NAF gradients were typically between 75-120 %, which was considered to be an acceptable range. Gradients with lower or higher recoveries were discarded.

Table 3-2: Recovery of marker enzyme activities during the NAF procedure
A. thaliana Col-0 leaf material was lyophilized for 96 h and part of it was used for NAF. The first column shows the percentage of enzyme activity in lyophilised material compared with non-lyophilised material. The second column shows the sum of enzyme activities in all the gradient fractions expressed as a percentage of the corresponding activity in unfractionated lyophilized material. Values are mean ± SD from three independent gradients.

Marker enzyme	**Recovery of activity [%]**	
	Lyophilisation	**Non-aqueous fractionation**
Phosphoribulokinase	86.6 ± 3.8	109.8 ± 4.0
$NADP^+$ dependent GAP dehydrogenase	13.2 ± 1.9	38.8 ± 3.1
Transketolase	82.5 ± 3.1	97.5 ± 12.9
UDP-glucose pyrophosphorylase	81.3 ± 2.7	82.5 ± 6.7
Phosphoenolpyruvate carboxylase	78.8 ± 1.3	113.2 ± 2.5
α-glucosidase	96.5 ± 1.1	91.5 ± 5.4
Acid invertase	75.2 ± 6.9	81.1 ± 4.8

The markers that were used in this study showed good recoveries after lyophilisation and NAF treatment. Therefore, they are considered to be a robust measure for the fractionation of the different subcellular compartments: chloroplast, cytosol and vacuole.

Since it cannot be ruled out that a differential loss in individual fractions took place, it was decided not to use NADP-GAPDH as a plastidial marker. PEPC and UGPase were used as markers for the cytosol, while α-glucosidase and acid invertase were used as markers for the

vacuole. To minimise the effect of any technical variation in the assays of the marker enzymes the mean values of the two markers for each compartment were used for subsequent calculations. Figure 3-2 shows a typical gradient and the distribution of the marker enzymes.

Figure 3-2: Marker enzyme distribution of a typical *A. thaliana* Col-0 NAF gradient

Activity in each fraction is expressed as a percentage of the total activity of all ten fractions. Fraction number 1 contains very little cell material. The plastidial particles are enriched at the top of the gradient, while the vacuolar particles accumulate at the bottom. The cytosolic particles distribute more evenly throughout the gradient. Average values of the two plastidial markers PRK and TK, two cytosolic markers UGPase and PEPC, and two vacuolar markers α-glucosidase and acid invertase were used for all subsequent calculations.

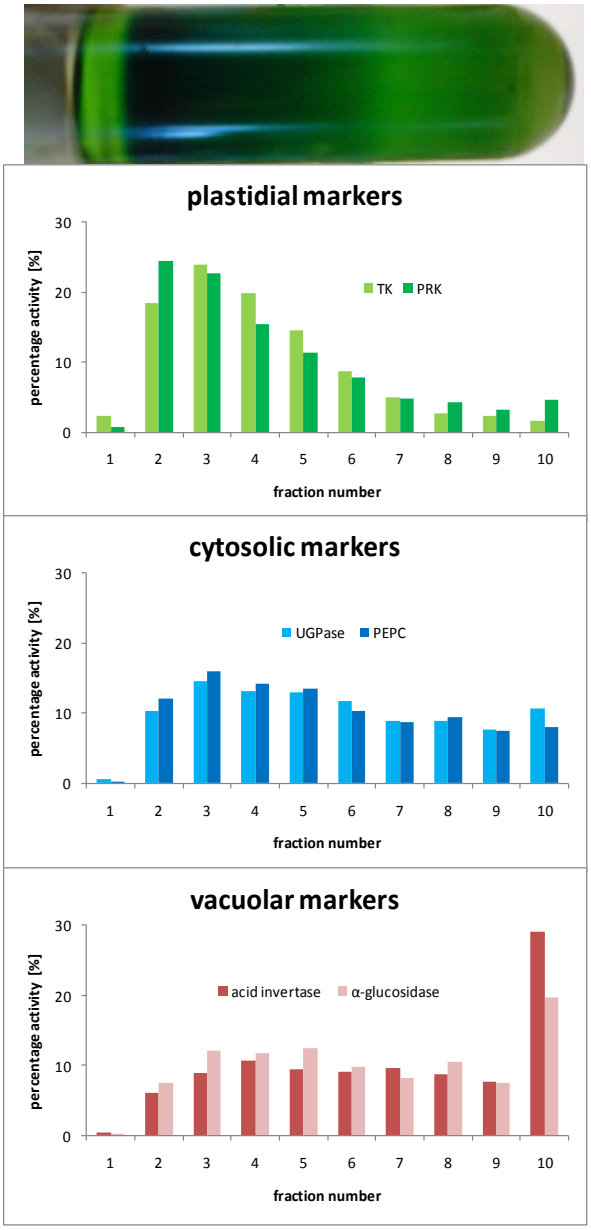

Scatter plots were drawn to assess the agreement between the two markers for each compartment for three gradients. These show a strong linear correlation between the two markers for chloroplasts and those for the cytosol (Fig. 3-3). There was generally also a good agreement between the vacuolar marker enzymes, if not quite as good as for the plastid and cytosolic markers. Comparison of the scatter plots from different gradients shows that the agreement of the marker enzymes for each compartment was reproducible between different gradients.

Figure 3-3: Linear correlation between the two marker enzymes for each compartment

The activities of the two marker enzymes for each of the three compartments, plastid, cytosol and vacuole, are plotted against each other to assess their agreement by linear regression analysis. Data are shown for three separate gradients. (a,b,c) shows the plastidial markers TK and PRK, (d,e,f) the cytosolic markers UGPase and PEPC and (g,h,i) the vacuolar markers acid invertase and α-glucosidase for each gradient. Linear regression analysis was done using Microsoft Excel.

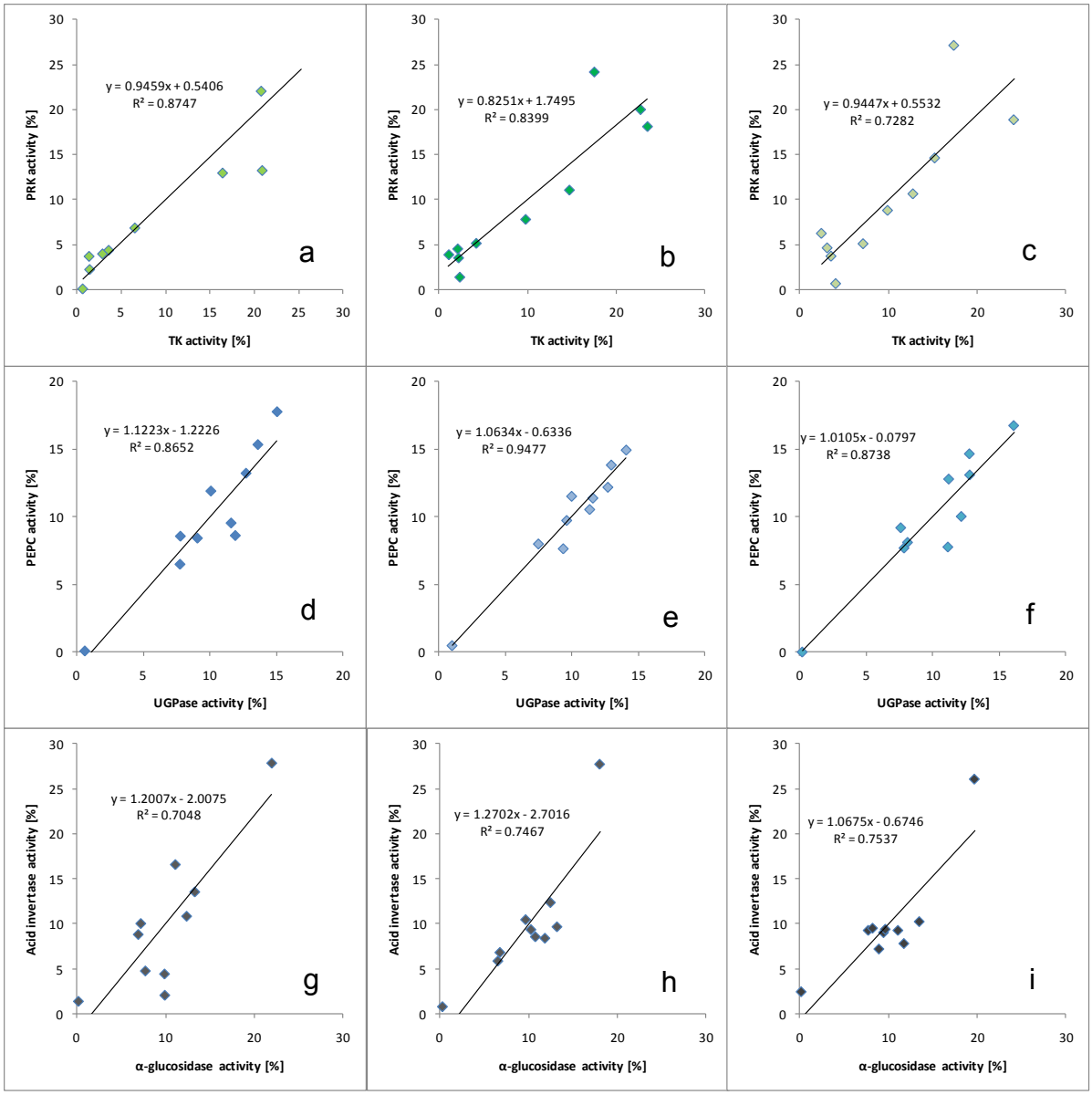

However, it was found that even gradients prepared with the same material on the same day showed some variation in the distribution of marker enzymes, which is most likely due to slight differences in the density profile arising during preparation of the gradients. Due to this technical variation, the distribution of metabolites was calculated separately for each individual gradient using the R-based computer tool Bestfit (Krueger et al., 2011), which compares metabolite and enzyme values from the same gradient. The program generates differential equations to describe the distribution of the marker enzymes, and uses these as a basis to calculate the percentage distribution of the metabolites in each compartment. The program checks all possible combinations of percentage distribution for two and three compartments for the best agreement with the marker enzymes. It was observed that the initial density range used for the NAF gradients gives a satisfactory separation of chloroplast, cytosol and vacuole (Fig. 3-2) from *A. thaliana* leaf material, so no further optimisation of the gradient itself or centrifugation conditions was felt to be necessary.

The next step in the validation of the NAF procedure was to check whether the metabolites that are measured by the different analytical platforms were extracted completely from the different fractions, and that no significant loss or degradation occurs during the treatment. Hot ethanolic extracts were made for enzymatic analysis of free sugars, starch and protein (Gibon et al., 2004a). For LC-MS/MS analysis of phosphorylated compounds, nucleotides and organic acids, a chloroform/methanol extraction procedure was used (measurements performed by Dr. Stéphanie Arrivault, MPIMP), while for the GC-MS analysis of amino acids a methanolic extraction was used (measurements performed by Marek Szecowka, MPIMP). Extreme care was taken during the harvesting of the material to ensure that metabolism was not perturbed by shading of the plants or by slow freezing. The total amount of each metabolite recovered from the NAF gradients was compared with the amount in the original, unfractionated lyophilized powder to ensure that the metabolites are not degraded during the procedure (see table 3-3). For complete extraction from the dried gradient fractions, samples were agitated with metal ball bearings in a ball mill during the extraction, and the chloroform phase from the chloroform/methanol extraction was washed three times with water to ensure complete recovery of polar metabolites into the aqueous methanol phase.

Although the vacuole stores primary metabolites like free hexoses, sucrose, organic acids and amino acids, there is evidence from several sources that phosphorylated compounds are mostly

absent from the vacuole of plants (Bligny et al., 1990; Martinoia et al., 2007; Neuhaus, 2007). Therefore, to simplify the analysis and minimize errors due to the slightly greater technical variation in the vacuolar marker enzyme assays, a two compartment analysis between chloroplast and cytosol was performed for all phosphorylated compounds. For all other metabolites, such as organic acids and amino acids a three compartment analysis between chloroplast, cytosol and vacuole was performed. For some metabolites like malate or sucrose even a three-compartment model may not be suitable, because substantial amounts of these metabolites can be present in other compartments than those included in the three compartment model, e.g. the apoplast and the vascular tissue, and the distribution of material from these compartments within the NAF gradients is not known. For the two compartment analysis the values for the vacuole were set to zero in the Bestfit program. The concentration of each metabolite in the specific compartment was estimated according to Winter et al. (1994), based on the assumption that the individual compartments in *A. thaliana* leaves have similar volumes to those in spinach leaves. The volumes estimated for spinach were 546 µl [mg Chl]$^{-1}$ for the vacuole, 65 µl [mg Chl]$^{-1}$ for the chloroplast stroma and 24 µl [mg Chl]$^{-1}$ for the cytosol (Winter et al., 1994).

Table 3-3: Subcellular distribution and *in vivo* concentration of organic acids in *A. thaliana* Col-0 leaves

The leaves were harvested after 8 h in the light period in a 12 h day/ 12 h night cycle. Recovery values are the comparison of the amount measured after the NAF procedure to lyophilized unprocessed plant material in percentage. Percentage distribution of metabolites for the compartments has been calculated as the mean of three independent gradients and the concentrations were calculated from the percentage distribution, total amount and the volumes for the three compartments in spinach leaves according to Winter et al. (1994). The three-compartment model was used for the calculation. Values for amount and recovery are mean ± SD from three independent gradients.

Metabolite	Amount [nmol g FW^{-1}]	Recovery [%]	Amount in plastid [%]	Amount in cytosol [%]	Amount in vacuole [%]	Concentration in plastid [µM]	Concentration in cytosol [µM]	Concentration in vacuole [µM]
2-OG	85.7 ± 9.4	91 ± 6	6	35	59	79	1250	92
aconitate	11.4 ± 0.1	87 ± 14	0	0	100	0	0	21
citrate	2222 ± 357	137 ± 7	0	0	100	0	0	4077
fumarate	1154 ± 47	95 ± 3	0	0	100	0	0	2117
glycerate	169 ± 65	86 ± 36	31	47	22	805	3306	68
isocitrate	34.3 ± 4.8	64 ± 7	0	0	100	0	0	63
malate	3833 ± 1119	80 ± 9	0	0	100	0	0	7032
pyruvate	99.2 ± 35.6	114 ± 22	24	31	45	366	1281	82
shikimate	35.6 ± 7.6	102 ± 9	37	22	41	202	326	27
succinate	89.6 ± 7.6	75 ± 4	4	17	79	55	634	130

Table 3-4: Subcellular distribution and *in vivo* concentration of amino acids, nitrate and putrescine in *A. thaliana* Col-0 leaves

The leaves were harvested after 8 h in the light period in a 12 h day/ 12 h night cycle. Recovery values are the comparison of the amount measured after the NAF procedure to lyophilized unprocessed plant material in percentage. Percentage distribution of metabolites for the compartments has been calculated as the mean of three independent gradients and the concentrations were calculated from the percentage distribution, total amount and the volumes for the three compartments in spinach leaves according to Winter et al. (1994). The three-compartment model was used for the calculation. Values for amount and recovery are mean ± SD from three independent gradients.

Metabolite	Amount [nmol g FW^{-1}]	Recovery [%]	Amount in plastid [%]	Amount in cytosol [%]	Amount in vacuole [%]	Concentration in plastid [mM]	Concentration in cytosol [mM]	Concentration in vacuole [mM]
alanine	228 ± 24	87 ± 18	16	14	70	0.56	1.33	0.29
arginine	164 ± 18	115 ± 15	42	0	58	1.06	0.00	0.17
asparagine	380 ± 25	98 ± 13	30	17	53	1.76	2.69	0.37
aspartate	1050 ± 346	93 ± 25	19	46	35	3.07	20.13	0.67
glutamate	3682 ± 1042	98 ± 30	30	42	28	16.99	64.43	1.89
glutamine	2349 ± 177	95 ± 4	11	0	89	3.97	0.00	3.84
glycine	543 ± 59	100 ± 15	28	33	39	2.34	7.47	0.39
isoleucine	38.9 ± 4.5	95 ± 13	33	0	67	0.20	0.00	0.05
methionine	10.7 ± 0.7	97 ± 9	42	13	45	0.07	0.06	0.01
nitrate	224000 ± 4100	96 ± 8	0	0	100	0.00	0.00	411
phenylalanine	53.1 ± 6.9	106 ± 7	48	0	52	0.39	0.00	0.05
proline	641 ± 90	104 ± 8	31	24	45	3.06	6.41	0.53
putrescine	91.1 ± 14.4	104 ± 10	40	0	60	0.56	0.00	0.10
serine	4265 ± 326	96 ± 6	36	22	42	23.62	39.09	3.29
threonine	459 ± 58	103 ± 13	42	0	58	2.96	0.00	0.49
tyrosine	9.86 ± 1.20	99 ± 13	45	0	55	0.07	0.00	0.01
valine	139 ± 16	96 ± 10	32	0	68	0.69	0.00	0.17

Table 3-5: Subcellular distribution and *in vivo* concentration of phosphorylated compounds in *A. thaliana* Col-0 leaves

The leaves were harvested after 8 h in the light period in a 12 h day/ 12 h night cycle. Recovery values are the comparison of the amount measured after the NAF procedure to lyophilized unprocessed plant material in percentage. Percentage distribution of metabolites for the compartments has been calculated as the mean of three independent gradients and the concentrations were calculated from the percentage distribution, total amount and the volumes for the three compartments in spinach leaves according to Winter et al. (1994). The two-compartment model was used for the calculation. Values for amount and recovery are mean ± SD from three independent gradients.

Metabolite	Amount [nmol g FW^{-1}]	Recovery [%]	Amount in plastid [%]	Amount in cytosol [%]	Concentration in plastid [µM]	Concentration in cytosol [µM]
ADP	15.2 ± 3.4	97 ± 17	63	37	147	235
ADPG	1.77 ± 0.46	103 ± 26	100	0	27	0
AMP	11.1 ± 4.2	89 ± 41	72	28	123	129
DHAP	7.30 ± 1.72	71 ± 2	23	77	26	234
Fru6P	153 ± 53	104 ± 24	34	66	801	4211
Fru1,6BP	8.93 ± 2.3	97 ± 8	70	30	96	112
Glc1P	11.7 ± 2.4	72 ± 14	8	92	14	448
Glc6P	173 ± 51	93 ± 32	17	83	452	5980
Gly3P	13.4 ± 3.6	108 ± 33	10	90	21	501
NAD	9.84 ± 2.45	79 ±14	29	71	44	291
NADP	4.42 ± 0.8	83 ± 4	98	2	67	3.7
PEP	56.5 ± 10.1	108 ± 25	6	94	52	2215
3PGA	487 ± 134	119 ± 40	44	56	3299	11372
R5P	1.14 ± 0.16	80 ± 7	49	51	8.6	24
RuBP	46.7 ± 8.2	92 ± 10	83	17	596	331
Suc6P	1.17 ± 0.28	121 ± 20	16	84	2.9	41
Sed7P	28 ± 5.4	82 ± 14	82	18	353	210
Sed1,7BP	9.56 ± 3.02	113 ± 25	75	25	110	99
Tre6P	0.358 ± 0.108	115 ± 26	16	84	0.88	12
UDPG	47.7 ± 14.3	109 ± 21	0	100	0	1989
XU5P + Ru5P	5.94 ± 2.17	81 ± 45	100	0	91	0

Table 3-6: Subcellular distribution and *in vivo* concentration of sugars and sugar alcohols in *A. thaliana* Col-0 leaves

The leaves were harvested after 8 h in the light period in a 12 h day/ 12 h night cycle. Recovery values are the comparison of the amount measured after the NAF procedure to lyophilized unprocessed plant material in percentage. Percentage distribution of metabolites for the compartments has been calculated as the mean of three independent gradients and the concentrations were calculated from the percentage distribution, total amount and the volumes for the three compartments in spinach leaves according to Winter et al. (1994). The three-compartment model was used for the calculation. Values for amount and recovery are mean ± SD from three independent gradients.

Metabolite	Amount [nmol g FW^{-1}]	Recovery [%]	Amount in plastid [%]	Amount in cytosol [%]	Amount in vacuole [%]	Concentration in plastid [mM]	Concentration in cytosol [mM]	Concentration in vacuole [mM]
fructose	1279 ± 148	101 ± 15	0	12	88	0.00	6.40	2.07
glucose	3267 ± 565	98 ± 6	12	23	65	6.03	31.31	3.90
inositol	922 ± 108	104 ± 7	66	0	34	9.36	0.00	0.57
sucrose	3577 ± 528	89 ± 1	19	31	50	10.46	46.21	3.28
trehalose	20.8 ± 3.0	100 ± 16	50	0	50	0.16	0.00	0.02

The recovery for lyophilized material versus fresh material was very good with only three metabolites being outside the 80 – 120 % interval (see Appendix Table 8-1). Recovery values for fractionated versus unfractionated material were also in a satisfactory range. Out of 52 measured metabolites, 45 showed recovery values in the range of 80 – 120 %, 5 lay between 70 – 130 % and only citrate with 137 % and isocitrate with 64 % recovery showed greater deviation from 100 %. It can therefore be concluded that there was no little or no loss of most metabolites during the lyophilisation or the NAF procedure. The higher deviations in recovery of citrate or isocitrate might reflect slight variation in the ionisation state of these trivalent molecules in different fractions, which would affect the yield of monovalent parent ions detected in the LC-MS/MS analysis and thus the accuracy of the measurements of these two metabolites.

Phosphorylated compounds and nucleotide sugars are approximately evenly shared between cytosol and chloroplast. Only low amounts of hexoses and organic acids are found in the chloroplast and in the cytosol. The vacuole contains most of the free sugars and organic acids, and a substantial proportion of the amino acids.

Metabolites that are expected to be restricted to one compartment based on the known location of the enzymes that metabolise them can also be used to assess the success of the fractionation, bearing in mind that this does not take into account the possibility that uncharacterised enzymes and transporters could affect the basis for the assumption. RuBP is believed to be restricted to the chloroplast as PRK is localized to this compartment only and no known RuBP transporter exists in the chloroplast membrane. Nonetheless the Bestfit program predicts 17 % of RuBP to be

cytosolic. This is quite surprising and may either reflect the technical limitation of the method or indicate side reactions of RuBP that occur in the cytosol. Other metabolites that are expected to be mainly in the chloroplast are ADPG, Xu5P and Ru5P. These show an exclusive location to the chloroplast with 100 % for ADPG, Xu5P and Ru5P (Table 3-5). The marker metabolites for the cytosol are Suc6P and UDPG, which were found to be 84 % and 100 % cytosolic, respectively. Again the 16 % of Suc6P calculated to be plastidial could reflect the technical limitations of the method. The vacuole is known to store most of the organic acids that are synthesized during the day, while the pools in the rest of the cell are much smaller, although probably more dynamic. In agreement with this aconitate, citrate, fumarate, isocitrate and malate were calculated to be localised exclusively in the vacuole. Nitrate was used as a vacuolar marker previously (Krueger et al., 2009; Krueger et al., 2011) and was also calculated to be 100 % vacuolar in my study. Nonetheless enzymatic markers are preferable over metabolites because they are more robust against intracellular movements. Depending on environmental conditions the distribution of nitrate could change, especially because the nitrate reduction is taking place in the cytosol (Cookson et al., 2005).

The dataset that is provided here covers a much wider range of metabolites from primary metabolism than in any previous study. Unexpected behaviour of metabolites according to predicted pathways or previously published results will be discussed in chapter 5.

3.4 Proteomics analysis of non-aqueous gradient fractions

As an independent test of the reliability of the measurements of the marker enzyme activities for chloroplast, cytosol and vacuole, and to investigate the distribution of markers for other subcellular compartments, the abundance of approximately 1500 proteins was measured in the NAF samples by protein mass spectrometry by Dr. Waltraud Schulze (MPIMP, Golm). About half of the detected proteins have already been located in purified organelles (Wienkoop et al., 2010). It must be remembered that mass spectrometry measures protein abundance, but does not distinguish between active and inactive forms of enzymes, which can at least partly account for any differences in the distribution between MS measurements and enzyme activity measurements. As a first test the distribution patterns of the enzymatic markers measured by the two different approaches were compared (see figure 3-4).

Figure 3-4: Comparison of the distribution of the marker enzymes determined by activity measurement and protein mass spectrometry.
Enzyme activities were measured using robotized spectrophotometric assays and the corresponding proteins were quantified by protein mass spectrometry. Values in each fraction are expressed as percentage of total activity/protein recovered from the gradient, and represent means of three gradients.

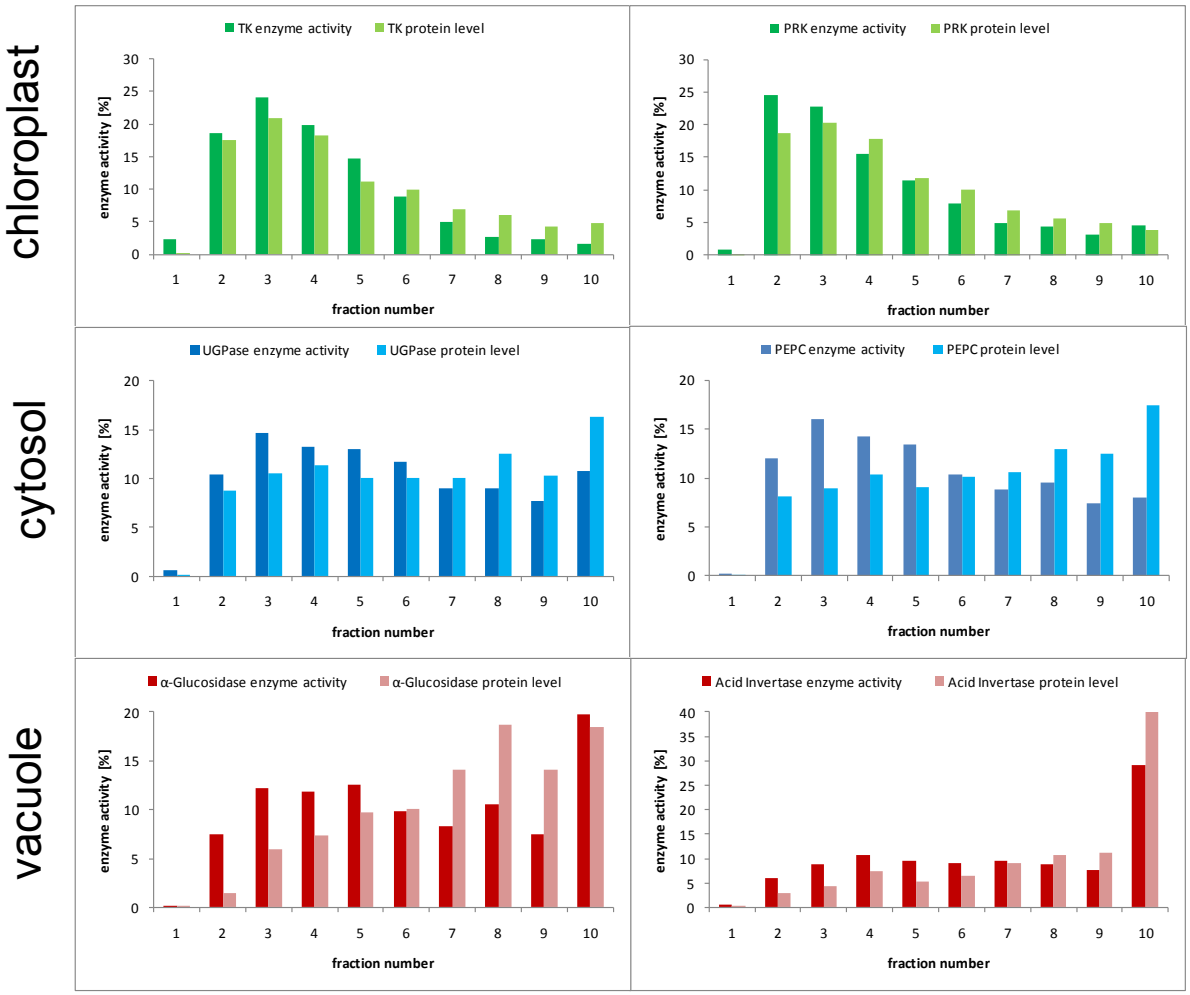

In general the distribution profiles of enzyme activity measurements and protein abundance show a good agreement, supporting the robustness of the marker enzyme activity data for calculating metabolite distributions. Slight differences can be explained by the fact that the protein mass spectrometry is less sensitive for low abundance proteins and that it does not distinguish between active forms of the enzyme and peptides from inactive or partially degraded protein. Plastidial markers accumulate at the top of the gradient, cytosolic markers distribute evenly across almost all fractions and the vacuole is strongly enriched at the bottom. Protein quantification by current proteomics techniques is subject to protein-to-protein variation and the linearity of the measurements depends on the abundance of the protein. Therefore, although the two approaches

for measuring the marker enzymes were in general agreement, the enzyme activity values were considered to be the most reliable basis for calculations of metabolite distributions. Nonetheless the proteomics data not only broadly confirm the enzyme activity measurements, but also provide information about the distribution of proteins from other subcellular compartments.

The distribution profiles of annotated proteins linked to various subcellular compartments are compared in Fig. 3-5.

Figure 3-5: Distribution profile of proteins across the non-aqueous fractionation gradient according to their subcellular compartments
Protein abundances in the 10 fractions from three independent gradients of *A. thaliana* Col-0 leaf material were measured by mass spectrometry. Mean values of the relative protein abundance from the three gradients are shown. Individual proteins in each class are represented by grey lines, and the average abundance of all the proteins in that class is shown by the red line. (a) represents 196 stromal proteins, (b) 130 cytosol proteins, (c) 17 peroxisomal proteins, (d) 42 mitochondrial proteins, (e) 6 vacuolar proteins, (f) 16 plasma membrane proteins, (g) 28 thylakoid proteins, (h) 30 chloroplast envelope proteins.

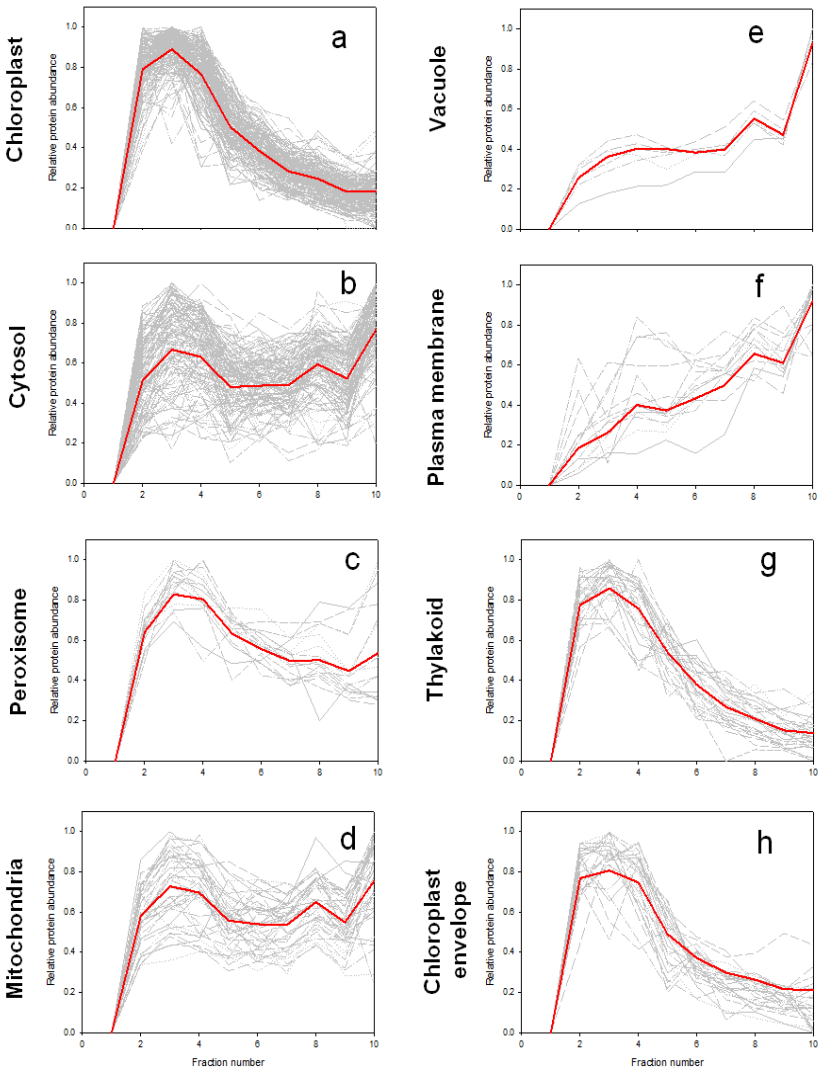

Figure 3-6: PCA analysis of the individual protein subcellular compartments

The individual subcellular protein classes were grouped and transformed into a principal component space in R. The plastidial proteins of the stroma, the thylakoid and the chloroplast envelope form a distinct class that was mostly well resolved from the other compartments. The vacuolar proteins were clustered with some plasma membrane proteins, and both were partially resolved from the cytosolic proteins. Cytosolic proteins were not resolved from mitochondrial or peroxisomal proteins.

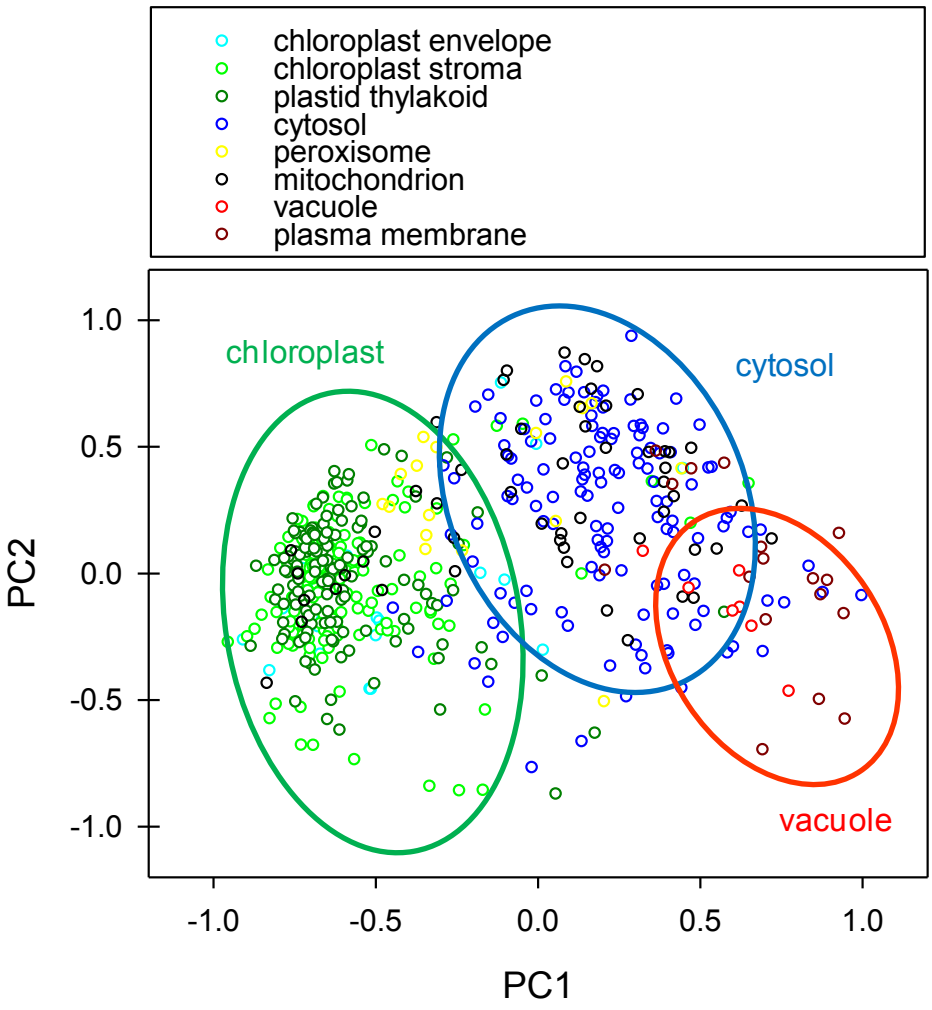

The distribution profiles of all detected proteins that are known to be specifically located in the stroma, cytosol, vacuole, peroxisome, mitochondria, thylakoids, chloroplast envelope or plasma membrane were compared to explore the possibility of resolving additional compartments. The distribution profiles of stroma, thylakoids and chloroplast envelope show a similar behaviour to each other with substantial enrichment at the top of the gradient (Fig. 3-5a, g, h). However, the distribution profiles of the proteins from the mitochondria and the peroxisome are almost indistinguishable from the cytosol (Fig. 3-5 b-d). The vacuole and the plasma membrane also behave similarly to each other with marked enrichment in the lower gradient fractions (Fig. 3-5 e-f). Principal component analysis supports these observations (Fig. 3-6). Here the chloroplastic

proteins from stroma, thylakoid and chloroplast envelope cluster within a single distinct group. The vacuolar proteins clustered quite closely with many of the plasma membrane proteins, and both were partially resolved from the cytosolic proteins. Mitochondria and peroxisomes overlap with each other and with the cytosol. From this it can be concluded that the density of the particles derived from peroxisomes and mitochondria is in the same range as the ones derived from the cytosol. These proteomic studies extended our knowledge about the behaviour of particles in a non-aqueous gradient. Although the data show little or no resolution of mitochondria or peroxisomes from the cytosol, or of the plasma membrane from the vacuole, at least we now know how these compartments distribute in the NAF gradients. This information could be useful to interpret some of the apparent anomalies in the distribution of metabolites assigned to the chloroplast, cytosol or vacuole using two- or three-compartment models.

3.5 Conclusions

It was not possible to adapt the methodology of NAF to *C. reinhardtii* cells. The principle of the methodology is to separate disrupted particles of different density. These particles are a conglomerate of proteins, metabolites and membranes, and according to their origin have slightly different densities. With *C. reinhardtii* material the various particles have the same density or the differences are so small that it was not possible to separate them. This is most likely due to too little variation in the membrane composition of the different subcellular compartments. The particles vary in their density depending on the mixture of membranes, metabolites and proteins. It is also possible that the metabolites are more evenly distributed between the different subcellular compartments in *C. reinhardtii* or that the comparatively low levels of starch in *C. reinhardtii* are insufficient to differentially affect the density of the chloroplast versus the cytosol. It is likely that the particles that are produced from the algal cells contain a mixture of chloroplast and cytosol. All species to which the methodology has been successfully applied in the past are higher plants. There is considerable variation in cell architecture between different chlorophyte algae, so the possibility of adapting the method to other unicellular green algae cannot be ruled out. However, all attempts to achieve a useful separation of subcellular compartments from *C. reinhardtii* by varying sonication, centrifugation or gradient parameters were unsuccessful. It is conceivable that non-aqueous gradients employing a combination of separation principles (e.g. density and hydrophobicity) might be more successful. Such approaches have been used to achieve separation of organelles that are poorly resolved by density gradient centrifugation alone,

such as mitochondria and peroxisomes, which are well separated when a gradient of PVP is included within the density gradient (Packer, 1987).

The application of robotised cycling assays increased the sensitivity and throughput of the marker enzyme assays, allowing two markers to be measured for each compartment and thus increasing the robustness of the NAF procedure. The NAF procedure was successfully combined with different sensitive MS techniques for metabolite measurements, providing an almost complete dataset of intermediates from primary carbon metabolism and its compartmentation pattern within leaf mesophyll cells. This dataset covers a much wider range of primary metabolites than previous studies and thereby allows a broader in-depth analysis of metabolic pathways. Tests of recoveries of metabolites validated the potential of the method to measure *in vivo* levels over a wide range of different metabolite classes and abundances.

The proteomics data verified the enzyme activity measurements and compartment based analysis clearly demonstrated the separation of chloroplast, cytosol and vacuole. In addition it revealed that the peroxisomes and mitochondria behave similarly to the cytosol in the gradient and that the vacuole distributes very much like the plasma membrane.

Since NAF is the only method so far available to determine the *in vivo* distribution of metabolites that turn over rapidly in mesophyll cells, the optimisation and validation of the method for *A. thaliana* leaves opened up many possibilities for further experiments to investigate primary metabolism and its regulation in this species. Mutants that are impaired in certain key functions of carbon metabolism are a convenient tool to learn more about the mechanisms of metabolic control. Investigating the effects of different environmental condition, e.g. higher or lower irradiance or CO_2 concentrations, could also extend our knowledge of the mechanisms that influence primary metabolism at the subcellular level, which can ultimately affect the growth of the whole plant.

I have established and validated an optimised procedure for NAF of *A. thaliana* leaves, suitable to address biological questions. In the next chapter I describe the application of this technique to investigate the control of carbon fixation by combining new knowledge about the compartmentation of metabolites in leaf mesophyll cells with information about the kinetic parameters of the corresponding enzymes.

Chapter 4: Control of carbon fixation

4.1 Introduction

In this chapter the results of the compartmentation analysis of Calvin-Benson cycle intermediates are used to systematically investigate regulation and control of the pathway. The control of carbon fixation is regulated at various levels and over different timescales. Photosynthesis responds rapidly, within seconds or minutes, to fluctuations in environmental conditions such as irradiance, CO_2 concentration or light quality. Photosynthesis is also regulated on a diurnal basis, linked to the daily 24 h cycle of light and dark, with related changes in temperature and CO_2 and water availability linked to transpiration and stomatal opening. In the longer term developmental and environmental adaptation of photosynthesis via transcriptional regulation and senescence related turnover of the photosynthetic machinery are very important mechanisms (Jiao et al., 2007). Long term adaptation can have two different reasons. First, growth of the plant will lead to developmental changes in the source-sink balance of the whole plant, requiring adjustment of photosynthetic capacity. Secondly environmental factors like photoperiod, light levels, temperature and nutrient availability are subject to seasonal changes and the plant needs to respond to these changes to guarantee effective photosynthesis. Here I will focus mainly on the short-term responses of photosynthesis to changes in environmental conditions.

The net synthesis of an end product of a biochemical pathway is dependent on the flux through this pathway. Every single enzymatic step has the potential to contribute to overall control of this flux. Control over the flux by an individual enzyme can be achieved by changing the velocity or direction of the reaction, altering the K_m for either substrate or product, or changing the amount of the enzyme itself. Early theories of metabolic control considered that the flux through a metabolic pathway is determined by the enzyme catalysing the so-called “rate-limiting steps”. Irreversible reactions were thought to be more suitable candidates for the “rate-limiting step” than reversible reactions (Newsholme and Crabtree, 1979). Reactions that are near equilibrium *in vivo*, i.e. where the change in Gibbs free energy is close to zero, can be considered to be freely reversible. According to previously held theories, a change in the enzyme activity catalysing such a reaction would have very little effect on the net flux, as both the forward and the reverse reactions would change in parallel. The net flux through reversible reactions would be strongly influenced by any change in the substrate/product ratio. Reactions that are greatly displaced from equilibrium, have

a large negative change in Gibbs free energy, such that the reaction is essentially irreversible. Consequently any change in the activity of the enzyme would be expected to affect the net flux. For this reason irreversible reactions were considered to be better targets for regulation to control flux. However, this concept is now considered to be too simplistic, as there are numerous examples of enzymes that catalyse irreversible reactions and show regulation of their activity but make only a small contribution to control of flux of a pathway. Indeed, it has been argued that their regulatory potential can be used to ensure that their activity is not limiting the flux through the pathway (Stitt, 1996). Such observations and the development of metabolic control theory by Kacser and Burns (1973) and Heinrich and Rapoport (1974) led to the idea that control of flux is shared by all enzymes in the pathway, albeit unequally and that few pathways contain a single rate-limiting step. Nevertheless, it is common for the enzymes catalysing non-equilibrium reactions to have more complex regulatory properties than those catalysing near equilibrium reactions.

Rubisco, fructose 1,6-bisphosphatase (Fru1,6BPase), sedoheptulose 1,7-bisphosphatase (Sed1,7BPase) and phosphoribulokinase (PRK) are the enzymes that previous studies have shown to catalyse irreversible steps in the Calvin-Benson cycle. However, overexpression or knockdown of such enzymes in the Calvin-Benson cycle often did not lead to marked changes in the rate of photosynthesis (Stitt, 1993; Stitt and Sonnewald, 1995; Haake et al., 1998; Haake et al., 1999; Stitt, 1999; Henkes et al., 2001; Raines, 2003), supporting the view that the traditional concept of flux control by irreversible reactions was too simplistic. It has been argued that reversible reactions might even have a bigger impact on the flux based on the premise that small changes in the substrate/product ratio of a reversible reaction can change the direction of the net flux catalysed by the enzyme, which can have a major impact on the whole network (Stitt et al., 2010a). By comparing the concentrations of substrates and products in a specific cell compartment with the catalytic properties of the enzymes that metabolise those compounds one can identify organizing metabolic principles (Bennett et al., 2009), i.e. control of the flux by the concentration of the metabolites. Bassham and Krause (1969) carried out a comprehensive analysis of the thermodynamic structure of carbon fixation, which can be used as a basis for understanding the network in more detail. Although the work by Bassham and Krause describes the thermodynamic structure of the whole set of Calvin-Benson cycle reactions, it did not take into account the issue of compartmentation of higher plant cells. In the time since this early work,

most studies have covered only a limited set of the Calvin-Benson cycle intermediates because paper chromatography and radioactive labelling were not used anymore and new analytical methods covering the bigger spectrum of intermediates were not developed at that time.

The irreversible enzymes Rubisco, Fru1,6BPase, Sed1,7BPase and PRK show regulatory properties. They are practically inactive in the dark and become activated in the light via redox modulation linked to the ferrodoxin/thioredoxin system. Rubisco is only indirectly activated by this system via Rubisco activase, which is a target of ferrodoxin/thioredoxin modulation. Rubisco activase facilitates the carbamylation of Rubisco and thus activates the enzyme. Carbamylation is the binding of CO_2 to the amino group of a lysine of the large subunit of Rubisco, which then also binds a Mg^{2+} ion (Wolosiuk et al., 1993). Besides the five enzymes mentioned above NADP-GAPDH, which catalyses a reversible reaction is also redox regulated. The activities of Fru1,6BPase, Sed1,7BPase, PRK and Rubisco are also dependent on the pH and the Mg^{2+} concentration (Buchanan and Schurmann, 1973; Portis and Heldt, 1976; Portis et al., 1977; Laing et al., 1981; Gardemann et al., 1983; Woodrow et al., 1984). Both stromal pH and Mg^{2+} concentration increase during the day when the light reactions of photosynthesis lead to pumping of protons into the thylakoids, with Mg^{2+} ions being transported in the opposite direction as counter ions (Wolosiuk et al., 1993). The activity of the Calvin-Benson cycle is also regulated by binding of PRK and NADP-GAPDH to the CP12 protein in their oxidised (disulphide) forms. The activity of these enzymes is decreased when they are bound in this multiprotein complex. The complex is disrupted upon illumination and thus is an additional mechanism for the regulation of the Calvin-Benson cycle to changing light conditions (Howard et al., 2008).

Much of our knowledge of the regulation of photosynthetic carbon fixation is based on studies with isolated chloroplasts (Buchanan and Schurmann, 1972; Schurmann and Buchanan, 1975; Robinson and Walker, 1979a; Flugge et al., 1980; Heldt et al., 1980; Laing et al., 1981). This leaves crucial questions, such as the integration of the Calvin-Benson cycle with end product synthesis, unanswered. Furthermore it is also unclear how closely the steady state condition of the Calvin-Benson cycle in isolated chloroplasts resembles that in intact leaf mesophyll cells, especially because the studies on isolated chloroplasts were usually performed under saturating CO_2 conditions.

In this chapter, I extend the comprehensive analysis of the Calvin-Benson cycle by Bassham and Krause (1969), taking into consideration the subcellular compartmentation of intermediates from the pathway. I compare *in vivo* concentrations of Calvin-Benson cycle intermediates from *A. thaliana* leaves with the K_m-values and binding site concentrations of the corresponding enzymes. The aim is to determine how reactions are balanced against each other to avoid accumulation of individual intermediates, especially for the regenerative phase of the cycle leading to production of RuBP. Over accumulation of individual metabolites could result in sequestration of inorganic phosphate and inhibitory effects on other enzymes. At the same time the plant needs to ensure that it provides enough metabolic precursors for other essential pathways, such as E4P for the shikimate pathway, R5P for nucleotide synthesis and GAP for the MEP pathway of isoprenoid synthesis. Conversely, excessive withdrawal of intermediates into these pathways, or for photosynthetic end production synthesis of sucrose and starch would restrict the rate of CO_2 fixation, and so all of the processes need to be tightly coordinated.

The effectiveness of the Calvin-Benson cycle depends on generating enough RuBP to keep Rubisco saturated with this substrate. I want to clarify how an appropriate balance between RuBP regeneration and the competing reactions of starch and sucrose synthesis is achieved.

4.2 The levels of metabolites of the Calvin-Benson cycle in the plastid stroma

In order to compare the values for Calvin-Benson cycle intermediates in studies from isolated spinach chloroplasts (Heldt et al., 1980) with the values measured by NAF in whole plant cell material from *A. thaliana* leaves, both datasets are displayed in Table 4-1. For both datasets the concentration in the plastid stroma was calculated according to Winter et al. (1994). In the current study 22 metabolic intermediates from primary carbon metabolism were measured by LC-MS/MS, compared with only 11 in isolated chloroplasts using ion exchange chromatography. Analysis by LC-MS/MS allowed measurement of Suc6P, Sed7P, Tre6P, NAD^+, $NADP^+$, PEP, UDPG, DHAP and Gly3P and resolution of R5P from the other pentose phosphates Xu5P and Ru5P. However, inorganic phosphate and ATP could not be measured in the LC-MS/MS analysis. Where comparisons can be made, the values for the metabolites in *A. thaliana* chloroplasts are all higher than those measured in spinach. While there is a good agreement in the

values for ADP and triose-phosphates, the values for ADPG, FBP, 3-PGA, RuBP, SBP and pentose monophosphates are 2.5- to 6-fold higher in plastids *in situ* in *A. thaliana*.

Table 4-1: Metabolite levels in the chloroplast stroma

The amounts and concentrations of metabolites in *A. thaliana* chloroplast stroma are derived from NAF data obtained from leaves harvested in the light and analysed by LC-MS/MS. The values are compared with data from isolated spinach chloroplasts from Heldt et al. (1980) analysed by ion-exchange chromatography. Original data from Heldt et al. was given in nmol mg Chl^{-1}. This was converted by assuming 1 g FW contains 1 mg Chl (Robinson et al., 1983). (ND = not determined)

Metabolite	**Amount in plastid [nmol g FW^{-1}]**		**Concentration in plastid [µM]**		**Ratio *A.thaliana*/spinach**
	A.thaliana	**spinach**	***A.thaliana***	**spinach**	
3-PGA	214	70.9	3297	1091	3.02
ADP	9.58	7.8	147	120	1.23
ADPG	1.77	0.69	27	11	2.57
AMP	7.99	ND	123	ND	ND
ATP	ND	2.63	ND	40	ND
DHAP	1.68	ND	26	ND	ND
DHAP+GAP	ND	2.94	ND	45	ND
E4P	ND	ND	ND	ND	ND
Fru1,6BP	6.25	2.2	96	34	2.84
Fru6P	52.02	ND	800	ND	ND
Glc1P	0.94	ND	14	ND	ND
Glc6P	29.41	ND	452	ND	ND
Glc6P+Fru6P+Glc1P	82.37	42.8	1267	658	1.92
Gly3P	1.34	ND	21	ND	ND
NAD	2.85	ND	44	ND	ND
NADP	4.33	ND	67	ND	ND
PEP	3.39	ND	52	ND	ND
Pi	ND	148.9	ND	2291	ND
R5P	0.56	ND	9	ND	ND
R5P+Ru5P+Xu5P	6.5	1.08	100	17	6.02
RuBP	38.76	9.43	596	145	4.11
Sed7P	22.96	ND	353	ND	ND
Sed1,7BP	7.17	2.15	110	33	3.33
Suc6P	0.19	ND	3	ND	ND
Tre6P	0.06	ND	1	ND	ND
UDPG	0	ND	0	ND	ND
Xu5P + Ru5P	5.94	ND	91	ND	ND

Isolated spinach chloroplasts can achieve rates of CO_2 fixation that equal the rates in intact leaves, so the capacity of the Calvin-Benson cycle to fix CO_2 is clearly not impaired by the

isolation procedure. Nevertheless removing chloroplasts from their natural cellular environment inevitably affects their metabolism due to loss of interaction with other parts of the cell. Consequently it would be expected that the metabolic network is poised in a different conformation when chloroplasts are separated from their natural physiological context even though the rates of photosynthetic CO_2 fixation are comparable. Differences between species could also be a contributing factor, for example, spinach leaves generally store less starch as a proportion of carbohydrate than *A. thaliana*. By similar arguments, metabolite data obtained from protoplast studies may also not reflect the nature of the metabolic network in cells within the intact leaf, due to the restriction of sucrose export from the cell and interactions with neighbouring cells. This could explain why the levels of key Calvin-Benson cycle intermediates, such as 3PGA and RuBP, were found to be 5- to 6-fold lower in barley leaf protoplasts (Keerberg et al., 2011) than the values I obtained for *A. thaliana* leaves. From these comparisons it is apparent that while isolated chloroplasts or protoplasts have some advantages as experimental model systems, NAF is currently the only suitable method for studying the subcellular compartmentation of metabolism in an intact physiological context. This is especially important for the study of the regulatory capacity of the metabolites in biochemical networks.

It has to be mentioned that the levels of the phosphorylated intermediates of the Calvin-Benson cycle measured in this study deviate from the levels measured previously by Arrivault et al. (2009). Table 4-2 compares the total levels of theses metabolites with each other. The levels of the metabolites measured in the NAF study should be in a similar range to the ones measured in ambient CO_2 and light in the study of Arrivault et al. (2009). Slight differences can be explained by the fact that these are independent experiments with different plant material that has been harvested in a different way. For the analysis performed by Arrivault et al. (2009) the plants were put into a box with direct CO_2 gassing via tubing with high airflow close to the leaf and a different light source, while for the NAF study the plants have been harvested inside the growth chamber. It is possible that theses different experimental conditions led to the different levels of most of the phosphorylated intermediates. Nonetheless comparison of the ratios of 3PGA/DHAP and Fru6P/Fru1,6BP indicate a situation that is similar to the ones in dark harvested leaves, while the ratios of S7P/SBP and RuBP/Ru5P are similar to the ones harvested in the light and at ambient CO_2 (Table 4-3).

Table 4-2: Comparison of the total amounts of metabolites in *A. thaliana* leaves in the NAF study against values measured by Arrivault et al. (2009)

Displayed are the total levels of the metabolites in the NAF study, plants grown in ambient CO_2 and light and plants that were 15 min in the dark at ambient CO_2. These levels are compared with each other and the turnover times ($T_{0.5}$) of these metabolites that were determined in Arrivault et al. (2009) are also shown. (ND = not determined)

Metabolite	Total Amount [nmol g FW^{-1}]			ratio ambient CO_2 and light/NAF	ratio ambient CO_2 and 15 min dark/NAF	$T_{0.5}$ (s^{-1})
	NAF study	Arrivault et al. (2009) ambient CO_2 and light	Arrivault et al. (2009) ambient CO_2 15 min dark			
aconitate	11.4 ± 0.1	22.8 ± 1.6	39.7 ± 2.5	2.00	3.48	ND
ADP	15.2 ± 3.4	24.3 ± 1.9	26 ± 3	1.60	1.71	0.07
AMP	11.1 ± 4.2	8.66 ± 0.59	17.9 ± 0.3	0.78	1.61	ND
ADPG	1.77 ± 0.46	1.021 ± 0.097	0.002 ± 0.002	0.58	0.001	0.5
aspartate	1050 ± 346	1642 ± 107	1647 ± 84	1.56	1.57	ND
citrate	2222 ± 357	1688 ± 117	2748 ± 50	0.76	1.24	ND
DHAP	7.30 ± 1.72	57.3 ± 4.2	3.6 ± 0.5	7.85	0.49	0.24
Fru6P	153 ± 53	128 ± 8	33.4 ± 2.3	0.84	0.22	3.23
Fru1,6BP	8.93 ± 2.3	31.2 ± 2.4	0.768 ± 0.077	3.49	0.09	0.79
fructose	1279 ± 148	374 ± 68	357 ± 38	0.29	0.28	ND
Glc1P	11.7 ± 2.4	11.4 ± 1.2	7.23 ± 0.45	0.97	0.62	1.9
Gly3P	13.4 ± 3.6	47.5 ± 2.5	37.5 ± 0.9	3.54	2.80	ND
Glc6P	173 ± 51	272 ± 15	95.4 ± 4	1.57	0.55	45.33
glucose	3267 ± 565	1168 ± 70	1155 ± 34	0.36	0.35	ND
glutamate	3682 ± 1042	4424 ± 319	3973 ± 225	1.20	1.08	ND
glycerate	169 ± 65	290 ± 11	206 ± 9	1.72	1.22	ND
isocitrate	34.3 ± 4.8	49.9 ± 2.2	67.7 ± 2.9	1.45	1.97	ND
malate	3833 ± 1119	3222 ± 186	4018 ± 175	0.84	1.05	ND
NAD	9.84 ± 2.45	14.0 ± 1.2	18.8 ± 0.5	1.42	1.91	ND
NADP	4.42 ± 0.8	3.16 ± 0.35	2.96 ± 0.06	0.71	0.67	0.01
2-OG	85.7 ± 9.4	90.4 ± 2.6	125 ± 7	1.05	1.46	ND
3-PGA	487 ± 134	168 ± 15	142 ± 5	0.34	0.29	0.7
PEP	56.5 ± 10.1	43.5 ± 1.6	43.2 ± 1.4	0.77	0.76	ND
pyruvate	99.2 ± 35.6	25.8 ± 4.8	31.3 ± 10.4	0.26	0.32	ND
R5P	1.14 ± 0.16	3.28 ± 0.83	1.29 ± 0.24	2.88	1.13	0.08
RuBP	46.7 ± 8.2	118 ± 11	4.29 ± 0.8	2.53	0.09	0.98
Suc6P	1.17 ± 0.28	0.985 ± 0.109	0.247 ± 0.09	0.84	0.21	0.23
Sed7P	28 ± 5.4	87.5 ± 4.3	96.6 ± 5.1	3.13	3.45	2.21
SedBP	9.56 ± 3.02	27.9 ± 2.4	0.954 ± 0.237	2.92	0.10	0.7
shikimate	35.6 ± 7.6	34.1 ± 3.3	35.4 ± 1.6	0.96	0.99	ND
succinate	89.6 ± 7.6	122 ± 7	227 ± 8	1.36	2.53	ND
sucrose	3577 ± 528	3510 ± 256	3036 ± 95	0.98	0.85	ND
T6P	0.358 ± 0.108	0.12 ± 0.007	0.108 ± 0.018	0.34	0.30	ND
UDPG	47.7 ± 14.3	151 ± 4	117 ± 3	3.17	2.45	35.95
X5P + Ru5P	5.94 ± 2.17	39.1 ± 1.6	3.5 ± 0.2	6.58	0.59	0.33

Table 4-3: Ratios of total levels of 3PGA/DHAP, Fru6P/Fru1,6BP, Sed7P/Sed1,7BP and RuBP/R5P in *A. thaliana* leaves in this study and in ambient CO_2 and light and ambient CO_2 and dark measured by Arrivault et al. (2009)

Ratio	NAF study	Arrivault et al. (2009) ambient CO_2 and light	Arrivault et al. (2009) ambient CO_2 15 min dark
3PGA/DHAP	66.71	2.93	39.44
Fru6P/Fru1,6BP	17.13	4.10	43.49
Sed7P/Sed1,7BP	2.93	3.14	101.26
RuBP/R5P	40.96	35.98	3.33

Although the harvest of the plants for this study was done extremely carefully, the ratio of DHAP/3PGA and Fru6P/Fru1,6BP indicate the possibility that the plants were subjected to a very short shading period at the harvest, which led to a 7-fold decrease of DHAP and X5P + Ru5P, which is in agreement with their very short turnover times of 0.24 and 0.33 s, respectively. Most of the other metabolites show moderate changes of a factor of 2 to 3. The recovery values of the metabolites were all in a satisfactory range, so the possibility of degradation of metabolites by lyophilisation or the NAF procedure can be ruled out (Table 3-5 and Table 8-1). In order to verify the measurements of DHAP by LC-MS/MS the measurements were repeated in TCA extracts on a Sigma Photometer, which gave a value in the same range (7.9 nmol g FW^{-1}). To account for the possibility of decreased metabolite levels due to very short shading, all further data evaluation steps are critically assessed by testing whether a qualitatively different answer is obtained by taking the metabolite levels of Arrivault et al. (2009) with the compartmentation pattern from this study.

4.3 Comparison of metabolite concentrations with the binding site concentrations and the K_m values of the corresponding enzymes

Information about the *in vivo* concentrations of metabolites can be linked to enzymological data to explore the structure of biochemical networks in more detail (Bennett et al., 2009). A further application of combining such datasets is to test predictions from published mathematical models of the Calvin-Benson cycle, to assess the validity and usefulness of those models.

Here I systematically compare estimated metabolite concentrations with published values for the K_m values of the enzymes, and with estimates of the enzyme binding site concentrations derived from the proteomics data reported in chapter 3. Proteomics data from this study and information about the structure of the Calvin-Benson cycle enzymes from the BRENDA enzyme database

(http://www.brenda-enzymes.info/) (Schomburg et al., 2002) were used to calculate the concentrations of the holoenzymes and the metabolite-binding site concentrations for the catalytic and regulatory subunits (Table 4-4).

Table 4-4: Protein amount and concentrations of holoprotein and subunits of the Calvin-Benson cycle enzymes from *A. thaliana*
The protein amount was determined by quantitative proteomics (measurement performed by Dr. Waltraud Schulze) and was used to calculate the concentrations of the subunits of each enzyme in the plastid stroma. Concentration of the holoprotein was calculated by division of the number of subunits (http://www.brenda-enzymes.info/). Information about the holoprotein calculations is also available in supplementary data from Piques et al. (2009). For RubisCO only the large subunit was used for the calculation. (NA= not applicable, ND = not determined).

Enzyme	**EC-number**	**Protein amount [nmol g FW^{-1}]**	**Enzyme structure**	**Concentration [µM]**		
				catalytic subunits	**regulatory subunits**	**holoprotein**
RubisCO LSU (catalytic subunit)	4.1.1.39	13.65 *51.7*[a]	8 LSU : 8 SSU	210.1 *795.4*[a]	NA	26.3 *99.4*[a]
RubisCO SSU (regulatory subunit)	4.1.1.39	198.35		NA	3051	
Phosphoglycerate kinase	2.7.2.3	5.17	Monomer	79.5	NA	260.0
Glyceraldehyde-3-phosphate dehydrogenase A (catalytic subunit)	1.2.1.9	3.76	A_4 (minor), A_2B_2	57.9	NA	22.3 (A_2B_2) 14.5 (A_4)
Glyceraldehyde-3-phosphate dehydrogenase B (regulatory subunit)	1.2.1.9	2.07		NA	31.8	
Triosephosphate isomerase	5.3.1.1	3.13	Homodimer	48.2	NA	24.1
Aldolase	4.1.2.13	8.10	Homotetramer	124.6	NA	31.1
Fructose-1,6-bisphosphatase	3.1.3.11	4.28	Homodimer	65.8	NA	32.9
Transketolase	2.2.1.1	*1.8*[a]	Homodimer	*27*[a]	ND	*13.5*[a]
Sedoheptulose-1,7-bisphosphatase	3.1.3.37	3.96	Homodimer	60.9	NA	30.5
Ribose-5-phosphate isomerase	5.3.1.6	ND	Homodimer	ND	ND	ND
Ribulose-5-phosphate epimerase	5.1.3.1	1.51	Octamer	23.3	NA	2.9
Phosphoribulokinase	2.7.1.19	6.79	Homodimer	104.5	NA	52.3

[a] Value estimated from maximum catalytic activity in *A. thaliana* leaves multiplied by the specific activity of the spinach enzyme

Surprisingly the molar amount of the large Rubisco subunit is approximately 14-fold lower than the value for the small subunit. It is known that mass spectrometry based proteomics measurements tend to underestimate the amounts of high abundance proteins (Ishihama et al., 2005), and Rubisco can represent up to 50 % of all soluble protein in the leaves of C_3 plants (Portis and Parry, 2007). Therefore, the concentration for Rubisco may well be an underestimate of the true value in leaves. Technical problems with the measurement of Rubisco in *A. thaliana* leaves by mass spectrometry have been reported previously (Piques et al., 2009). An estimate of the concentration of Rubisco based on enzyme activity measurements gave an approximately 4-fold higher value. For further calculations this value was used. NADP-GAPDH can exist in two different forms (Price et al., 1995). A minor form consists of four A subunits (A_4), while the major form is a heterotetramer of two A and two B subunits (A_2B_2). In the table the theoretical concentration for both isoforms is given, although the actual concentration of the A_4 form might be much lower. For further calculations the A_2B_2 form was used.

In order to compare the binding site concentrations of the enzymes with their corresponding metabolite concentrations, it is first necessary to estimate the concentrations of metabolites that are missing from the dataset. This was done using the stromal concentrations of the Calvin-Benson cycle intermediates (Table 4-5), with the assumption that the reversible TK, TPI and Ru5P epimerase reactions are close to equilibrium and that therefore the mass action ratio (MAR) is essentially the same as the equilibrium constant *K´*. Values for *K´* were taken from Bassham and Krause (1969). For the calculation of a missing metabolite in an enzymatic reaction, the following formula was used:

$$vA + wB \leftrightarrow xC + yD$$

$$K' = \frac{[C]^x \times [D]^y}{[A]^v \times [B]^w} \approx MAR$$

Equation 1: Generalised reaction of two substrates (A,B) giving two products (C,D) and formula used to estimate the mass action ratio (MAR) from the equilibrium constant (*K´*)

v, *w*, *x*, *y* represent the stochiometric amounts of the corresponding reactants.

The calculation also required estimates of ATP, P_i and NADPH concentrations. For this purpose ATP was estimated from the measured ADP concentration, assuming an ATP/ADP ratio of 3 (Gardestrom and Wigge, 1988), NADPH was estimated from the measured $NADP^+$ concentration, assuming an NADPH/$NADP^+$ ratio of 0.5 (Heineke et al., 1991) and P_i was measured by NMR to be approximately 4000 µM in the plastid (Pratt et al., 2009).

Table 4-5: Estimation of the unknown concentrations of Calvin-Benson cycle intermediates

The concentrations of the missing metabolites were estimated using the measured concentrations of related metabolites and published values of equilibrium constants (*K´*) or *in vivo* ratios for the concentrations of the known and unknown metabolites. The stromal P_i concentration is based on published NMR data. Concentrations based on the values measured by Arrivault et al. (2009) are shown in parantheses.

Metabolite	Calculation basis	*K´*	calculated concentration [µM]	Reference
ATP	ATP/ADP ratio = 3		441 (705)	(Gardestrom and Wigge, 1988)
E4P	transketolase reaction	$\frac{[E4P][Xu5P]}{[F6P][GAP]} = 0.084$	2.3 (2.8)	(Bassham and Krause, 1969)
GAP	triosephosphate isomerase reaction	$\frac{[GAP]}{[DHAP]} = 0.045$	1.3 (10)	(Bassham and Krause, 1969)
NADPH	NADPH/$NADP^+$ ratio = 0.5		34 (24)	(Heineke et al., 1991)
Ru5P	ribulose-5-phosphate epimerase reaction and measured concentration of Ru5P+Xu5P = 92 µM	$\frac{Xu5P}{Ru5P} = 1.5$	37 (243)	(Bassham and Krause, 1969)
Xu5P	(Ru5P + Xu5P) – Ru5P = Xu5P (92-37=55)	$\frac{Ru5P}{Xu5P} = 1.5$	55 (362)	(Bassham and Krause, 1969)
P_i	NMR data		4000	(Pratt et al., 2009)

With the complete dataset of measured and estimated concentrations, it is now possible to systematically compare the concentrations and ligand-binding properties of the enzymes from the Calvin-Benson cycle with the corresponding metabolite concentrations *in vivo* (Table 4-6).

Table 4-6: Comparison of Calvin-Benson cycle active site enzyme concentrations with concentrations of the corresponding substrates, products and K_m values

K_m values were taken from the BRENDA database (http://www.brenda-enzymes.info/) and refer to the enzymes from spinach leaves, unless indicated differently. The concentration of CO_2 was assumed to be 6 µM in the plastid stroma according to Heldt and Heldt (2005) The ratios of the metabolite concentrations to the binding site concentrations and the K_m values are also shown. For the ratio of reactant to binding site concentration a value close to one or lower than one indicates that most substrate is bound to the enzyme (shown in bold), a value higher than one indicates free substrate. The values based on the metabolite levels measured by Arrivault et al. (2009) are shown in parentheses. (NA = no data available, ND = not determined).

Enzyme	active binding site concentration [µM]	Reactant	Concentration [µM]	K_m [µM]	$\frac{[reactant]}{[binding\ site]}$	$\frac{[reactant]}{K_m}$
Rubisco	795	**RuBP**	596 (1505)	1.5	**0.7 (1.9)**	397 (1003)
		CO_2	6	10	**0.007**	0.6
		3PGA	3297 (1137)	NA	4.1 **(1.4)**	ND
PGK	80	**3PGA**	3297 (1137)	1100	41.2 (14.2)	3.0 (1.0)
		ATP	441 (705)	300	5.5 (8.8)	1.5 (2.3)
		1,3BPGA	ND	NA	ND	ND
		ADP	147 (235)	NA	1.8 (2.9)	ND
GAPDH	58	**1,3BPGA**	ND	15	ND	ND
		NADPH	34 (23)	30	**0.6 (0.4)**	1.1 (0.8)
		GAP	1.3 (10)	31	**0.02 (0.18)**	0.04 (0.3)
		$NADP^+$	67 (47)	17	**1.2 (0.8)**	3.9 (2.8)
TPI	48	**GAP**	1.3 (10)	440	**0.03 (0.2)**	0.003 (0.02)
		DHAP	26 (204)	NA	**0.5** (4.3)	ND
Aldolase (Fru1,6BP)	125	**GAP**	1.3 (10)	NA	**0.01 (0.08)**	ND
		DHAP	26 (204)	NA	**0.2 (1.6)**	ND
		Fru1,6BP	96 (335)	9.1[a]	**0.8** (2.7)	10.5 (36.9)
Fru1,6BPase	66	**Fru1,6BP**	96 (335)	2.3	**1.5** (5.1)	41.7 (145)
		Fru6P	800 (669)	NA	12.1 (10.1)	ND
		P_i	4000	NA	60.6	ND
Transketolase (1)	27	**Fru6P**	800 (669)	3200	29.6 (24.8)	0.3 (0.2)
		GAP	1.3 (10)	NA	**0.05 (0.4)**	ND
		E4P	2.3 (2.8)	NA	**0.09 (0.1)**	ND
		Xu5P	55 (362)	67	2.0 (13.1)	0.8 (5.4)
Aldolase (Sed1,7BP)	125	**E4P**	2.3 (2.8)	NA	**0.02 (0.02)**	ND
		DHAP	26 (204)	NA	**0.2 (1.6)**	ND
		Sed1,7BP	110 (321)	6[b]	**0.9** (5.2)	18.3 (53.5)
Sed1,7BPase	61	**Sed1,7BP**	110 (321)	50	**1.8** (5.3)	2.2 (6.4)
		Sed7P	353 (1103)	NA	5.8 (18.1)	ND

		P_i	4000	NA	65.6	ND
Transketolase (2)	27	**Sed7P**	353 (1103)	NA	13.1 (40.1)	ND
		GAP	1.3 (10)	NA	**0.05 (0.4)**	ND
		R5P	9 (26)	NA	**0.3 (1.0)**	ND
		Xu5P	55 (362)	67	2.0 (13.1)	0.8 (5.4)
R5P isomerase	ND	**R5P**	9 (26)	880	ND	0.01 (0.03)
		Ru5P	37 (243)	660[a]	ND	0.06 (0.4)
Ru5P epimerase	23	**Xu5P**	55 (362)	NA	2.4 (15.7)	ND
		Ru5P	37 (243)	220	**1.6** (10.6)	0.2 (1.1)
PRK	105	**Ru5P**	37 (243)	222	**0.4** (2.3)	0.2 (1.1)
		ATP	441 (705)	625	4.2 (6.7)	0.7 (1.1)
		RuBP	596 (1505)	NA	5.7 (14.3)	ND
		ADP	147 (235)	NA	**1.4** (2.2)	ND

[a] pea, [b] carrot,

The catalytic binding side concentrations of the following enzymes are higher than the concentration of their respective substrates shown in parentheses: Rubisco (RuBP, CO_2), TPI (DHAP, GAP), Fru1,6BP aldolase (DHAP and GAP), TK (GAP), Sed1,7BP aldolase (E4P and DHAP) and PRK (Ru5P). The catalytic activity of Rubisco is also very dependent on the absolute concentration of CO_2 and the ratio of CO2:O2. It has previously been shown that Rubisco exerts a very high control over photosynthesis in low or ambient CO_2 conditions, but practically none in elevated CO_2 (Stitt et al., 1991). The concentration of 3PGA, the substrate for the PGK reaction is more than 40-fold higher than the PGK binding site concentration. Transketolase catalyzes two reactions within the Calvin-Benson cycle, and the active binding site concentration is higher than the substrate concentration of GAP. For Fru1,6BPase and Sed1,7BPase the substrate concentrations are slightly higher than the corresponding binding site concentrations. Ratios could not be calculated for Ru5P epimerase as no protein data were available. In summary, one can say that most of the enzymes from the Calvin-Benson cycle are filled with their substrate, with the exceptions of aldolase, transketolase and TPI, which both catalyze reversible reactions. PRK catalyses an irreversible reaction and the concentration of the catalytic binding site is higher than the substrate concentration of Ru5P. These conclusions are also mostly valid based on the analysis of the dataset from Arrivault et al. (2009), with the exception of similar or lower binding site concentrations than metabolite concentrations for DHAP for the TPI reaction and Ru5P for

the PRK reaction. For Fru1,6BPase and Sed1,7BPase the substrate concentrations would be approximately 5-fold higher than the binding site concentrations.

The extent to which an enzyme is actually saturated by its substrate will depend not only on the ratio of binding site concentration to metabolite concentration, but also on the binding affinity, represented by the K_m value of the enzyme for the metabolite, compared to the concentration of the metabolite. The K_m value is the concentration of substrate at which the enzyme reaction reaches half its maximal velocity (Table 4-6). Strictly speaking this is only true for enzymes that follow Michaelis-Menten kinetics. For the enzymes of the Calvin-Benson cycle it is valid to assume that they follow Michaelis-Menten kinetics (Zhu et al., 2007), although at least the plastidial Fru1,6BPase has been shown to have cooperative kinetics in the presence of Fru6P (Gardemann et al., 1986).

For the following enzymes the calculated stromal concentrations of the substrates shown in parantheses are substantially above the literature K_m values for the spinach enzymes: Sed1,7BPase (Sed1,7BP), Fru1,6BPase (Fru1,6BP), PGK (3PGA) and Rubisco (RuBP) with Rubisco and Fru1,6BPase having more than 10-fold higher values of the substrates RuBP and Fru1,6BP, respectively, than the literature K_m values (Table 4-6). For the following enzymes the calculated stromal concentrations of the substrates shown in parantheses are substantially below the K_m value: TPI (GAP), PRK and Ru5P epimerase (Ru5P), R5P isomerase (R5P) and transketolase (Fru6P). These data indicate that the first transketolase reaction, using Fru6P as substrate, and the last three reactions for the regeneration of RuBP (Ru5P epimerase, R5P isomerase and PRK) are particularly substrate limited. These conclusions are mostly valid based on the analysis of the dataset from Arrivault et al. (2009) with the exception of Ru5P in the PRK and the Ru5P epimerase reaction, where the concentration also rises to be slightly higher than the respective K_m values.

In order to obtain a complete picture of the control and regulation of the Calvin-Benson cycle, the *in vivo* change in Gibbs free energy for each reaction was calculated from the mass action ratio and the standard Gibbs free energy change according to the formula:

$$vA + wB \leftrightarrow xC + yD \;; \qquad MAR = \frac{[C]^x \times [D]^y}{[A]^v \times [B]^w}$$

$$free\ energy\ change\ in\ vivo = \Delta G = \Delta G^{0\prime} + RT\ ln\ (MAR)$$

Equation 2: Standard equation for calculation of change in Gibbs free energy *in vivo* on the basis of the mass action ratio (MAR).
$\Delta G^{0'}$ = standard free energy change, R (gas constant) = 8.314 J mol^{-1} K^{-1}, T (temperature) = 298 K, ln = natural logarithm,

The Gibbs free energies of the Rubisco, Fru1,6BPase and Sed1,7BPase and PRK reactions are all highly negative with values of -25, -36, -38 and -32 kJ mol^{-1}, respectively (Table 4-7). These four reactions are displaced from equilibrium and can be considered as irreversible. The values for all enzymes, including the ones that catalyze reversible reactions are in relatively good agreement with the values calculated for *Chlorella pyrenoidosa* by Bassham and Krause (1969) in steady state photosynthesis, with the exception of the two aldolase reactions in *A. thaliana*, were the values are positive with approximately 15 kJ mol^{-1}. This would mean that the aldolase reactions would favourably run in the direction of cleavage of Fru1,6BP and Sed1,7BP *in vivo*. This difference can be explained by the differences in the DHAP concentration that are about 25-fold lower in *A. thaliana* than measured in *Chlorella pyrenoidosa*. DHAP levels that were measured in A. thaliana leaves previously by Arrivault et al. (2009) were about 7-fold higher (57.3 nmol g FW^{-1}) than measured in this study (7.3 nmol g FW^{-1}). Therefore the calculations of the change in Gibbs free energy for the two aldolase reactions have to be looked at very carefully, because the measurements of DHAP might underestimate the real *in vivo* levels. Since the calculations for the missing metabolites GAP and E4P are also dependent on the DHAP concentration these also have to be looked at critically. The low DHAP levels could be due to the plants being shaded for a very short time during the harvest. In order to assess this issue all changes in Gibbs free energy were also calculated based on the levels estimated by using the alternative concentrations estimated from data in Arrivault et al. (2009) (given in parentheses in Table 4-6). The general trend for all reactions is the same by using this dataset. The two aldolase reactions still have a positive change of Gibbs free energy. This problem is discussed in chapter 6.2.

Table 4-7: Estimated Gibbs free energy change for each reaction of the Calvin-Benson cycle *in vivo*
Values for standard ΔG and steady state ΔG have been taken from Bassham et al. (1969). Steady-state ΔG for the *A. thaliana* NAF gradient data was calculated by computing the mass action ratio for each enzyme on the basis of product and substrate concentration. For the Fru1,6BPase and Sed1,7BPase reaction [H_2O] = 55.5 M was used. The steady-state ΔG for the *A. thaliana* NAF gradient data was also calculated based on the concentrations estimated by using the data of Arrivault et al. (2009) (shown in parantheses).

Enzyme	**[a]standard $\Delta G^{0'}$ [kJ mol^{-1}]**	**steady-state ΔG [kJ mol^{-1}]**	
		Chlorella pyronosa[a]	*A. thaliana*[b]
RubisCO	-35.17	-41.03	-25.25 (-32.87)
PGK / GAPDH	18.00	-6.70	-16.14 (-8.35)
TPI	-7.54	-0.84	0.00[c]
Aldolase (Fru1,6BP)	-21.77	-1.67	15.10 (7.99)
Fru1,6BPase	-14.24	-27.21	-36.07 (-36.17)
Transketolase (Fru6P+GAP-> E4P+Xu5P)	6.28	-3.77	0.00[c]
Aldolase (Sed1,7BP)	-23.45	-0.84	12.66 (9.35)
Sed1,7BPase	-14.24	-29.73	-38.44 (-34.83)
Transketolase (S7P+GAP-> R5P+Xu5P)	0.42	-5.86	0.00[c]
R5P isomerase	2.09	-0.42	-1.49 (-3.56)
Ru5P epimerase	0.84	-0.42	0.00[c]
PRK	-21.77	-15.91	-31.26 (-33.69)

[a] from Bassham (1969), [b] from NAF data, [c] assumed to be at equilibrium to estimate concentrations of non-measured metabolites

4.4 Control of the flux through the Calvin-Benson cycle – a holistic view

From the analysis described above it is now possible to investigate the role of each enzyme from the Calvin-Benson cycle in terms of control of regeneration of RuBP under steady state

conditions. Enzymes that are substrate limited are responsive to changes of the substrate concentration, and if they catalyse reversible directions than they are also responsive to changes of the product concentration. If an enzyme is not substrate limited it is relatively insensitive to changes of the substrate concentration, but responsive to changes in the amount or activity status, e.g. via redox regulation, of the enzyme.

Rubisco: Rubisco catalyses the irreversible reaction of carboxylation or oxygenation of RuBP. With -25 kJ mol^{-1} change in free energy under the situation discussed here it is an irreversible reaction that is far from equilibrium. The Rubisco binding site is not filled with its substrate CO_2, and the concentration of RuBP is very close to the binding site concentration. Further the K_m for RuBP is very low, much lower than the binding site or the total metabolite pool. Any increase in RuBP will therefore lead to an increased number of RubisCO binding sites that are occupied by RuBP. The estimated CO_2 concentration (6 μM) is nominally in the same order as the K_m for CO_2 (10 μM). However if entry of CO_2 is a limiting factor, the actual concentration at the RubisCO active site may often be lower, while the K_m for CO_2 will be higher in the presence of atmospheric levels of the competititive inhibitor O_2. The *Km* for O_2 is 295 μM in tobacco. In presence of normal O_2 levels in the air (21 %) the *Km* for CO_2 will increase to approximately 20 μM (Terashima et al., 2006). Therefore Rubisco is likely to be responsive to any change in the concentrations of RuBP, CO_2 and O_2.

PGK: The change in Gibbs free energy could not be calculated for the reaction alone due to the lack of BPGA data. PGK is saturated with its substrates 3PGA and ATP and therefore relatively insensitive to any changes if the substrate concentrations.

NADP-GAPDH: The combined reactions of PGK and NADP-GAPDH show a negative change in free energy with a value of -16.14 kJ mol^{-1}. The concentrations of the substrate NADPH and the product $NADP^+$ are close to the binding site concentration of the enzyme and the concentration of NADPH (34 μM) is close to the Km for this metabolite (30 μM). It is possible that the activity of the enzyme is also directly regulated by the levels of $NADP^+$ that was shown to influence the activity of the $NADP^+$ dependent malate dehydrogenase in C_4 plants (Carr et al., 1999).

TPI: As GAP was not measured, to estimate its concentration the TPI reaction was assumed to be at equilibrium. The reaction is freely reversible *in vitro* and the activity is usually very high *in vivo*. The enzyme shows largely unfilled binding sites for GAP and DHAP. However, the levels

measured for DHAP might underestimate the real *in vivo* concentration, as pointed out above. The concentration of GAP is more than 300-fold lower than the K_m of the enzyme, therefore any change in the GAP concentration would influence the catalytic rate of TPI massively. The net reaction catalysed by TPI will be in the direction of conversion of GAP to DHAP. In order to test if the change of Gibbs free energy is influenced strongly by different ratios of GAP and DHAP the ΔG for the ratios DHAP:GAP 10:1 (ΔG = -1.83 kJ mol^{-1}) and 2:1 (ΔG = -5.82 kJ mol^{-1}) was calculated. Even relatively large changes in ratio of DHAP to GAP do not influence ΔG strongly.

Fru1,6BP aldolase: The aldolase reaction is reversible *in vitro*. Surprisingly under the *in vivo* conditions it shows a change of Gibbs free energy of 15.1 kJ mol^{-1}, which clearly favours the synthesis of DHAP and GAP. This can be explained by the fact that the DHAP levels that were measured in this study might underestimate the real *in vivo* concentration, which is discussed in chapter 6.2. The concentration of the substrates GAP and DHAP are lower than the catalytic binding site concentration of the enzyme and an increase in the concentration of these would increase the catalytic rate of aldolase. This would still be the case for GAP if the levels were about 7-fold higher as measured previously by Arrivault et al. (2009) and the concentration of DHAP would be slightly higher than the binding site concentration.

Fru1,6BPase: This reaction has a large negative Gibbs free energy change of -36 kJ mol^{-1} and so like almost all hydrolytic reactions is essentially irreversible. The binding site concentration of the enzyme is lower than the level of its substrate Fru1,6BP, and comparison with the K_m also reveals that it is relatively insensitive to changes in the substrate concentration. However, the enzyme is subject to feedback inhibition by its product Fru6P, and this is competitive to Fru1,6BP. This renders the enzyme more sensitive to changes of its substrate. Under the situation discussed here with 800 µM Fru6P and 96 µM Fru1,6BP this would decrease the catalytic activity of the enzyme by approximately 50 %, and with the alternative dataset by Arrivault et al. (2009) with 669 µM Fru6P and 335 µM Fru1,6BP by approximately 20 % (Gardemann et al., 1986).

Transketolase: In order to estimate the concentration of E4P in the stroma it was assumed that the TK reaction is close to equilibrium, as the reaction is freely reversible *in vitro*. For the two reactions that TK catalyses the binding site concentration is lower than the substrate concentration of Fru6P or Sed7P, but not for E4P or GAP. For both reactions, the flux is

therefore likely to depend strongly on the GAP level. As discussed above the GAP and E4P values here might be lower than the real *in vivo* levels. Even if the metabolite concentrations would be 7-fold higher for GAP and 1.2-fold higher for E4P (as estimated using the overall metabolite levels from Arrivault et al. (2009)), the binding site concentration would still be higher than the concentrations of these two metabolites. For the reaction involving Fru6P the K_m value is approximately 4-fold higher than the Fru6P concentration and a change in Fru6P concentration would influence the catalytic behaviour of the enzyme. In order to test if the change of Gibbs free energy is influenced strongly by different ratios of substrates and products the ΔG was calculated for a 10-fold equilibrium constant (ΔG = 5.71 kJ mol^{-1}) and a tenth of the equilibrium constant (ΔG = -5.71 kJ mol^{-1}). Even relatively large changes in ratio of substrates and products do not influence ΔG strongly.

Sed1,7BP aldolase: : Using the metabolite levels estimated from my measurements, this aldolase reaction appears to have a positive Gibbs free energy change of 12.6 kJ mol^{-1}, making it practically irreversible under the circumstances discussed here and driving the synthesis of DHAP and E4P. The flux during operation of the Calvin-Benson cycle would be in the opposite direction. This value might not reflect the *in vivo* situation as the DHAP and E4P concentrations are likely to be underestimated, as pointed out above and discussed in detail in chapter 6.2. The enzyme has unfilled binding sites for both substrates E4P and DHAP and therefore is likely to respond to changes in the substrate concentrations, even if the real *in vivo* levels were as high as measured by Arrivault et al. (2009).

Sed1,7BPase: This reaction has a large negative Gibbs free energy change of -38 kJ mol^{-1}. The enzyme binding site concentration is lower than the concentration of Sed1,7BP. The concentration Sed1,7BP is twice as high as the K_m. Therefore Sed1,7BPase is relatively insensitive to changes in the substrate concentration.

R5P isomerase: R5P isomerase has a moderate negative Gibbs free energy change of -1.5 kJ mol^{-1} and so is freely reversible. The concentration of the substrate R5P is approximately 100-fold lower than the K_m. R5P isomerase is therefore very likely to respond to a change in the substrate concentration.

Ru5P epimerase: The concentrations of substrate and product are both higher than the binding site concentration.

PRK: PRK has a negative Gibbs free energy change of -31 kJ mol^{-1} and catalyses an irreversible reaction. The catalytic binding site is only 50 % filled with the substrate Ru5P and the concentrations of both substrates, Ru5P and ATP, are below the respective K_m*s* and changes of either would influence the catalytic rate of PRK. The values of Ru5P and ATP might be underestimated as pointed out above. Use of the metabolite levels measured by Arrivault et al (2009) would put the concentrations of Ru5P and ATP slightly above the respective K_m value.

If the substrate concentration is much higher than the K_m this leads to a relative insensitivity of the flux to changes in substrate concentration through the cycle at this particular stage, unless the enzyme is regulated in a different way, e.g. redox regulation. Rising or falling substrate concentrations would not lead to big changes of the general flux through the cycle. This is especially the case for Rubisco. The bidirectional enzymes TPI, aldolase and R5P isomerase have unfilled binding sites. All three enzymes catalyze reactions that provide substrates for other biochemical pathways than the Calvin-Benson cycle. TPI precedes a branch point, producing DHAP, which can be retained in the Calvin-Benson cycle for regeneration of RuBP or can leave the chloroplast via the triose-phosphate:phosphate translocator to be used in the cytosol for sucrose synthesis. Transketolase and aldolase will influence the level of E4P, which is the substrate for the shikimate pathway that produces aromatic amino acids and aromatic secondary metabolites. Likewise, transketolase and R5P isomerase will influence the levels of R5P that can be used for the synthesis of nucleotides. Intuitively, branch points could be an effective site for regulation to determine partitioning of metabolites between the Calvin-Benson cycle and other pathways. This implies that there is a big flexibility at these steps of flux through the cycle to decrease the regeneration of RuBP and at the same time increase the flux into other biochemical pathways. This finding is strengthened by the observation that a moderate decrease of aldolase leads to a strong decrease of photosynthesis, altered carbon partitioning and growth inhibition in potato leaves (Haake et al., 1998).

The finding that the last three enzymes in the regeneration phase of RuBP, which are Ru5P epimerase, R5P isomerase and PRK show lower substrate concentrations than K_m values (Table 4-6) could indicate their important role for the regeneration of RuBP.

For the enzymes Rubisco, NADP-GAPDH, Fru1,6BPase, Sed1,7BPase and PRK it is known that they are activated in the light via the ferrodoxin/thioredoxin system. Additionally Fru1,6BPase,

Sed1,7BPase, PRK and Rubisco activities are dependent on the pH and the Mg^{2+} concentration, which change with varying light conditions and PRK and NADP-GAPDH activities are also controlled by binding with CP12 to form a multiprotein complex that also reacts to variations in light strength. These control mechanisms coordinate the activities of several enzymes in the cycle to adjust changes in the flux through the cycle in response to short term changes in environmental conditions, and to coordinate the Calvin-Benson cycle with the ATP and NADPH production of the light reactions. These sophisticated control mechanisms do not necessarily mean that these enzymes have a major influence on control of the flux through the cycle. These control mechanisms allow a fast adjustment to a changed flux through the cycle, and so these enzymes may be responding to a change in flux rather than initiating the change of the flux themselves (Stitt, 1996).

One way to assess the quantitative control of an enzyme for the flux of a pathway is to determine the flux control coefficient (FCC), which is defined as the fractional change in flux, which results from a fractional change in enzyme activity. The value is generally between 0 (no control) and 1 (rate limiting) although negative values are possible for enzymes in competing pathways. Experiments with mutants and transgenic plants have shown that changing the amount of a Calvin-Benson cycle enzyme can have a big influence on the flux through the cycle, but the specific contribution of each enzyme to overall control is greatly influenced by environmental conditions and only very rarely does a single enzyme exert complete control over flux in the sense of a classical “rate-limiting step”. Additionally a severe effect on the overall flux is usually only observed if the decrease in the amount of an enzyme is greater than 50 %. Transgenic tobacco plants with decreased Rubisco content showed that Rubisco has a strong control over net carbon fixation in limiting CO_2, but very little control in saturating CO_2 (Stitt et al., 1991). The flux control coefficient was determined to be between 0.2 and 0.8, depending on the environmental conditions. It has to be emphasized that Rubisco is the key player in control if CO_2 is limiting (Stitt, 1996). A decrease in the amount of plastidial GAPDH did not lead to altered 3-PGA levels (Price et al., 1995). A decrease in the amount of plastidial aldolase led to increased triose-phosphate levels, and decreased ribulose-1,5-bisphosphate and glycerate-3-phosphate levels (Haake et al., 1998). Tobacco plants with decreased transketolase enzyme had lower levels of RuBP and 3PGA, but increased levels of Fru6P (Henkes et al., 2001). A decrease in the

amount of sedoheptulose-bisphosphatase enzyme revealed lower sugar and starch levels (Olcer et al., 2001; Lawson et al., 2006). Table 4-8 shows the FCC for the Calvin-Benson cycle enzymes.

Table 4-8: Experimental estimates of flux control coefficients for enzymes in the Calvin–Benson cycle

Table was modified from Stitt et al. (2010b). The flux control coefficient (FCC) was estimated under ambient growth conditions.

Enzyme	FCC	Species	Reference	Comments
Rubisco	0.35	Tobacco	(Mate et al., 1993), (Stitt et al., 1991)	FCC under moderate light conditions. FCC is 1 in saturating light and 0 in low light.
Aldolase	0.2	Potato	(Haake et al., 1998)	Ambient photosynthesis is inhibited under a wide range of growth irradiances.
Fru1,6BPase	0.1-0.2	Tobacco	(Kossmann et al., 1994)	Rates under saturating CO_2 and high or low light. FCCs are overestimated because they are based on a transgenic line with more than 60% decrease in activity.
Transketolase	ND	Tobacco	(Henkes et al., 2001)	FCC=0.8 under saturating light and ambient CO_2, and 1 under saturating light and saturating CO_2. A small decrease in TK activity led to a decrease in aromatic amino acids and phenylpropanoids.
Sed1,7BPase	0.2-0.35	Tobacco	(Harrison et al., 2001), (Olcer et al., 2001)	FCC approaches 1 under saturating light and CO_2. Overexpression increases the rate of photosynthesis in tobacco (Lefebvre et al., 2005).
PRK	ND	Tobacco	(Paul et al., 1995)	FCC approaches 0.8 when plants that were grown under low light are transferred to high light (Paul et al., 2000).

Mathematical modelling of the Calvin-Benson cycle has also been used to assess the distribution of control of flux through the cycle. According to one model, assimilation flux is mainly controlled by Rubisco and Sed1,7BPase (Poolman et al., 2000), while a different model proposes GAPDH and transketolase to be key players (Fridlyand and Scheibe, 1999). This could mean that the distribution of control is not fixed and changes with different conditions or that the conclusions of the different models are wrong.

The data presented here shows that the non regulated enzymes TPI, aldolase, transketolase and R5P isomerase, which link RuBP regeneration in the Calvin-Benson cycle with different pathways have largely unfilled catalytic binding sites or substrate concentrations that are much lower than the respective K_m values, and catalyze bidirectional reactions. Small changes in the substrate/product ratio will greatly influence the catalytic rate at this particular stage of the pathway, while the other enzymes will be relatively insensitive to these changes. Figure 4-1 summarises the analysis performed in this thesis for the enzymes of the Calvin-Benson cycle.

Figure 4-1: Thermodynamic behaviour of the Calvin-Benson cycle enzymes under steady-state photosynthesis

The individual reactions are catalysed by the following enzymes: (1) RubiscCO; (2) PGK; (3) NADP-GAPDH; (4) TPI; (5) Fru1,6BP aldolase; (6) Fru1,6BPase; (7) transketolase; (8) Sed1,7BP aldolase; (9) Sed1,7BPase; (10) transketolase (11) R5P isomerase; (12) Ru5P epimerase; (13) PRK. Branch points to other pathways are indicated by blue arrows. Non-equilibrium steps are shown with red arrows. Enzymes that have unfilled catalytic binding sites are shown in green. Metabolites, which have concentrations below the K_m values of the corresponding enzyme, are shown in green and bold font.

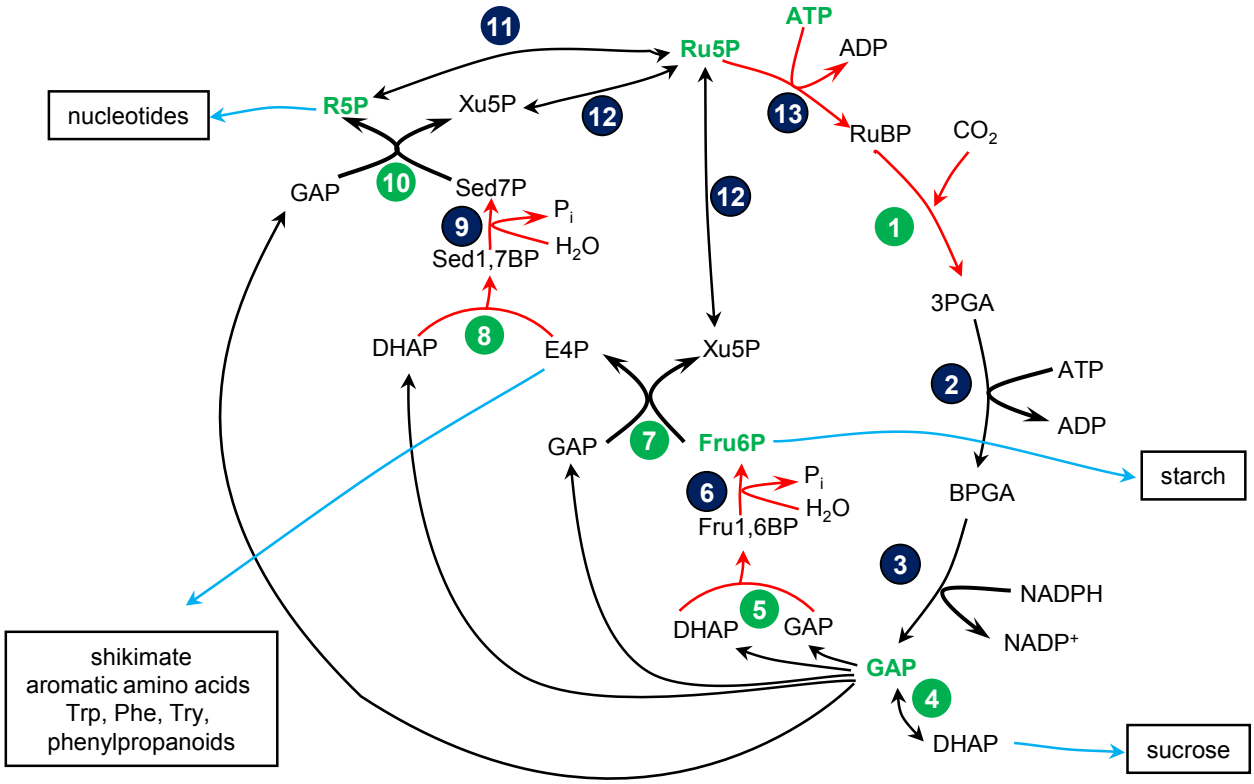

4.5 Comparison with existing Calvin-Benson-cycle models

Several mathematical models of the Calvin-Benson cycle have been published (Pettersson and Ryde-Pettersson, 1988; Fridlyand and Scheibe, 1999; Poolman et al., 2000; Poolman et al., 2001; Kreim and Giersch, 2007). The model by Pettersson and Ryde-Petterson (1988) is the only one that resolves the complete regeneration phase of RuBP and gives calculated values for nearly all metabolites. The model by Fridlyand and Scheibe (1999) uses measured values in sunflower leaves to calculate most of the other intermediates. In order to investigate the validity of these two comprehensive models the calculated values from both models are compared with the experimental data I obtained from *A. thaliana* leaves (Table 4-9).

Table 4-9: Comparison of measured and calculated Calvin-Benson cycle metabolite levels

Values were derived from the NAF analysis of *A. thaliana* leaves (this study) and calculated levels from the mathematical models of Pettersson et al. (1988), and Fridlyand and Scheibe (1999) for C_3 plants. The values based on the metabolite levels measured by Arrivault et al. (2009) are shown in parentheses. The levels in the Fridlyand model were based on measured amounts of some metabolites in sunflower leaves. (ND = not determined)

Metabolite	Stromal concentration [µM]		
	A. thaliana	after Petersson et al.	after Fridlyand et al.
3PGA	3297 (1137)	590[a]	11700
ADP	147 (235)	ND	ND
ATP	441[a] (705)	390[a]	ND
DHAP	26 (204)	270[a]	840
E4P	2[a] (3)	40[a]	50[a]
Fru1,6BP	96 (335)	24[a]	ND
Fru6P	800 (669)	1360[a]	1400
GAP	1.3[a] (10)	10[a]	ND
NADP+	67 (47)	ND	ND
NADPH	34[a] (23)	210[a]	ND
R5P	9 (26)	60[a]	150[a]
Ru5P	37 (243)	20[a]	60[a]
RuBP	596 (1505)	140[a]	5200
Sed7P	353 (1103)	220[a]	400[a]
Sed1,7BP	110 (321)	130[a]	300
Xu5P	55[a] (362)	40[a]	90[a]

[a] calculated values

Comparison of the values in the two different models already shows that the range of predicted concentrations can differ enormously, for example by a factor of more than 30 for RuBP.

Nonetheless most of the metabolites measured here fall within the range of the predicted values of the two different models. The variations can partly be explained by the fact that the models use different environmental conditions. The mathematical model of Pettersson and Ryde-Pettersson (1988) assumes a fixed external orthophosphate concentration of 0.5 mM, which gives results that are in relatively good agreement with experiments with isolated chloroplasts and an external orthophosphate concentration of 0.5 mM (Portis et al., 1977). However, this assumption might not reflect the *in vivo* situation in intact plant leaf tissue, as the cytosolic orthophosphate concentration is reported to be 0.07 mM, which is about 7-fold lower than the value used in the model (Pratt et al., 2009). This is likely to have a strong effect on the predicted rate of withdrawal of triose-phosphates from the chloroplast via the triose-phosphate/phosphate translocator and thus influence the levels of the other Calvin-Benson cycle intermediates in the plastid stroma. Some of the metabolite levels in the Fridlyand model were derived from experimental measurements in sunflower leaves, and the others were calculated based on the measured metabolites. Differences in the levels of the metabolites can be explained by species dependent differences and also by the assumption that the stromal volume is 30 µl [mg Chl]$^{-1}$, in contrast to the calculations from the *A. thaliana* data, which assumed a stromal volume of 65 µl [mg Chl]$^{-1}$. The levels of most metabolites measured in *A. thaliana* leaves are in the range that is predicted by the two different models, with the exception of DHAP, GAP, E4P and R5P. The relatively low levels of these metabolites in *A. thaliana* compared with the two models can partly be explained by species dependent differences or differences in the environmental conditions, as the sunflower were grown in longer photoperiods and with higher irradiance. Nonetheless the DHAP levels that were measured in this study, and consequently GAP and E4P levels are likely to underestimate the real *in vivo* concentration, as discussed above. Use of the total levels of metabolites measured by Arrivault et al. (2009) leads to a better agreement of the predicted concentrations of DHAP and GAP, but not E4P of the two models.

4.6 Conclusions

The systemic comparison of the levels of Calvin-Benson cycle intermediates with the catalytic properties revealed new information about the regulation of the cycle. The metabolite levels that are measured here reflect the *in vivo* situation in intact leaf tissue at steady state photosynthesis. Levels of these metabolites in isolated chloroplasts or protoplasts deviate a lot from the levels in leaves and are therefore not suitable for the investigation of their potential role in regulation. For

the first time a nearly complete set of these intermediates is measured with subcellular resolution in higher plant leaves.

Comparison of metabolite concentrations with catalytic binding site concentrations and K_m values of the corresponding enzymes shows the regulatory potential of the readily reversible enzymes TPI, aldolase, transketolase and R5P isomerase. These enzymes are also the branch points to other biochemical pathways, i.e. carbon export from the chloroplast for sucrose synthesis, shikimate pathway and nucleotide biosynthesis. The fitness of a plant depends on how successful it is at balancing various demands for carbon for growth and other processes given the prevailing experimental conditions and nutrient availability. At a biochemical level this is reflected in the distribution of photoassimilate between the Calvin-Benson cycle, allowing further carbon acquisition, sucrose and starch synhthesis for growth and survival through the night, and allocation of carbon to secondary metabolite synthesis for defence against pathogens or abiotic stress. Taking these thoughts into account it makes sense that the enzymes in the cycle that are the branch points between RuBP regeneration and provision of substrates for other pathways can have a major influence on the flux through the Calvin-Benson cycle. In the next chapter I will investigate the metabolic control of two of the major fluxes out of the Calvin-Benson cycle, namely starch and sucrose synthesis.

Chapter 5: Control of carbon end product metabolism

5.1 Introduction

There are two main end products of carbon fixation, i.e. sucrose and starch. Sucrose is the mobile transport sugar that is exported from the leaves (source) to other parts of the plant that are not photosynthatically active (sinks), such as the roots, to provide them with energy for metabolism and growth. Starch is synthesised in the chloroplast during the day and acts as an energy reserve for the night. Starch is also an integrating factor for the regulation of plant growth, as it negatively correlates with biomass (Sulpice et al., 2009). The triose-phosphates DHAP and GAP are either exported to the cytosol via the triose-phosphate/phosphate translocator (Fliege et al., 1978) or they remain in the plastid stroma. The triose-phosphates that remain in the chloroplast are converted to Fru1,6BP by means of Fru1,6BP aldolase, which is used by Fru1,6BPase to make Fru6P. Fru6P is isomerised to Glc6P by PGI and subsequently converted into Glc1P by PGM. Glc1P acts together with ATP as the substrates for the synthesis of ADPGlc by AGPase, which is the direct precursor for starch, the main carbon end product in the plastid. This generally accepted scheme for the synthesis of starch has been challenged by the hypothesis that most of the ADPGlc is synthesized in the cytosol via ADP-mediated cleavage of sucrose by sucrose synthase, and then transported into the plastid via an ADPGlc transporter in the plastid envelope (Baroja-Fernandez et al., 2004). According to this theory, starch synthesis would be dependent on previous sucrose synthesis. ADPGlc is used by starch synthase to elongate an existing glucose chain and thus increases the starch content. The branching and debranching enzymes introduce defined branch points into the linear glucose chain, making the starch molecule a densely packed glucose polymer molecule that is osmotically inert (Zeeman et al., 2007). Starch acts as a storage reserve, which can be mobilized in the night to provide the plant with reduced carbon for its metabolism. This is mainly achieved by the action of β-amylase that cleaves off maltose units from the starch granule. The maltose is transported to the cytosol by the maltose transporter MEX1 for respiration or sucrose synthesis (Niittylä et al., 2004; Weise et al., 2004; Smith et al., 2005).

The triose-phosphates that leave the chloroplast are mainly used for the synthesis of the second main end product of carbon fixation, i.e. sucrose. The same reactions as for starch biosynthesis up to Glc1P are carried out by cytosolic isoforms of Fru1,6BP aldolase, Fru1,6BPase, PGI and

PGM. Then UGPase uses Glc1P and UTP to make UDPGlc, which is used by SPS in combination with Fru6P to form Suc6P. The phosphate group of Suc6P is cleaved off by sucrose phosphatase to form sucrose (Lunn and MacRae, 2003). Sucrose is the main transport sugar in plants and can be moved via the phloem stream to non-photosynthesizing parts of the plant, e.g. the roots.

Sucrose and starch metabolism, including degradation of starch during the night, are controlled at various levels to guarantee an appropriate balance between the two end products and to guarantee sufficient provision of carbon during the diurnal cycle. AGPase is redox regulated by the ferrodoxin/thioredoxin system and is only active in the light, which prevents starch synthesis during the night. Additionally AGPase is activated by a high 3PGA/P_i ratio (Ghosh and Preiss, 1966), which is an indirect measure of the availability of triose-phosphates and how much is being exported to the cytosol. If less P_i is released in the cytosol because sucrose synthesis is restricted, then less P_i enters the chloroplast and more triose-phosphates remain in the chloroplast and can be used for starch synthesis. Sucrose synthesis is regulated by a feed forward mechanism involving Fru2,6BP, which is an inhibitor of the cytosolic Fru1,6BPase. If the levels of triose-phosphate in the cytosol rise the level of Fru2,6BP drops and as a consequence the activity of cytosolic Fru1,6BPase will be increased (Stitt and Heldt, 1985; Stitt, 1987), which ultimately provides the substrates and the allosteric activators of SPS leading to sucrose biosynthesis. SPS is also regulated by reversible multi-site protein phosphorylation (Lunn and MacRae, 2006). This is especially important for the regulation of night-time sucrose synthesis from starch, which bypasses the cytosolic Fru1,6BPase and so is not regulated by Fru2,6BP. Tre6P may act as a signal of the sucrose status in the cytosol and thereby coordinate sucrose and starch metabolism (for a more detailed description of starch and sucrose metabolism, see section 1.4.2). Rising sucrose levels lead to increased Tre6P levels and Tre6P promotes the redox activation of AGPase, which increases starch synthesis (Kolbe et al., 2005; Lunn et al., 2006). Tre6P is synthesised by only a single enzyme that is localised in the cytosol, i.e. trehalose6-phosphate synthase1 (TPS1). So far it has not been shown how Tre6P mediates the redox activation of AGPase, i.e. whether it enters the chloroplast and interacts directly with AGPase and thioredoxins, or if it acts externally through some interaction at the chloroplast envelope.

In this chapter I want to resolve in which part of the cell ADPGlc is synthesised and thus distinguish between the contradictory theories about the pathway of starch synthesis. In order to

do so I show the subcellular distribution of ADPGlc in wild type plants and ADPGlc levels in *pgm* and *adg1* mutants that are deficient in plastidial PGM and AGPase activities, respectively.

I also investigated the subcellular localisation of Tre6P, to see if this signal metabolite is present in the chloroplast, which would be consistent with a direct interaction with AGPase/thioredoxin, or if it is restricted to the cytosol, which would suggest a less direct role of action in redox activation of AGPase.

In addition to these specific aims, I also look at the pathways of sucrose and starch synthesis as a whole. A comprehensive analysis of the *in vivo* levels of the metabolites with the catalytic properties of the corresponding enzymes was done to further our understanding of how these competing pathways are regulated and coordinated with each other. The comparative analysis with the dataset from Arrivault et al (2009) was not performed for the synthesis pathways of sucrose and starch, as the levels of the pathway intermediates are very similar (Table 4-2). Possible shading for a fraction of a second seems not to influence these pathways, like it does for the Calvin-Benson cycle. This is understandable because the turnover times of the pools in end-product synthesis are much lower than those of the Calvin-Benson cycle intermediates (Stitt et al., 1980; Arrivault et al., 2009).

5.2 The role of ADPGlc in starch synthesis in photosynthetically active cells

In the heterotrophic tissue of cereal endosperms the precursor of starch, ADPGlc is synthesized in the cytosol by a cytosolic AGPase (Denyer et al., 1996) and is then imported into the amyloplast by the BRITTLE-1 transporter (Shannon et al., 1998). In leaves AGPase is exclusively localised in the chloroplast, and so the chloroplasts have generally been regarded as the only sites of ADPGlc synthesis in leaves (Zeeman et al., 2002).

This generally accepted pathway of starch synthesis in leaves has been called into question. The alternative theory claims that the direct precursor of starch ADPGlc is not synthesized in the chloroplast by means of AGPase, but by the ADP-mediated cleavage of sucrose in the cytosol by means of sucrose synthase, with subsequent import of ADPGlc via an adenylate translocator into the chloroplast (Pozueta-Romero et al., 1991a). These reactions would directly link sucrose and starch biosynthesis (Baroja-Fernandez et al., 2001). The alternative theory is based on a series of

experiments carried out by Pozueta-Romero and co-workers. Expression of a bacterial ADPGlc-cleaving adenosine diphosphate sugar pyrophosphatase in the cytosol of potato leaves led to reduced ADPGlc and starch levels, while expression of this enzyme in the chloroplast had no effect on the starch levels (Baroja-Fernandez et al., 2004). Further evidence to support the theory came from overexpression of sucrose synthase in transgenic potato leaves, which showed elevated levels of ADPGlc and starch, while a decrease in the amount of sucrose synthase had the opposite effect. In addition, it was reported that transgenic *A. thaliana* plants that lack plastidial phosphoglucomutase or AGPase have normal levels of ADPGlc (Munoz et al., 2005). The mutant plants lacking the plastidial phosphoglucomutase or AGPase are essentially starchless. To account for this observation, the alternative theory invokes a role for these enzymes in turnover and resynthesis of starch in the plastid (Baroja-Fernandez et al., 2005). Although the results of Pozueta-Romero and colleagues cannot be fully explained on the basis of the classical textbook view of starch synthesis, their alternative theory of starch synthesis challenged on the grounds that it fails to account for some well established observations, e.g. from starch deficient mutants, and so has not been widely accepted by the plant science community (Neuhaus et al., 2005).

The most important arguments against this theory are as follows. There is no evidence for a permanent turnover of starch during the day, so the starchless phenotype of the *pgm* and *adg1* mutants cannot be explained if there is substantial import of ADPGlc from the cytosol as the alternative theory proposes. Inhibition of enzymes needed for sucrose synthesis including the cytosolic PGI and Fru1,6BPase, led to lower sucrose but higher starch levels, which does not fit to a sucrose dependent starch synthesis (Neuhaus et al., 1989; Zrenner et al., 1996). Potato plants that have decreased transport activity of the triosephosphate/phosphate translocator have elevated levels of starch and reduced levels of sucrose, which also argues against a sucrose dependent pathway of starch synthesis (Riesmeier et al., 1993). Mutants that are impaired in starch degradation were crossed with the starchless *pgm* mutant and the progeny were still starchless, which is also consistent with a predominant synthesis of ADPGlc in the chloroplast rather than the cytosol (Streb et al., 2009). A mutant impaired in plastidial PGI is also essentially starchless, which argues against the turnover and resynthesis of starch (Yu et al., 2000). Finally, quadruple *A. thaliana* knockout mutants that lack all four of the cytosolic sucrose synthase isoforms expressed in mesophyll cells have normal starch levels (Barratt et al., 2009), showing that sucrose synthase is not required for starch synthesis. Despite this apparently overwhelming evidence

against the alternative pathway, Pozueta-Romero and colleagues continue to challenge the conventional pathway of starch synthesis (Baroja-Fernandez et al., 2009).

The vast majority of experimental evidence argues against the alternative theory of starch synthesis. Nonetheless so far the intracellular distribution of ADPGlc has not been rigorously determined. Here the non-aqueous fractionation technique has been used to measure the ADPGlc levels and the intracellular distribution between chloroplast and cytosol in leaves of wild type *A. thaliana* Col-0 plants. In leaves harvested in the light the level of ADPGlc was found to be 1.77 nmol g FW^{-1}. Previous published data measured by an HPLC technique indicated ADPGlc levels levels in wild type and the starch deficient *pgm* and *adg1* mutants that were about 7-fold lower than this, at around 0.25 nmol g FW^{-1} (Munoz et al., 2005). This is in the range of the levels that were measured in the *pgm* and *adg1* mutants here (Table 5-1), which were 0.38 and 0.07 nmol g FW^{-1}, respectively.

Table 5-1: Comparison of ADPGlc levels in *A. thaliana* Col-0 wild type, *adg1* and *pgm* leaves

Plant genotype	**ADPGlc level [nmol g FW^{-1}]**
Col-0	1.77
pgm	0.38
adg1	0.07

The measurements performed in this study via an LC-MS/MS technique (Arrivault et al., 2009) are far more sensitive and reliable than the HPLC technique, because of the highly specific mass-based detection system used in the LC-MS/MS approach and the use of internal standards to correct for ion suppression and interference by other compounds in the plant extract.

The general difference in ADPGlc levels between wildtype and the two starch deficient mutants already argues in favour for the classical pathway of starch synthesis, but the subcellular distribution of ADPGlc in wild type leaves provides even stronger proof. In wild type leaves ADPGlc was found to be localised exclusively in the chloroplast (see Table 3-5). This finding clearly supports the classical starch synthesis with ADPGlc synthesis in the chloroplast by means of ADPGlc pyrophosphorylase. Nonetheless the very low but detectable levels of ADPGlc found in the *pgm* and *adg1* mutants indicate that ADPGlc might also be produced via an AGPase independent route possibly by sucrose synthase in the cytosol, but this ADPGlc is not available for starch synthesis. In comparison to wild type plants, the levels of ADPGlc were about 6-fold

lower in the *pgm* mutant and 35-fold lower in *adg1* mutant. The higher levels of ADPGlc in *pgm* compared to *adg1* might be explained by the elevated sucrose levels in *pgm* than in wild type plants, possibly leading to higher rates of ADPGlc production via sucrose synthase. The physiological significance of the presumed cytosolic pool of ADPGlc is unclear. Cytosolic ADPGlc might be a dead end pool, since no reactions are known that consume ADPGlc in the cytosol besides sucrose synthase in the reverse direction.

The finding that ADPGlc is exclusively localised to the chloroplast in wild type plants adds further weight to the evidence from the quadruple sucrose synthase knockout mutant, which has wild type starch levels (Barratt et al., 2009), and the starch degradation mutants in a *pgm* background, which were starchless (Streb et al., 2009). Taken all these observations into account this leads me to the reject the alternative theory for the pathway of starch synthesis. Therefore all further discussion is based in the classical pathway of starch synthesis.

5.3 Calculation of concentrations of metabolites, comparison with K_m values and binding sites of the corresponding enzymes

In order to analyse the competing pathways of sucrose and starch synthesis in more detail, the estimated enzyme concentrations from the proteomics analysis are set into relation with K_m values of the enzymes and the concentrations of the corresponding metabolites (Table 5-1 and 5-3). The information about the catalytic characteristics of the enzymes has been taken from the BRENDA database. The change in Gibbs free energy for each reaction under the steady-state conditions discussed here was calculated (Table 5-2 and 5-4).

5.3.1 Starch synthesis

Table 5-1 shows a comparison of metabolite levels and enzyme properties in the pathway of starch synthesis, and the factors that are likely to influence the activities of the individual enzymes are discussed below.

Table 5-2: Comparison of starch synthesis enzyme concentrations with concentrations of the corresponding substrates, products and K_m values
K_m values are used from the BRENDA database. All values were determined in spinach, except phosphoglucomutase (*Pisum sativum*) and starch synthase and AGPase (*Arabidopsis thaliana*). The plastidial pyrophosphate concentration was estimated based on measurements of cytosolic pyrophosphate concentration by Weiner et al. (1987). Calculated are ratios of the substrate concentration against the binding site concentrations and the K_m values.

Enzyme	active binding site concentration [µM]	Reactant	Concentration in plastid [µM]	K_m [µM]	$\frac{[reactant]}{[binding\ site]}$	$\frac{[reactant]}{K_m}$
pPGI	0.3	**Fru6P**	800	300	2666	2.7
		Glc6P	452	580	1506	0.8
pPGM	7	**Glc6P**	452	NA	64.3	ND
		Glc1P	14	360[b]	2	0.04
AGPase	3	**Glc1P**	14	60	4.7	0.2
		ATP	441	73	147	6
		ADPGlc	27	100[d]	9.1	ND
		PP_i	1[a]	NA	0.3	ND
Pyrophosphatase	ND	**PP_i**	1[a]	70[c]	ND	0.01
		P_i	4000[c]	NA	ND	ND
Starch synthase	ND	**ADPGlc**	27	280	ND	0.1
		starch	ND	NA	ND	ND
		ADP	147	NA	ND	ND

[a] spinach data from Weiner et al. (1987), [b] pea, [c] *A. thaliana* data from Pratt et al. (2009), [d] *A. thaliana* data from Haedrich et al. (unpublished)

Table 5-3: Change of Gibbs free energy for starch synthesis
Values for standard $\Delta G^{0'}$ have been taken from Tiessen et al. (2002). Steady-state ΔG for the *A. thaliana* NAF gradient data has been calculated by computing the mass action ratio for each enzyme on the basis of product and substrate concentration and using the formula: $free\ energy\ change\ in\ vivo = \Delta G = \Delta G^{0\prime} + RT\ ln\ (MAR)$. Steady-state ΔG for starch synthase was not calculable due to lack of metabolite data or values for standard $\Delta G^{0'}$. For the PPase reaction $[H_2O]$ = 55.5 M was used.

Enzyme	standard $\Delta G^{0'}$ [kJ mol^{-1}]	steady-state ΔG [kJ mol^{-1}] in *A. thaliana*
PGI	-3.2[a]	-1.8
PGM	6.9	-1.7
AGPase	0	-13.5
PPase	-17.1	-20.2

PGI: The change in free energy is with -1.8 kJ mol^{-1} small and the reaction is freely reversible. The concentrations of substrate and product exceed the binding site concentration by a factor of more than 1000. The concentration of the substrate Fru6P is nearly 3-fold higher than the

respective K_m, while the product concentration of Glc6P is very close to the respective K_m. Thus moderate changes of the concentration of the product Glc6P would influence the catalytic rate of the cPGI reaction.

PGM: The chloroplastic PGM catalyses a freely reversible reaction with a Gibbs free energy change of -1.7 kJ mol^{-1}. The concentration of the substrate Glc6P is about 64-fold higher than the binding site concentration. For the product Glc1P the concentration is about twice as high as the binding site concentration. Comparison with the K_m for the product Glc1P, which is about 25-fold higher than the concentration, shows that the reaction is relatively insensitive to changes in the product concentration and that the PGM reaction operates the direction of Glc1P production.

AGPase: The AGPase reaction has a negative Gibbs free energy change of -13.5 kJ mol^{-1} *in vivo*, which makes the reaction essentially irreversible. The standard free energy change is very low, i.e., at equilibrium the combined concentrations of the substrates are similar to the combined concentrations of the products. However, the back reaction of ADPGlc to its substrates Glc1P and ATP is prevented by the removal of PP_i by the irreversible alkaline pyrophosphatase reaction (ΔG = -20.2 kJ mol^{-1}). This differs to the situation for the chemically similar reaction catalysed by UGPase in the cytosol (see below). The concentration of Glc1P is 5-fold lower than the respective K_m.

Starch synthase: The concentration of the substrate ADPGlc is about 10-fold lower than the respective K_m. It was not possible to estimate the Gibbs free energy because of the difficulty of measuring the effective concentration of starch.

The comparison of the catalytic binding sites of PGI, PGM and AGPase with the corresponding metabolite concentrations involved in starch biosynthesis shows that the enzymes are present at much lower concentrations than their substrates. No peptides were found for pyrophosphatase, soluble starch synthase I – IV or granule bound starch synthase. Therefore the binding site concentration for those enzymes could not be estimated. Comparison of the K_m values of the enzymes with the metabolite concentrations in the stroma shows that the substrate concentrations for the AGPase reaction (Glc1P) and starch synthase (ADPGlc) reactions are lower than the respective K_m values. Changes in the substrate concentration at these steps in the pathway would therefore be expected to affect starch synthesis more strongly than at the steps catalysed by PGI and PGM. This situation is radically different to the situation in the Calvin-Benson cycle, where

many of the enzymes show a much higher active binding site concentration in comparison to the substrate concentration.

Analysis of regulatory steps in a pathway depends not only on *in vivo* levels of substrates and products but also on *in vivo* levels of activating and inhibiting metabolites. Unfortunately such data is very limited and only available for very few enzymes in plants. For AGPase a detailed analysis of inhibitory properties has been carried out with the purified spinach enzyme (Ghosh and Preiss, 1966). The inhibitor constant K_i is the dissociation constant of an enzyme-inhibitor complex. The K_i value indicates the concentration range of the inhibitor that will affect the catalytic activity of an enzyme by binding either to the catalytic site of the enzyme (competitive inhibition) or an allosteric regulatory site of the enzyme (non competitive inhibition). Competitive inhibitors are very often close analogues of the substrate, and increase the K_m for the substrate with which they compete, but do not alter the maximum catalytic activity of the enzyme. A non competitive inhibitor does not alter the K_m but lowers maximum catalytic activity. Whatever the mode of action, accumulation of an inhibitor will alter the reaction rate at this particular step and thereby is also likely to influence the flux of the whole pathway. If the concentration of such an inhibitor is close to the K_i value of the enzyme it indicates that significant inhibition of the enzyme will be occurring *in vivo*. AGPase is inhibited by a high phosphate and a low 3PGA concentration. A ratio of P_i/3PGA of approximately 10 decreases the activity by 50% in vitro (Ghosh and Preiss, 1966). The ratio of P_i/3PGA *in vivo* is 1.2 and the inhibitory effect on AGPase relatively weak. AGPase is also inhibited competitively by ADP at the ATP binding site and the K_i value was determined to be 1.2 mM (Ghosh and Preiss, 1966), but the *in vivo* concentration of ADP, calculated to be 0.14 mM, is nearly 10-fold lower than the K_i. The K_m value for ATP is 0.073 mM, but the *in vivo* concentration, estimated to be 0.441 mM, is 6-fold higher than the K_m. Comparison of these values indicates that inhibition of AGPase by ADP and P_i is very low and its influence on the total overall flux is likely to be negligible. Figure 5-1 gives an overview of the contribution of metabolic control of starch synthesis at each individual step.

Figure 5-1: Control of starch synthesis

The individual reactions are catalysed by the following enzymes: (1) PGI; (2) PGM; (3) AGPase; (4) Alkaline pyrophosphatase; (5) Starch synthase. Irreversible steps are shown with red arrows. All enzymes are at lower concentrations than their substrates. Metabolites, which have concentrations below the K_m values of the corresponding enzyme, are shown in green and bold font.

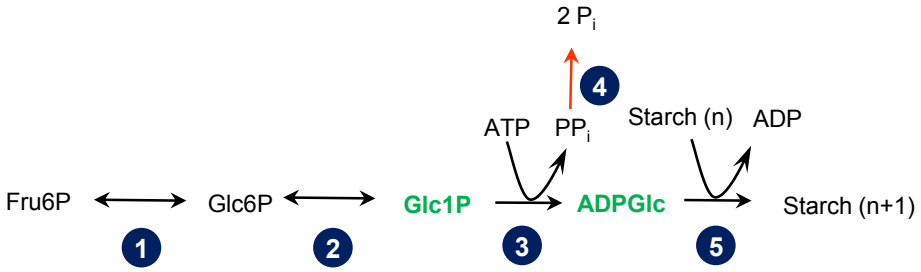

5.3.2 Sucrose synthesis

Table 5-3 shows a comparison of metabolite levels and enzyme properties in the pathway of sucrose synthesis, and the factors that are likely to influence the activities of the individual enzymes are discussed below.

Table 5-4: Comparison of sucrose synthesis active site enzyme concentrations with concentrations of the corresponding substrates, products and K_m values

K_m values are used from the BRENDA database. Calculated are ratios of the substrate concentration against the binding site concentrations and the K_m values. Values in italics are taken from the literature. For PP_i from Weiner et al. (1987), for P_i from Pratt et al. (2009) and for UDP and UTP from Dancer et al. (1990). (NA = no data available, ND = not determined).

Enzyme	active binding site concentration [µM]	Reactant	Concentration [µM]	K_m [µM]	$\frac{[reactant]}{[binding\ site]}$	$\frac{[reactant]}{K_m}$
cTPI	16	**GAP**	12	440[b]	0.7	0.03
		DHAP	234	NA	14.6	ND
cAldolase (Fru1,6BP)	415	**GAP**	12	NA	0.03	ND
		DHAP	234	NA	0.6	ND
		Fru1,6BP	112	2.3[a]	0.3	48.5
cFru1,6BPase	1	**Fru1,6BP**	112	1.5[a]	112	74.4
		Fru6P	4211	NA	4211	ND
		P_i	*75*[c]	NA	75	ND
cPGI	0.9	**Fru6P**	4211	300	4679	14.0
		Glc6P	5980	580	6644	10.3
cPGM	19	**Glc6P**	5980	NA	314	ND
		Glc1P	448	360[b]	23.5	1.2
UGPase	6	**Glc1P**	448	140[c]	74.7	3.2
		UTP	*700*[a]	31[c]	116.7	22.6
		UDPGlc	1989	40[c]	331.5	49.7
		PP_i	*300*[a]	NA	50	ND
SPS	5	**UDPGlc**	1989	1300[a]	397	1.5
		Fru6P	4211	800[a]	842	5.3
		Suc6P	41.0	NA	8.2	ND
		UDP	*350*[a]	NA	70	ND
SPP	ND	**Suc6P**	41.0	105[a]	ND	0.4
		sucrose	46 mM	NA	ND	ND
		P_i	*75*[c]	NA	ND	ND

[a] spinach data from Weiner et al. (1987) or Dancer et al. (1990), [b] pea, [c] *A. thaliana* data from Pratt et al. (2009)

Table 5-5: Change of Gibbs free energy for sucrose synthesis

Values for standard $\Delta G^{0'}$ have been taken from Lunn et al. (1990) and for the cFru1,6BPase from Newsholme and Leech (1983). Steady-state ΔG for the *A. thaliana* NAF gradient data has been calculated by computing the mass action ratio for each enzyme on the basis of product and substrate concentration and using the formula: $free\ energy\ change\ in\ vivo = \Delta G = \Delta G^{0\prime} + RT\ ln\ (MAR)$. Steady-state ΔG for cytosolic TPI and Fru1,6BPase aldolase, was not calculable due to lack of metabolite data or values for standard $\Delta G^{0'}$. For the cFru1,6BPase and the sucrose phosphatase reaction [H_2O] = 55.5 M was used.

Enzyme	standard $\Delta G^{0'}$ [kJ mol^{-1}]	steady-state ΔG [kJ mol^{-1}] in *A. thaliana*
cFru1,6BPase	-8.6	-33.1
cPGI	-3.2	-2.3
cPGM	7.3	0.87
UGPase	2.9	4.5
SPS	-5.7	-21.5
SPP	-16.5	-32.6

cTPI: The concentration of GAP is lower than active binding site concentration and nearly 40-fold lower than the K_m. The reaction is therefore relatively sensitive to changes in the concentration of GAP, even if the values were underestimated, as discussed in chapter 4.

cAldolase (Fru1,6BP): The concentration of GAP and DHAP is lower than the respective binding site concentration, although the actual *in vivo* concentration of DHAP and GAP might be 7-fold higher. Then the concentration of DHAP but not GAP would be higher than the binding site concentration. The concentration of the product Fru1,6BP is nearly 50-fold higher than the respective K_m. Due to uncertainty about the measurement of the DHAP concentration ΔG has not been calculated.

cFru1,6BPase: With a Gibbs free energy change of -33.1 kJ mol^{-1} this reaction can be considered to be irreversible *in vivo*. The concentration of the substrate Fru1,6BP is far above the binding site concentration of the enzyme and the respective K_m. The K_m value of the cytosolic Fru1,6BPase is very dependent on the concentration of the competitive inhibitor Fru2,6BP (Stitt and Heldt, 1985), but Fru2,6BP was not measured in this study.

cPGI: With a Gibbs free energy change of -2.3 kJ mol^{-1} this reaction is freely reversible and close to equilibrium. The concentrations of Fru6P and Glc6P are several thousand times higher than the catalytic binding site concentration and at least 10-fold higher than the respective K_m values. Thus the enzyme is relative insensitive to changes in the concentrations of either of these hexose-phosphates.

cPGM: The cytosolic PGM reaction has a small positive Gibbs free energy change of 0.87 kJ mol^{-1}, indicating that the reaction is likely to be freely reversible, and the substrate concentration is higher than that of the enzymes´ binding sites. The concentration of Glc1P is relatively close to the respective K_m value of PGM, and thus moderate changes in the concentration of Glc1P could influence the catalytic rate.

UGPase: The reaction has a moderate positive ΔG of 4.5 kJ mol^{-1}, and is slightly displaced from equilibrium under the conditions discussed here. This could be because values for the concentration of pyrophosphate are taken from published data for spinach leaves and not in *A. thaliana* leaves. The enzyme is completely filled with its substrates and the concentrations are at least 3-fold higher than the respective K_m values. Therefore UGPase will be relatively insensitive to changes in the concentration of substrates and products. It must however be taken into account that the various products and substrates may act as competitive inhibitors for each other.

SPS: The SPS reaction has a strong negative ΔG of -21.5 kJ mol^{-1}, and is far removed from equilibrium *in vivo* and can be considered to be irreversible. The concentration of the substrates exceeds the catalytic binding site concentration by a factor of at least 390. The concentration of UDPGlc is only slightly higher than the respective K_m. Therefore SPS will be mainly sensitive to changes of UDPGlc.

SPP: The SPP reaction has a strong negative ΔG of -32.6 kJ mol^{-1}, and is far removed from equilibrium *in vivo* and can be considered to be irreversible. The concentration of the substrate Suc6P is about 60 % lower than the K_m value of Suc phosphatase. An increase of Suc6P concentration would enhance the catalytic rate of this enzyme massively.

For sucrose biosynthesis a similar observation as for starch biosynthesis can be made. With the exception of the Fru1,6BP aldolase, all enzymes in the pathways are present at much lower concentrations than their substrates and products. SPP has to be excluded from this conclusion because no proteomics data was available. Comparison of the K_m values with the metabolite concentrations reveals that for the last two steps in the pathway, SPS and SPP, the substrate concentrations, UDPGlc and Suc6P, are very close to the respective K_m*s*. Again changes in the substrate concentration for these reactions would have a much stronger effect on sucrose biosynthesis than at the other steps in the pathway catalysed by TPI, aldolase, Fru1,6BPase, PGI, PGM and UGPase. The cytosolic Fru1,6BPase (Jang et al., 2003) and SPS (Harbron et al., 1981;

Amir and Preiss, 1982) have important regulatory properties. The K_i values are compared with the *in vivo* metabolite concentrations. For spinach leaf SPS Suc6P acts as a competitive inhibitor towards UDPGlc and the K_i value was determined to be 0.4 mM (Amir and Preiss, 1982), however the *in vivo* concentration for Suc6P is only 0.041 mM, which is approximately 10-fold lower than the K_i. Therefore it can be concluded that inhibition of the SPS reaction by Suc6P is minimal under the conditions discussed here. The same holds true for the inhibition of SPS by Fru1,6BP, which is a competitive inhibitor towards Fru6P. Here the K_i value was determined to be 0.8 mM (Harbron et al., 1981), while the *in vivo* concentration of Fru1,6BP in the cytosol is only 0.12 mM, i.e. more than 6-fold lower. Glc6P is a allosteric activator of SPS, acting to increase the affinity for Fru6P and UDPGlc (Reimholz et al., 1994), and P_i acts antagonistically to Glc6P. For the pea cytosolic Fru1,6BPase the K_i value of the non competitive inhibitor AMP is 0.12 mM (Herzog et al., 1984; Jang et al., 2003), while the *in vivo* concentration of AMP in the cytosol is 0.13 mM, which is very close to the K_i. Here the concentration of AMP will lead to a significant inhibition of the Fru1,6BPase, and could at least partially restrict the flux to sucrose. Fru2,6BP is a powerful competitive inhibitor of the cytosolic Fru1,6BPase (Herzog et al., 1984), but the concentration of this inhibitior was not measured in the current study. But it can be assumed that it is present in *A. thaliana* leaves and will act synergistically with AMP to increase the K_m of the cytosolic Fru1,6BPase for its substrate Fru1,6BP. Figure 5-2 gives an overview of the contribution of metabolic control of sucrose synthesis at each individual step.

Figure 5-2: Control of sucrose synthesis

The individual reactions are catalysed by the following enzymes: (1) cTPI; (2) cFru1,6BP aldolase; (3) cFru1,6BPase; (4) cPGI; (5) cPGM; (6) UGPase; (7) SPS; (8) Suc phosphatase. Irreversible steps are shown with red arrows. Enzymes that have unfilled catalytic binding sites are shown in green. Metabolites, which have concentrations below the K_m values of the corresponding enzyme, are shown in green and bold font.

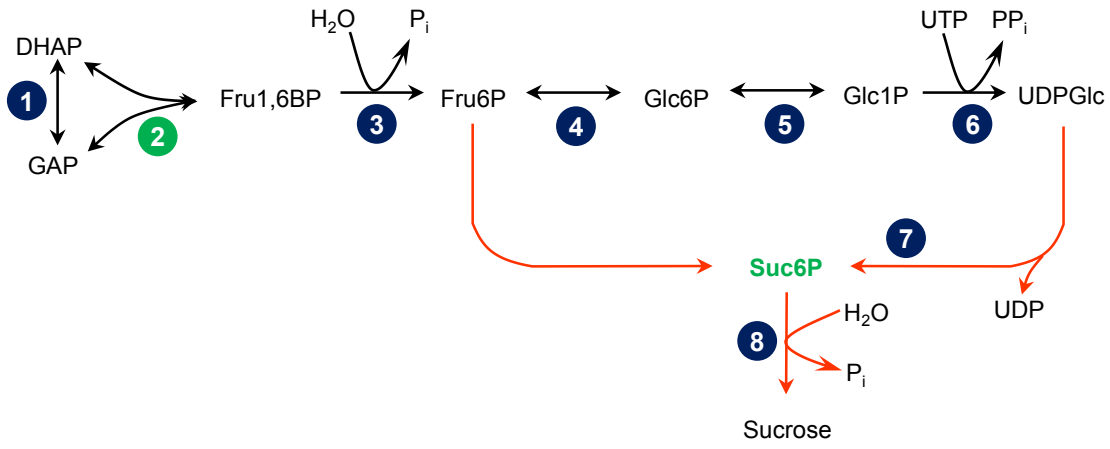

5.4 The role of Tre6P as a signalling molecule between cytosol and chloroplast

The synthesis of sucrose and starch needs to be tightly regulated to ensure that the partitioning of carbon fulfils the immediate and longer term (diurnal) needs of the plant for growth and survival during periods when photosynthesis is not possible (dark) or restricted by unfavoured environmental conditions. AGPase is activated by a high 3PGA/P_i ratio (Ghosh and Preiss, 1966), which is a measure of the availability of photoassimilate in the chloroplast. Sucrose synthesis is regulated by Fru2,6BP, which is an inhibitor of the cytosolic Fru1,6BPase. Increased levels of triose-phosphates in the cytosol lead to decreased levels of Fru2,6BP, which stimulates sucrose biosynthesis by relieving the inhibition of the cytosolic Fru1,6BPase.

Tre6P plays an important role in the physiology of plants. Modification of the enzymes in Tre6P synthesis and degradation has strong effects on the physiology and also influences leaf anatomy and flowering time (Paul, 2007). There is strong evidence that Tre6P links metabolism and development (Paul et al., 2008). In addition to that Tre6P could play an important role in the coordination of carbon end product metabolism, where Tre6P could act as a signalling molecule between the sucrose status in the cytosol and regulation of starch synthesis in the chloroplast. Incubation of isolated chloroplasts with Tre6P leads to an activation of ADPGlc pyrophosphorylase in the chloroplast (Kolbe et al., 2005) and thereby promotes starch synthesis.

It was also shown that rising levels of sucrose are accompanied by increasing levels of Tre6P in *A. thaliana* leaves (Lunn et al., 2006). The Tre6P synthase family includes 11 members in *A. thaliana,* of which only TPS1 shows catalytic activity and is most likely exclusively expressed in the cytosol (Almeida et al., 2007; Paul et al., 2008). The proposed model works as follows. A high sucrose status in the cytosol triggers Tre6P synthesis. Tre6P then acts as a mediator of the high energy status in the cytosol to the chloroplast by activating starch synthesis via ADPGlc pyrophosphorylase activation and thereby adjusts the carbon partitioning between starch and sucrose.

The study of incubation of isolated chloroplasts with Tre6P does not clarify if Tre6P acts directly in the chloroplast on ADPGlc pyrophosphorylase. So far no transporter for Tre6P at the plastidial membrane has been reported. It is also possible that Tre6P interacts with some other compound in the cytosol that then moves to the chloroplast or it triggers a signal cascade by binding to a receptor at the chloroplast membrane. In order to test these different possibilities it is helpful to know how Tre6P is shared between the two compartments chloroplast and cytosol. The NAF data revealed that Tre6P is 16% plastidial and 84% cytosolic. This corresponds to a plastidial concentration of 0.88 µM. The enzyme concentration of ADPGlc pyrophosphorylase is about 3 µM, which sets the two partners in a realistic physiological range for possible interaction. However, Suc6P was also predicted to be 16% plastidial and this should be purely cytosolic. Therefore it is possible that the plastidial Tre6P is a cytosolic contamination and repetitions of the experiments are necessary to test this.

5.5 Conclusions

Comparison of the concentrations of the sucrose synthesis intermediates in the cytosol and starch synthesis intermediates in the chloroplast with the catalytic properties of the catalyzing enzymes provided new insights into the control of the pathways under steady state photosynthesis conditions. Here I present a nearly complete dataset of these intermediates resolved at a subcellular level, representing the *in vivo* levels at steady state photosynthesis.

The finding that ADPGlc is exclusively localised in the chloroplast in *A. thaliana* leaves supports the classical starch synthesis model and argues strongly against a sucrose dependent ADPGlc production in the cytosol being a substantial source of ADPGlc for starch synthesis. However, residual levels of ADPGlc in the starch deficient *pgm* and *adg1* mutants show that there is

another route for synthesis of ADPGlc that is independent of these enzymes. The levels of ADPGlc in the *adg1* mutant are about 35-fold lower than the levels in wild type plants. It seems likely that this small amount of ADPGlc derives from a side reaction of sucrose synthase, but it does not make a significant contribution to the provision of ADPGlc for the synthesis of starch.

For starch biosynthesis it was shown that the catalytic binding sites of the enzymes PGM, PGI and AGPase are filled with their substrates, while comparison with the K_m values revealed that AGPase and starch synthase are more susceptible to changes in the respective metabolite concentration Glc1P and ADPGlc.

Analysis of sucrose biosynthesis revealed that the cytosolic substrate concentrations UDPGlc for the SPS reaction and Suc6P for the sucrose phosphatase are very close to the K_m of the enzymes. For SPS and cytosolic Fru1,6BPase data for the K_i values were available. Comparison of the K_i values with the *in vivo* concentration of the competitive inhibitors Suc6P and Fru1,6BP revealed that the concentration of the inhibitors is low relative to the K_i values of the enzymes. It can be concluded that the effect on the SPS reaction is insignificant. In contrast to that the *in vivo* concentration of the non competitive inhibitor AMP is exactly in the range of the K_i of the cytosolic Fru1,6BPase. Here the binding of AMP reduces the maximal catalytic activity of the enzyme and the flux to sucrose is decreased.

A general comparison of the Calvin-Benson cycle with the sucrose and starch synthesis pathways reveals that metabolite concentrations in the Calvin-Benson cycle are generally very close to the concentration of the active binding sites, while for the synthesis pathways of sucrose and starch the metabolite concentrations are much higher than the active binding site concentrations. Third this comparison indicates that starch synthesis and sucrose synthesis pathways have much higher levels of metabolites than enzyme binding sites, as is usually the case in primary metabolic pathways. This contrasts (with caution as the results need to be confirmed with a new data set) with the Calvin-Benson cycle, which appears to be a rather unusual metabolic pathway with very high concentrations of enzymes, which are required to catalyse the very rapid fluxes around the cycle that are required during photosynthesis. It appears to operate with levels of metabolites that are in the same range or sometimes lower than the enzyme active site concentrations.

For a possible interaction of Tre6P with AGPase the data is inconclusive. The predicted plastidial pool of Tre6P could also be a cytosolic contamination. Further experiments are necessary to test the subcellular distribution of Tre6P.

The analysis performed for carbon end product metabolism revealed new insights in the control of sucrose and starch metabolism and helped to clarify the starch synthesis debate.

Chapter 6: General discussion

6.1 Introduction

The aim of the work presented in this thesis was to investigate control and regulation of photosynthetic carbon fixation and carbon end product synthesis. More specifically, the *in vivo* concentrations of pathway intermediates from the Calvin-Benson cycle, sucrose and starch synthesis were determined in the different cellular compartments of cytosol and chloroplast and analysed systematically for their role in metabolic control of these pathways. Subsidiary aims were to clarify the role of Tre6P as a potential mediator between cytosol and chloroplast, linking sucrose and starch metabolism and to determine the subcellular location of ADPGlc to resolve the disputed pathway of starch synthesis.

In the light period when photosynthesis takes place, CO_2 is fixed in the plastid stroma via the Calvin-Benson cycle. This fixed carbon is either used to fix more carbon or intermediates of the cycle are withdrawn for synthesis of starch in the chloroplast or sucrose in the cytosol. Starch is the energy reserve for night metabolism, when it is remobilised, while sucrose is a mobile transport sugar that can be exported to other parts of the plant. This partitioning of carbon into sucrose and starch is coordinated with the Calvin-Benson cycle, to avoid too many intermediates of the cycle being used for starch and sucrose synthesis, which would limit CO_2 fixation. At the same time the partitioning of photoassimilate between sucrose and starch needs to be balanced to fulfil the energetic needs of the plant. The plant must store enough carbon in the form of starch for the night and support the sink tissue with enough energy in the form of sucrose. Photosynthetic carbon metabolism has been studied extensively and the regulation of key enzymes in all three pathways has been characterized, and gives us a general understanding of how this balance is achieved. However, many open questions remain, especially in terms of metabolic control of the flux through the different pathways. Our knowledge about the subcellular compartmentation of the pathway intermediates *in vivo* is fragmentary. Even the generally accepted pathway of starch synthesis has been called into question, in part due to uncertainty about the subcellular distribution of the starch precursor ADPGlc. In order to address these questions the non-aqueous fractionation technique was used to resolve the subcellular

distribution of these pathway intermediates, and the *in vivo* concentrations were calculated and compared systematically with the catalytic characteristics of the corresponding enzymes.

6.2 Identification of regulatory steps in carbon fixation

The subcellular distribution pattern of the pathway intermediates of the Calvin-Benson cycle has been measured with LC-MS/MS after non-aqueous fractionation of *A. thaliana* leaf material harvested in steady-state photosynthetic conditions. The missing metabolite values of GAP and E4P were calculated based on the assumption that the mass action ratio for the TPI and TK reaction is close to the equilibrium constant. The *in vivo* concentration of these intermediates in the plastid stroma has been calculated by using published values for the volume of spinach chloroplasts (Winter et al., 1994) as such data were not available for *A. thaliana*. The comprehensive analysis of the Calvin-Benson cycle in *Chlorella pyrenoidisa* carried out by Bassham and Krause (1969) has been used as a basis to calculate changes of Gibbs free energy for each reaction in the cycle under the conditions discussed here. The BRENDA database was used to compare the actual *in vivo* concentrations of each metabolite with the K_m value of the corresponding enzymes. With the proteomics measurement and knowledge about the structure of the enzymes it was possible to calculate the concentration of the catalytic binding sites in the plastid stroma, and to compare these with the corresponding metabolite concentration. Taking all these data together it was possible to investigate every single step of the cycle in terms of metabolic control by assessing if an enzyme catalyses a reversible or irreversible reaction, if the substrate concentration is lower or higher than the binding site concentration and how the *in vivo* concentrations of the metabolites relate to the respective K_m values.

Every enzymatic step in a biochemical pathway has the potential to contribute to the control of flux to the end product of the pathway. The general concept for control of the flux distinguishes between reversible and irreversible reactions, and considers that irreversible reactions are more important for the control because an increase in the activity of an enzyme would alter the reaction rate, while for reversible reactions an increase in activity would not influence the net outcome so effectively because the forward and reverse reaction would be altered in the same way (Newsholme and Crabtree, 1979). Most of the enzymes that catalyse irreversible reactions of the Calvin-Benson cycle show sophisticated control mechanisms. Rubisco, Fru1,6BPase, Sed1,7BPase and PRK are activated by the ferrodoxin/ thioredoxin system and are sensitive to

changes in pH and Mg^{2+} concentration. Therefore it was concluded that these enzymes must be the key players in controlling the flux. This concept might be too simplistic, because the reason for the regulation of these enzymes might not be to initiate a change in the flux, but to compensate changes of the flux that has been initiated by a different enzyme (Stitt, 1996). For a reversible reaction a change in substrate/product ratio can alter the direction of the reaction and thus have a major influence on the overall flux to the end product. In agreement with that the control over the flux by Fru1,6BPase and PRK is low, but slightly higher in the case of Sed1,7BPase (Raines, 2003). It is known that Rubisco can exert considerable control of the flux, but this pivotal role is very dependent on the environmental conditions, especially on the CO_2 concentration (Stitt et al., 1991). Aldolase catalyses a freely reversible reaction and has significant control over the flux (Haake et al., 1998).

The analysis carried out in the frame of this thesis revealed new insights into the metabolic control over the flux in the Calvin-Benson cycle under steady-state photosynthesis conditions. Interestingly the two aldolase reactions, which are readily reversible *in vitro*, showed large positive Gibbs free energy changes *in vivo* of approximately 15 kJ mol^{-1} under the environmental conditions discussed here. This is most likely due to an underestimation of the *in vivo* concentration of DHAP because of short time shading of the leaves and the very fast turnover time of DHAP. The plastidial pool is likely to have a shorter turnover time and thus to be depleted more strongly. This is in agreement with the observation that the plastidial pool was determined to be only 23 % (Table 3-5) of the total DHAP here, which is contrasting to the study by Gerhardt et al. (1987), where DHAP was determined to be 47 % plastidial. Another explanation would be that some of the Fru1,6BP and Sed1,7BP might be bound; it is known for example that these compounds may bind to the RubicO binding site, which is present at very high concentrations. Unpublished data form 13C-labelling kinetics (S. Arrivault, unpubl. data) indicates that, at least for Fru1,6BP, a substantial part of the pool is not in isotopic equilibrium with DHAP, which would be consistent with this possibility. A further contributing factor might be that these reactions were actually running in the opposite direction at the moment when the metabolism was quenched on the leaf material for this study. However, this would not explain the positive free energy changes obtained also when the calculations are performed with overall metabolite levels taken from Arrivault et al. (2009), which is an additional indicator that the plastidial pool of DHAP might be higher than the measured 23 % here.

The following enzymes in the Calvin-Benson cycle have higher catalytic binding site concentrations than substrate concentrations: Rubisco, TPI, aldolase (for both reactions), and transketolase (for both reactions), while for the irreversible reactions of Fru1,6BPase, Sed1,7BPase and PRK the substrate concentrations are higher than the catalytic binding site concentration. This data could indicate that the irreversible reactions, with the exeption of Rubisco are relatively insensitive to fluctuations in substrate concentrations, while the reversible reactions of TPI, aldolase and transketolase are very susceptible to changes in substrate or product concentration. This observation is strengthened by the fact that the following metabolites have concentrations that are lower than the K_m values of the respective enzymes: GAP (TPI), Fru6P (TK), R5P (R5P isomerase) and ATP and Ru5P (PRK). With the exception of PRK these are all freely reversible reactions. Another interesting finding is that the enzymes that have higher binding site concentrations than metabolite concentrations or where the metabolite concentration is lower than the K_m value are branch points to other pathways. This is the case for GAP (TPI) that links the Calvin-Benson cycle with sucrose synthesis, TK (Fru6P) that links the Calvin-Benson cycle with starch synthesis, TK and Sed1,7BP aldolase (E4P) that connect the cycle with the shikimate pathway and R5P isomerase (R5P), which provides the substrate for nucleotide biosynthesis. In terms of metabolic control for the Calvin-Benson cycle these steps may exert more influence than the regulated irreversible steps of Fru1,6BPase and Sed1,7BPase.

The fitness and growth of a plant very much depends on how much of the fixed carbon is used for different purposes than fixing more carbon. Sucrose and starch are the two main end products of carbon fixation. Sucrose is the mobile transport sugar and is extremely important for growth and metabolism of non-photosynthetic parts of the plant, e.g. the roots. Starch is the energy reserve for the night and plants that do not make starch grow much more slowly than wild type plants (Caspar et al., 1985; Lin et al., 1988). The shikimate pathway is necessary for the synthesis of aromatic compounds including essential aromatic amino acids, and also important for synthesis of secondary metabolites that are essential for the fitness of the plant (Herrmann, 1995). Finally R5P can be used for nucleotide biosynthesis that can fulfil many different functions including energy metabolism, DNA replication and transcription. Taking all this findings together the Calvin-Benson cycle is most susceptible to metabolic control at the steps in the pathway that connect to other biochemical reactions with the ultimate aim to fine balance Ru5P regeneration with primary and secondary metabolism.

6.3 Characterization of the subcellular distribution of ADPGlc and Tre6P reveals new insights into the coordination of sucrose and starch metabolism

The biochemical pathways of sucrose and starch synthesis need to be tightly regulated in order to fulfil the metabolic needs of the whole plant. On the one hand the plant needs to make sure that it stores enough starch in the chloroplast during the day to keep metabolism running during the night, on the other hand enough sucrose needs to be synthesised to provide other parts of the plant with carbon and energy. The export of triose-phosphates from the chloroplast to the cytosol is coupled to exchange of inorganic phosphate from the cytosol into the chloroplast. This phosphate is used in the chloroplast for synthesis of ATP. The chloroplast is not only a donor of energy to the cytosol but also receives necessary components from the cytosol to keep photophosphorylation running. A few key players in coordinating these processes have been determined.

AGPase, the enzyme that synthesises ADPGlc, which is the direct precursor of starch, is activated by thioredoxin in the light, and thus inactive in the dark. Starch synthesis does not occur during the night. Sucrose synthesis is regulated in a more complex manner involving the signal metabolite Fru2,6BP. Fru2,6BP is an inhibitor of the cytosolic Fru1,6BPase and is synthesised by fructose-6-phosphate, 2-kinase/ fructose 2,6-bisphosphatase (F2KP). An increase of triose-phosphates and a decrease of orthophosphate in the cytosol lead to a decline of Fru2,6BP levels and thus synthesis of Fru6P is increased (Stitt and Heldt, 1985; Stitt, 1987). This in turn leads to activation of SPS by increased availability of the substrates UDPGlc and Fru6P, and the higher concentration of the allosteric activator Glc6P. All together these mechanisms result in sucrose synthesis being activated. SPS is also regulated by reversible protein phosphorylation. This mechanism is important in the regulation of night-time sucrose synthesis from starch, which bypasses the cytosolic Fru1,6BPase and so is not regulated by Fru2,6BP. If sucrose levels rise too much in the leaf, inhibition of SPS, possibly via changes in its phosphorylation status, leads to accumulation of Fru6P, which allosterically activates the kinase activity of the F2KP, leading to an increase in the level of Fru2,6BP and inhibiton of the cytosolic F1,6BPase. This inhibition decreases the release of orthophosphate in the cytosol, which restricts the export of triose-phosphates from the chloroplast via the triose-phosphate/phosphate antiporter. As a consequence orthophosphate levels in the stroma decrease, which leads to less ATP production and rising

3PGA levels in the chloroplast. Higher 3PGA and lower P_i together act to activate AGPase allosterically, and thus increase the flux of carbon into starch synthesis (Stitt and Quick, 1989).

Although the mechanisms described above already provide a framework to explain how the synthesis of sucrose and starch are coordinated, additional control mechanisms have been discussed. It has been proposed that the direct precursor of starch ADPGlc is not synthesized in the chloroplast by means of AGPase, but by the cleavage of sucrose in the cytosol by means of sucrose synthase, and subsequent import of ADPGlc into the chloroplast (Pozueta-Romero et al., 1991a). The attractiveness of this idea is that this would directly link sucrose and starch biosynthesis (Baroja-Fernandez et al., 2001). Starch synthesis would always be dependent on sucrose levels. With the work carried out in the frame of this thesis it was possible to show that ADPGlc is exclusively localised to the chloroplast. In addition it was shown that the levels of ADPGlc in the starch-deficient mutants *pgm* and *adg1* are much lower than in wild type plants, although they have normal or even elevated levels of sucrose and normal sucrose synthase activity. This argues very much in favour of AGPase-dependent ADPGlc production in the chloroplast. Even if ADPGlc were produced by sucrose synthase in the cytosol and the import into the chloroplast would be reasonably fast at least residual levels of this metabolite would be expected in the cytosol. Even though the idea of linking sucrose and starch synthesis with one single reaction, i.e. sucrose synthase, may sound appealing, this mechanism does not exist *in vivo*.

Tre6P has been implicated in regulation of photoassimilate partitioning of sucrose and starch. Tre6P is synthesized in the cytosol by TPS1 (Paul, 2007; Paul et al., 2008). Elevated levels of sucrose in the cytosol lead to increased Tre6P levels (Lunn et al., 2006). Tre6P promotes the redox activation of AGPase. Based on these findings the following hypothesis has been formulated, elevated sucrose levels lead to increased Tre6P, which enters the chloroplast and acts as a feed forward activator of AGPase and thus increases starch synthesis (Kolbe et al., 2005). So far no functional Tre6P transporter in the chloroplast membrane has been characterised, so it is unclear if Tre6P can enter the chloroplast and act directly on AGPase. To answer this question the subcellular distribution pattern of Tre6P in mesophyll cells has been investigated in this thesis. The levels of Tre6P that have been found in the chloroplast are close to the cytosolic crosscontamination. Therefore no definite conclusion about Tre6P being able to enter the chloroplast can be drawn.

Taken together these findings give new insights into the coordination of partitioning of photoassimilates. The idea of a direct sucrose-dependent starch synthesis due to synthesis of ADPGlc by sucrose synthase has been proven wrong.

6.4 Identification of regulatory steps in sucrose and starch synthesis

The subcellular distribution of the phosphorylated intermediates of starch und sucrose synthesis has been determined by non-aqueous fractionation. The *in vivo* concentration of these intermediates in the plastid stroma for starch and in the cytosol for sucrose has been calculated by using published values on the volume of the chloroplast stroma and cytosolic compartments in spinach leaves (Winter et al., 1994). The published values for standard free energy of the individual reactions for sucrose from Lunn and ap Rees (1990) and for starch from Tiessen et al. (2002) were used to calculate the steady-state Gibbs free energy changes of each reaction. K_m values for the catalysing enzymes were taken from the BRENDA database and were compared with corresponding metabolite concentration *in vivo*. The same was done with the concentration of the catalytic binding sites of these enzymes. By analysis of these parameters it was possible to investigate each individual step of starch and sucrose synthesis in terms of metabolic control. Therefore the reversibility of each enzymatic step, the filling of an enzyme with substrate and the ratio of *in vivo* concentrations of the metabolites against the respective K_m values were determined.

The analysis of each individual step of sucrose synthesis revealed that nearly all enzymes have lower binding site concentrations than substrate concentration. The only exception is the cytosolic aldolase that has a higher binding site concentration than the concentration of DHAP and GAP. As discussed above the levels of DHAP and GAP might be underestimated in this study. This contrasts with the situation for the Calvin-Benson cycle in the chloroplast, where approximately half of the enzymes in the pathway have higher binding site concentrations than substrate concentrations. The cytosolic aldolase catalyses the first reaction of sucrose synthesis by using the exported triose-phosphates from the chloroplast. The comparison of K_m values with *in vivo* metabolite concentrations showed that Suc6P, the substrate of the SPP reaction, is more than 50 % lower than the K_m. The concentration of UDPGlc, the substrate for the SPS reaction is only slightly higher than the K_m. The Gibbs free energy changes of the SPS and SPP reactions are highly negative, and the reactions can be considered to be irreversible. SPS is inhibited by its

product Suc6P and by Fru1,6BP, but the concentration of these inhibitors *in vivo* is relatively low, and the effect on SPS likely to be insignificant. The concentration of AMP, a non-competitive inhibitor of the cytosolic Fru1,6BPase, is exactly in the range of the K_i. Here the binding of AMP reduces the maximal catalytic activity of the enzyme and the flux to sucrose is decreased. Taken together, these data show that the first enzyme in sucrose synthesis, the aldolase and the last two enzymes, SPS and sucrose phosphatase are likely to contribute to control of the flux in terms of being sensitive to changes in substrate levels.

For starch synthesis, the redox modulation of AGPase links its activity status directly to the availability of light (Hendriks et al., 2003). AGPase is also activated by increased levels of 3PGA and decreased levels of orthophosphate that reflect lower sucrose synthesis in the cytosol (Smith et al., 2010). By this mechanism reduced sucrose synthesis leads to increased starch synthesis and vice versa.

In terms of metabolic control the pivotal role of AGPase is supported by the fact that the concentration of the substrate Glc1P is about 5-fold lower than the K_m value. The concentration of the competitive inhibitor ADP and the ratio of P_i/3PGA are too low to have a significant inhibitory effect. The concentration of ADPGlc, the substrate of starch synthase is about 10-fold lower than the K_m. Alkaline pyrophosphatase prevents the reverse reaction of AGPase, i.e. conversion of ADPGlc and PP_i to Glc1P and ATP. AGPase and starch synthase are likely to contribute to control of the flux to starch in terms of being sensitive to changes in their substrate levels.

Taken together the findings for metabolic control of sucrose and starch synthesis reveal that the last steps of the pathways are the ones that are sensitive to changes in substrate concentration. In contrast to the Calvin-Benson cycle the regulated reactions of SPS and AGPase are subject to metabolic control. Comparison of the concentrations of substrates and active binding site concentrations between the Calvin-Benson cycle and the sucrose and starch synthesis pathways shows that metabolite concentrations in the Calvin-Benson cycle are usually close to the concentration of the active binding sites, while for the synthesis pathways of sucrose and starch the metabolite concentrations are much higher than the active binding site concentrations.

6.5 Conclusions

Detailed analysis of the subcellular levels of pathway intermediates of the Calvin-Benson cycle, sucrose and starch synthesis revealed new insights into the metabolic control of the individual steps. For the Calvin-Benson cycle it was demonstrated that the reversible reactions of TPI, aldolase, transketolase and R5P isomerase, which link the cycle to other pathways, are more sensitive to changes in substrate concentration than the regulated irreversible reactions carried out by Fru1,6BPase and Sed1,7BPase. For sucrose synthesis the cytosolic aldolase, SPS and SPP are not filled with their respective substrates and the catalytic rate of these steps is sensitive to changes in substrate availability. SPS and SPP catalyse irreversible reactions. For starch synthesis it was shown that AGPase and starch synthase are not filled with their substrates. In terms of metabolic control these steps are most responsive to changes in the concentrations of Glc1P and ADPGlc. Furthermore it was shown that ADPGlc is exclusively synthesised in the chloroplast, which proves the alternative concept of sucrose dependent ADPGlc production by means of sucrose synthase in the cytosol to be wrong.

Because of the uncertainty about the DHAP levels the experiment has to be repeated for a publication to confirm the hypothesis that the plants were subject to a transient decrease in light intensity, which led to the unexpected DHAP values. I did not address this issue in my thesis because of technical problems with the NAF gradients. Recent NAF gradients showed unexpected distribution behaviour of plastidial metabolites that co-localised with the vacuolar markers. This is most likely due to unbroken cells in the gradient. The reason for this could be the necessity of using of a new nylon net for filtration after sonication, as the old net was used up.

6.6 Outlook

The analysis performed here investigates the metabolic control of the Calvin-Benson cycle under steady state photosynthesis conditions. In nature photosynthesis is exposed to changes in environmental conditions. The flux of photosynthetic carbon metabolism, i.e the Calvin-Benson cycle and starch and sucrose synthesis, is driven by light and light intensity is changing continually. It would be interesting to investigate how this metabolic control changes when the environmental conditions change and especially how the flux is optimised. Easy and non invasive manipulation would be to vary the light strength, the CO_2 concentration or the phosphate availability. In addition transgenic plants with altered levels of plastidial TPI or R5P isomerase

could be used to verify the hypothesis that they play a major role in control of the Calvin-Benson cycle. For aldolase (Haake et al., 1998) and transketolase (Henkes et al., 2001) it was already shown that a decrease in the amount of these enzymes leads to severe effects in plants. For sucrose and starch synthesis the role of the key players AGPase and SPS has been confirmed. In addition control potential for the cytosolic aldolase was shown. Transgenic plants with altered cytosolic aldolase activity should be tested for the effect on sucrose synthesis. If the control potential is validated by independent transgenic experiments a next step would be to test if the same mechanisms apply in crop plants, and if manipulation of carbon partitioning into the different end products can increase the yield. In order to test if Tre6P is the direct mediator of the sucrose status more experiments are necessary. By putting plants into an extended night, after about 4 h after reillumination sucrose levels will be higher than in plants that had a normal day/night rhythm. In such conditions it would be expected that more Tre6P would enter the chloroplast and NAF gradients could be used to clarify if the Tre6P distribution would be different to the plants with a normal day/night rhythm.

Chapter 7: Appendix

7.1 Acknowledgements

First of all I want to thank Prof. Dr. Mark Stitt for giving me the opportunity to work in his group on an interesting and challenging project and his helpful support throughout the whole time of my PhD.

Particularly thanks to Dr. John Lunn, who has supported me a lot in the past years. I always could rely on him, no matter if my questions where concerned with work in the lab, references or experimental strategies.

In addition, thanks to Dr. Alisdair Fernie and Dr. Oliver Ebenhöh for guiding me in the right direction as being members of the evaluation committee.

I am deeply thankful to Dr. Stéphanie Arrivault with whom I have been collaborating the most in my project. Without her this research would not have been possible.

I also want to thank Regina Feil for supporting this project with her measurements and especially for helping to resolve the mystery of starch synthesis in mesophyll cells.

Thanks to Marek Szecowka and Alisdair Fernie for GC-MS measurements.

Many thanks to Dr. Waltraud Schulze for doing the proteomics work.

Thank you to Nicole, Bea, Manuela, Christine and Melanie for their help in the lab and with plant growth.

Thanks to the Greenteam and the media kitchen staff for the perfect working conditions.

Finally, special thanks to my parents and Nadine for their constant support throughout my studies, although they never really understood what I did during that time.

7.2 Abstract (English)

Metabolism in plant cells is highly compartmented, with many pathways involving reactions in more than one compartment. For example, during photosynthesis in leaf mesophyll cells, primary carbon fixation and starch synthesis take place in the chloroplast, whereas sucrose is synthesized in the cytosol and stored in the vacuole. These reactions are tightly regulated to keep a fine balance between the carbon pools of the different compartments and to fulfil the energy needs of the organelles. Classical fractionation methods such as sucrose density gradient centrifugation can be used for enzyme localization, but the separation of organelles by these methods is generally too slow compared to the very short turnover times of pathway intermediates to provide useful information about the distribution of metabolites. To circumvent this problem I applied a technique which fractionates the cells under non-aqueous conditions, whereby the metabolic state is frozen at the time of harvest and held in stasis throughout the fractionation procedure. Highly sensitive robotized cycling assays were used to measure marker enzymes in the various cell fractions. Application of liquid chromatography linked to tandem mass spectrometry (LC-MS/MS) has considerably extended the range of metabolites, especially phosphorylated pathway intermediates that can be measured in the cell fractions. These methods were used to investigate the subcellular compartmentation of metabolites in *Arabidopsis thaliana* leaves harvested in the light under steady state photosynthetic conditions.

With the combination of non-aqueous fractionation and mass spectrometry based metabolite measurements (LC-MS/MS, GC-MS) it was possible to investigate the intracellular distributions of the intermediates of photosynthetic carbon metabolism and its products in subsequent metabolic reactions. With the knowledge about the *in vivo* concentrations of these metabolites under steady state photosynthesis conditions it was possible to calculate the mass action ratio and change in Gibbs free energy *in vivo* for each reaction in the pathway, to determine which reactions are near equilibrium and which are far removed from equilibrium. The K_m value and concentration of each enzyme were compared with the concentrations of its substrates *in vivo* to assess which reactions are substrate limited and so sensitive to changes in substrate concentration.

Several intermediates of the Calvin-Benson cycle are substrates for other pathways, including dihydroxyacetone-phosphate (DHAP,sucrose synthesis), fructose 6-phosphate (Fru6P, starch

synthesis), erythrose 4-phosphate (E4P,shikimate pathway) and ribose 5-phosphate (R5P, nucleotide synthesis). Several of the enzymes that metabolise these intermediates, and so lie at branch points in the pathway, are triose-phosphate isomerase (DHAP), transketolase (E4P, Fru6P), sedoheptulose-1,7-bisphosphate aldolase (E4P) and ribose-5-phosphate isomerase (R5P) are not saturated with their respective substrate as the metabolite concentration is lower than the respective K_m value. In terms of metabolic control these are the steps that are most sensitive to changes in substrate availability, while the regulated irreversible reactions of fructose-1,6-bisphosphatase and sedoheptulose-1,7-bisphosphatase are relatively insensitive to changes in the concentrations of their substrates.

In the pathway of sucrose synthesis it was shown that the concentration of the catalytic binding site of the cytosolic aldolase is lower than the substrate concentration of DHAP, and that the concentration of Suc6P is lower than the K_m of sucrose-phosphatase for this substrate. Both the sucrose-phosphate synthase and sucrose-phosphatase reactions are far removed from equilibrium *in vivo*.

In wild type *A. thaliana* Columbia-0 leaves, all of the ADPGlc was found to be localised in the chloroplasts. ADPglucose pyrophosphorylase is localised to the chloroplast and synthesises ADPGlc from ATP and Glc1P. This distribution argues strongly against the hypothesis proposed by Pozueta-Romero and colleagues that ADPGlc for starch synthesis is produced in the cytosol via ADP-mediated cleavage of sucrose by sucrose synthase. Based on this observation and other published data it was concluded that the generally accepted pathway of starch synthesis from ADPGlc produced by ADPglucose pyrophosphorylase in the chloroplasts is correct, and that the alternative pathway is untenable. Within the pathway of starch synthesis the concentration of ADPGlc was found to be well below the K_m value of starch synthase for ADPGlc, indicating that the enzyme is substrate limited.

A general finding in the comparison of the Calvin-Benson cycle with the synthesis pathways of sucrose and starch is that many enzymes in the Calvin Benson cycle have active binding site concentrations that are close to the metabolite concentrations, while for nearly all enzymes in the synthesis pathways the active binding site concentrations are much lower than the metabolite concentrations.

In conclusion, my results confirm the classical pathway of starch synthesis and the detailed analysis of *in vivo* concentrations of pathway intermediates presented in this thesis provided new insights into the control of the Calvin-Benson cycle and starch and sucrose synthesis.

7.3 Wissenschaftliche Zusammenfassung (Deutsch)

Metabolismus in Pflanzenzellen ist stark kompartimentiert. Viele Stoffwechselwege haben Reaktionen in mehr als einem Kompartiment. Zum Beispiel wird während der Photosynthese in pflanzlichen Mesophyllzellen Kohlenstoff in Form von Stärke in den Chloroplasten synthetisiert, während es im Zytosol in Form von Sacharose gebildet und in der Vakuole gespeichert wird. Diese Reaktionen sind strikt reguliert um ein Gleichgewicht der Kohlenstoffpools der verschiedenen Kompartimente aufrecht zu erhalten und die Energieversorgung aller Teile der Zelle für anabolische Reaktionen sicher zu stellen. Klassische Fraktionierungsmethoden wie etwa Sacharosedichtegradienten können genutzt werden, um Enzymlokalisierungen zu bestimmen, aber diese Methoden sind zu langwierig um sinnvolle Informationen über Metabolite zu erhalten, die sehr kurze Umsetzungsraten haben. Um dieses Problem zu umgehen wende ich eine Methode an, bei der die Zellen unter nicht-wässrigen Bedingungen fraktioniert werden und daher der metabolische Status der während der Ernte herrschte über den ganzen Zeitraum der Auftrennung beibehalten wird. Hochsensitive automatisierte Enzymassays werden benutzt, um die Verteilung von Markerenzymen in den verschiedenen Zellfraktionen zu bestimmen. Die Anwendung von Flüssigchromotagraphie in Verbindung mit Tandemmassenspekrometrie hat die Anzahl der messbaren Metabolite wesentlich erweitert, speziell der phosphorilierten Stoffwechselintermediate. Diese Methode wurde verwendet, um die subzelluläre Kompartimentierung von Metaboliten in Zellen von *Arabidopsis thaliana* Blättern, die im Licht geerntet wurden, zu untersuchen.

Durch die Kombination von nichtwässriger Fraktionierung und verschiedener Massenspektrometrietechniken (Flüssigchromotagraphie- und Gaschromotagraphie basierende Massenspekrometrie) ist es möglich die intrazelluläre Verteilung der meisten Intermediate des photosynthetischen Kohlenstoffstoffwechsels und der Produkte der nachgelagerten metabolischen Reaktionen zu bestimmen. Das Wissen über die *in vivo* Konzentrationen dieser Metabolite wurde genutzt um die Änderung der freien Gibbs Energie *in vivo* zu bestimmen. Mit Hilfe dessen kann bestimmt werden, welche Reaktion sich in einem Gleichgewichtszustand befinden und welche davon entfernt sind. Die Konzentration der Enzyme und der K_m Werte wurden mit den Konzentrationen der Metabolite *in vivo* verglichen, um festzustellen, welche Enzyme substratlimitiert sind und somit sensitiv gegenüber Änderungen der Substratkonzentration sind.

Verschiedene Intermediate des Calvin-Benson Zyklus sind gleichzeitig Substrate für andere Stoffwechselwege, als da wären Dihyroxyaceton-phosphat (DHAP, Saccharosesynthese), Fructose 6-phosphat (Fru6P, Stärkesynthese), Erythrose 4-phosphat (E4P, Shikimat Stoffwechselweg) und Ribose 5-phosphat (R5P, Nukleotidbiosynthese). Die Enzyme, die diese Intermediate verstoffwechseln, liegen an den Abzweigungspunkten zu diesen Stoffwechselwegen. Diese sind Trisose phosphat isomerase (DHAP), Transketolase (E4P), Sedoheptulose-1,7 biphosphat aldolase (E4P) und Ribose-5-phosphat isomerase (R5P), welche nicht mit ihren Substraten gesättigt sind, da die jeweilige Substratkonzentration geringer als der zugehörige K_m Wert ist. Für metabolische Kontrolle bedeutet dies, dass diese Schritte am sensitivsten gegenüber Änderungen der Substratkonzentrationen sind. Im Gegensatz dazu sind die regulierten irreversiblen Schritte von Fructose-1,6.biphosphatase und Sedoheptulose-1,7-biphosphatase relativ insensitiv gegenüber Änderungen der Substratkonzentration.

Für den Stoffwechselweg der Saccharosesynthese konnte gezeigt werden, dass die zytosolische Aldolase eine geringer Bindeseitenkonzentration als Substratkonzentration (DHAP) aufweist, und dass die Konzentration von Saccharose-6-phosphat geringer als der K_m Wert des synthetisierenden Enzyms Saccharose-phosphatase ist. Sowohl die Saccharose-phosphat-synthase, also auch die Saccharose-phosphatase sind *in vivo* weit von einem Gleichgewichtszustand entfernt.

In Wildtyp *Arabidopsis thaliana* Columbia-0 Blättern wurde der gesamte Pool von ADPGlc im Chloroplasten gefunden. Das Enzyme ADPGlc pyrophosphorylase ist im Chloroplasten lokalisiert und synthetisiert ADPGlc aus ATP und Glc1P. Dieses Verteilungsmuster spricht eindeutig gegen die Hypothese von Pozueta-Romero und Kollegen, dass ADPGlc im Zytosol durch ADP vermittelte Spaltung von Saccharose durch die Saccharose Synthase erzeugt wird. Basierend auf dieser Beobachtung und anderen veröffentlichten Ergebnissen wurde geschlußfolgert, dass der generell akzeptierte Stoffwechselweg der Stärkesynthese durch ADPGlc Produktion via ADPGlc pyrophosphorylase in den Chloroplasten korrekt ist, und die Hypothese des alternativen Stoffwechselweges unhaltbar ist. Innerhalb des Stoffwechselweges der Saccharosesynthsese wurde festgestellt, dass die Konzentration von ADPGlc geringer als der K_m Wert des Stärkesynthase ist, was darauf hindeutet, dass das Enzym substratlimitiert ist.

Eine generelle Beobachtung ist, dass viele Enzmye des Calvin-Benson Zyklus ähnliche Bindeseitenkonzentrationen wie Metabolitkonzentrationen aufweisen, wohingegen in den Synthesewegen von Saccharose und Stärke die Bindeseitenkonzentrationen der Enzyme viel geringer als die Metabolitkonzentrationen sind.

Zusammenfassend, konnte ich mit den Ergebnissen meiner Doktorarbeit den klassischen Stoffwechselweg der Stärkesynthese bestätigen und eine detailierte Analyse der *in vivo* Konzentrationen der Stoffwechselintermediate durchführen. Dies erbrachte neue Erkenntnisse im Bezug auf die Kontrolle des Calvin-Benson Zyklus und der Stärke und Saccharosesynthese.

Chapter 8: Additional data

8.1 Additional metabolite recovery data

Table 8-1: Recovery of metabolites in lyophilized vs fresh material

Values are given as means ± standard deviation

Metabolite	Recovery [%]	Metabolite	Recovery [%]
2OG	104 ± 8	malate	84 ± 14
3PGA	98 ± 17	maltose	100 ± 11
aconitate	129 ± 13	methionine	77 ± 20
ADP	76 ± 8	NAD	91 ± 6
ADPG	87 ± 13	NADP	93 ± 9
alanine	120 ± 8	ornithine	104 ± 11
AMP	78 ± 18	PEP	97 ± 24
arginine	115 ± 16	phenylalanine	109 ± 8
asparagine	102 ± 9	proline	105 ± 14
aspartate	93 ± 7	putrescine	106 ± 10
citrate	117 ± 11	pyruvate	95 ± 13
DHAP	90 ± 13	R5P	84 ± 18
Fru1,6BP	139 ± 7	RuBP	96 ± 5
Fru6P	82 ± 13	Sed1,7BP	164 ± 7
fructose	94 ± 9	Sed7P	101 ± 16
fumarate	96 ± 6	serine	98 ± 9
Glc1P	82 ± 9	shikimate	96 ± 9
Glc6P	87 ± 12	Suc6P	101 ± 14
Glucose	95 ± 12	succinate	154 ± 19
glutamate	99 ± 7	sucrose	96 ± 9
glutamine	109 ± 8	threonine	102 ± 9
Gly3P	63 ± 7	Tre6P	99 ± 16
glycerate	97 ± 5	trehalose	104 ± 11
glycine	96 ± 10	tyrosine	112 ± 7
inositol	99 ± 9	UDPG	74 ± 11
isocitrate	84 ± 13	valine	109 ± 6
Isoleucine	114 ± 7	Xu5P+Ru5P	85 ± 10

8.2 List of abbreviations

°C	degrees centigrade
x *g*	gravitational acceleration
µg	microgram
µl	micro liter
µm	micrometer
µmol	Micromole
ATP	Adenosine triphosphate
CO_2	carbon dioxide
g	gram
GC	gas chromatography
h	hour
HCl	hydrochloric acid
HEPES	4-(2-hydroxyethyl)-1-piperazineethanesulfonic acid
HPLC	High Pressure Liquid Chromatography
KOH	potassium hydroxide
LC	liquid chromatography
mg	milligram
$MgCl_2$	magnesium chloride
min	minute
mL	millilitre
mM	millimoles
mRNA	messenger RNA
MS	mass spectrometry
NADH	nicotinamide adenine dinucleotide
NAF	Non-aqueous fractionation
NaOH	sodium hydroxide
s	second
SNF1	sucrose non-fermenting1
Tris	Tris(-hydroxymethyl)aminomethane

8.3 References

Acamovic, T., and Brooker, J.D. (2005). Biochemistry of plant secondary metabolites and their effects in animals. Proceedings of the Nutrition Society **64,** 403-412.

Almeida, A.M., Santos, M., Villalobos, E., Araujo, S.S., van Dijck, P., Leyman, B., Cardoso, L.A., Santos, D., Fevereiro, P.S., and Torne, J.M. (2007). Immunogold localization of trehalose-6-phosphate synthase in leaf segments of wild-type and transgenic tobacco plants expressing the AtTPS1 gene from Arabidopsis thaliana. Protoplasma **230,** 41-49.

Amir, J., and Preiss, J. (1982). Kinetic characterization of spinach leaf sucrose-phosphate synthase. Plant physiology **69,** 1027-1030.

ap Rees, T. (1987). Compartmentation of plant metabolism. In The biochemistry of plants, D.D. Davies, ed (San Diego, CA, USA: Academic Press) **XII**.

ap Rees, T., and Macdonald, F. (1987). Isolation of amyloplasts from suspension cultures of soybean. Methods in Enzymology **148,** 218-226.

Arrivault, S., Guenther, M., Ivakov, A., Feil, R., Vosloh, D., van Dongen, J.T., Sulpice, R., and Stitt, M. (2009). Use of reverse-phase liquid chromatography, linked to tandem mass spectrometry, to profile the Calvin cycle and other metabolic intermediates in Arabidopsis rosettes at different carbon dioxide concentrations. Plant J **59,** 826-839.

Baker, A., Graham, I.A., Holdsworth, M., Smith, S.M., and Theodoulou, F.L. (2006). Chewing the fat: beta-oxidation in signalling and development. Trends Plant Sci **11,** 124-132.

Baroja-Fernandez, E., Munoz, F.J., and Pozueta-Romero, J. (2005). Response to Neuhaus et al.: No need to shift the paradigm on the metabolic pathway to transitory starch in leaves. Trends in plant science **10,** 156-158.

Baroja-Fernandez, E., Munoz, F.J., Akazawa, T., and Pozueta-Romero, J. (2001). Reappraisal of the currently prevailing model of starch biosynthesis in photosynthetic tissues: a proposal involving the cytosolic production of ADP-glucose by sucrose synthase and occurrence of cyclic turnover of starch in the chloroplast. Plant Cell Physiol **42,** 1311-1320.

Baroja-Fernandez, E., Munoz, F.J., Saikusa, T., Rodriguez-Lopez, M., Akazawa, T., and Pozueta-Romero, J. (2003). Sucrose synthase catalyzes the de novo production of ADPglucose linked to starch biosynthesis in heterotrophic tissues of plants. Plant Cell Physiol **44,** 500-509.

Baroja-Fernandez, E., Munoz, F.J., Zandueta-Criado, A., Moran-Zorzano, M.T., Viale, A.M., Alonso-Casajus, N., and Pozueta-Romero, J. (2004). Most of ADP x glucose linked to starch biosynthesis occurs outside the chloroplast in source leaves. Proc Natl Acad Sci U S A **101,** 13080-13085.

Baroja-Fernandez, E., Munoz, F.J., Montero, M., Etxeberria, E., Sesma, M.T., Ovecka, M., Bahaji, A., Ezquer, I., Li, J., Prat, S., and Pozueta-Romero, J. (2009). Enhancing sucrose synthase activity in transgenic potato (Solanum tuberosum L.) tubers results in increased levels of starch, ADPglucose and UDPglucose and total yield. Plant Cell Physiol.

Barratt, D.H., Derbyshire, P., Findlay, K., Pike, M., Wellner, N., Lunn, J., Feil, R., Simpson, C., Maule, A.J., and Smith, A.M. (2009). Normal growth of Arabidopsis requires cytosolic invertase but not sucrose synthase. Proc Natl Acad Sci U S A **106,** 13124-13129.

Bassham, J.A., and Krause, G.H. (1969). Free Energy Changes and Metabolic Regulation in Steady-State Photosynthetic Carbon Reduction. Biochimica et biophysica acta **189,** 207-&.

Bassham, J.A., Benson, A.A., and Calvin, M. (1950). The path of carbon in photosynthesis. The Journal of biological chemistry **185,** 781-787.

Bauwe, H., Hagemann, M., and Fernie, A.R. (2010). Photorespiration: players, partners and origin. Trends Plant Sci **15,** 330-336.

Benkeblia, N., Shinano, T., and Osaki, M. (2007). Metabolite profiling and assessment of metabolome compartmentation of soybean leaves using non-aqueous fractionation and GGMS analysis. Metabolomics **3,** 297-305.

Bennett, B.D., Kimball, E.H., Gao, M., Osterhout, R., Van Dien, S.J., and Rabinowitz, J.D. (2009). Absolute metabolite concentrations and implied enzyme active site occupancy in Escherichia coli. Nat Chem Biol **5,** 593-599.

Bligny, R., and Douce, R. (2001). NMR and plant metabolism. Current opinion in plant biology **4,** 191-196.

Bligny, R., Gardestrom, P., Roby, C., and Douce, R. (1990). 31P NMR studies of spinach leaves and their chloroplasts. The Journal of biological chemistry **265,** 1319-1326.

Bowsher, C.G., and Tobin, A.K. (2001). Compartmentation of metabolism within mitochondria and plastids. Journal of experimental botany **52,** 513-527.

Bradford, M.M. (1976). A rapid and sensitive method for the quantitation of microgram quantities of protein utilizing the principle of protein-dye binding. Analytical biochemistry **72,** 248-254.

Brown, L.A., and Baker, A. (2008). Shuttles and cycles: transport of proteins into the peroxisome matrix (review). Mol Membr Biol **25,** 363-375.

Buchanan, B.B., and Schurmann, P. (1972). A regulatory mechanism for CO 2 assimilation in plant photosynthesis: activation of ribulose-1,5-diphosphate carboxylase by fructose 6-phosphate and deactivation by fructose 1,6-diphosphate. FEBS Lett **23,** 157-159.

Buchanan, B.B., and Schurmann, P. (1973). Regulation of ribulose 1,5-diphosphate carboxylase in the photosynthetic assimilation of carbon dioxide. The Journal of biological chemistry **248,** 4956-4964.

Burrell, M., Earnshaw, C., and Clench, M. (2007). Imaging Matrix Assisted Laser Desorption Ionization Mass Spectrometry: a technique to map plant metabolites within tissues at high spatial resolution. Journal of experimental botany **58,** 757-763.

Calvin, M. (1950). The path of carbon in photosynthesis. Harvey Lect **Series 46,** 218-251.

Calvin, M., and Benson, A.A. (1948). The Path of Carbon in Photosynthesis. Science **107,** 476-480.

Calvin, M., Bassham, J.A., and Benson, A.A. (1950). Chemical transformations of carbon in photosynthesis. Fed Proc **9,** 524-534.

Carr, P.D., Verger, D., Ashton, A.R., and Ollis, D.L. (1999). Chloroplast NADP-malate dehydrogenase: structural basis of light-dependent regulation of activity by thiol oxidation and reduction. Structure **7,** 461-475.

Caspar, T., Huber, S.C., and Somerville, C. (1985). Alterations in Growth, Photosynthesis, and Respiration in a Starchless Mutant of Arabidopsis-Thaliana (L) Deficient in Chloroplast Phosphoglucomutase Activity. Plant physiology **79,** 11-17.

Cavalier-Smith, T. (2009). Predation and eukaryote cell origins: A coevolutionary perspective. International Journal of Biochemistry & Cell Biology **41,** 307-322.

Cline, K., and Dabney-Smith, C. (2008). Plastid protein import and sorting: different paths to the same compartments. Curr Opin Plant Biol **11,** 585-592.

Cookson, S.J., Williams, L.E., and Miller, A.J. (2005). Light-dark changes in cytosolic nitrate pools depend on nitrate reductase activity in Arabidopsis leaf cells. Plant physiology **138,** 1097-1105.

Cox, C.J., Foster, P.G., Hirt, R.P., Harris, S.R., and Embley, T.M. (2008). The archaebacterial origin of eukaryotes. Proc Natl Acad Sci U S A **105,** 20356-20361.

Dancer, J., Neuhaus, H.E., and Stitt, M. (1990). Subcellular compartmentation of uridine nucleotides and nucleoside-5' -diphosphate kinase in leaves. Plant physiology **92,** 637-641.

Denyer, K., Dunlap, F., Thorbjornsen, T., Keeling, P., and Smith, A.M. (1996). The major form of ADP-glucose pyrophosphorylase in maize endosperm is extra-plastidial. Plant physiology **112,** 779-785.

Deuschle, K., Chaudhuri, B., Okumoto, S., Lager, I., Lalonde, S., and Frommer, W.B. (2006). Rapid metabolism of glucose detected with FRET glucose nanosensors in epidermal cells and intact roots of Arabidopsis RNA-silencing mutants. The Plant cell **18,** 2314-2325.

Dodd, A.N., Borland, A.M., Haslam, R.P., Griffiths, H., and Maxwell, K. (2002). Crassulacean acid metabolism: plastic, fantastic. J Exp Bot **53,** 569-580.

Dunford, R.P., Catley, M.A., Raines, C.A., Lloyd, J.C., and Dyer, T.A. (1998). Purification of active chloroplast sedoheptulose-1,7-bisphosphatase expressed in Escherichia coli. Protein expression and purification **14,** 139-145.

Eckardt, N.A., Snyder, G.W., Portis, A.R., and Ogren, W.L. (1997). Growth and photosynthesis under high and low irradiance of Arabidopsis thaliana antisense mutants with reduced ribulose-1,5-bisphosphate carboxylase/oxygenase activase content. Plant Physiology **113,** 575-586.

Edwards, S., Nguyen, B.T., Do, B., and Roberts, J.K.M. (1998). Contribution of malic enzyme, pyruvate kinase, phosphoenolpyruvate carboxylase, and the krebs cycle to respiration and biosynthesis and to intracellular pH regulation during hypoxia in maize root tips observed by nuclear magnetic resonance imaging and gas chromatography-mass spectrometry. Plant physiology **116,** 1073-1081.

Elbers, R., Heldt, H.W., Schmucker, P., Soboll, S., and Wiese, H. (1974). Measurement of the ATP/ADP ratio in mitochondria and in the extramitochondrial compartment by fractionation of freeze-stopped liver tissue in non-aqueous media. Hoppe Seylers Z Physiol Chem **355,** 378-393.

Farre, E.M., Tiessen, A., Roessner, U., Geigenberger, P., Trethewey, R.N., and Willmitzer, L. (2001). Analysis of the compartmentation of glycolytic intermediates, nucleotides, sugars, organic acids, amino acids, and sugar alcohols in potato tubers using a nonaqueous fractionation method. Plant physiology **127,** 685-700.

Fernie, A.R., Carrari, F., and Sweetlove, L.J. (2004). Respiratory metabolism: glycolysis, the TCA cycle and mitochondrial electron transport. Curr Opin Plant Biol **7,** 254-261.

Fernie, A.R., Roessner, U., Trethewey, R.N., and Willmitzer, L. (2001). The contribution of plastidial phosphoglucomutase to the control of starch synthesis within the potato tuber. Planta **213,** 418-426.

Fliege, R., Flugge, U.I., Werdan, K., and Heldt, H.W. (1978). Specific transport of inorganic phosphate, 3-phosphoglycerate and triosephosphates across the inner membrane of the envelope in spinach chloroplasts. Biochim Biophys Acta **502,** 232-247.

Flugge, U.I., Freisl, M., and Heldt, H.W. (1980). Balance between Metabolite Accumulation and Transport in Relation to Photosynthesis by Isolated Spinach Chloroplasts. Plant physiology **65,** 574-577.

Fridlyand, L.E., and Scheibe, R. (1999). Regulation of the Calvin cycle for CO2 fixation as an example for general control mechanisms in metabolic cycles. Biosystems **51,** 79-93.

Furbank, R.T., Chitty, J.A., Von Caemmerer, S., and Jenkins, C. (1996). Antisense RNA Inhibition of RbcS Gene Expression Reduces Rubisco Level and Photosynthesis in the C4 Plant Flaveria bidentis. Plant physiology **111,** 725-734.

Gardemann, A., Stitt, M., and Heldt, H.W. (1983). Control of Co2 Fixation - Regulation of Spinach Ribulose-5-Phosphate Kinase by Stromal Metabolite Levels. Biochimica et biophysica acta **722,** 51-60.

Gardemann, A., Schimkat, D., and Heldt, H.W. (1986). Control of CO2 fixation
Regulation of stromal fructose-1,6-bisphosphatase in spinach by pH and Mg2+ concentration. Planta **168,** 536-545.

Gardestrom, P., and Wigge, B. (1988). Influence of Photorespiration on ATP/ADP Ratios in the Chloroplasts, Mitochondria, and Cytosol, Studied by Rapid Fractionation of Barley (Hordeum vulgare) Protoplasts. Plant physiology **88,** 69-76.

Geigenberger, P., Lerchl, J., Stitt, M., and Sonnewald, U. (1996). Phloem-specific expression of pyrophosphatase inhibits long-distance transport of carbohydrates and amino acids in tobacco plants. Plant Cell and Environment **19,** 43-55.

Gerhardt, R., and Heldt, H.W. (1984). Measurement of Subcellular Metabolite Levels in Leaves by Fractionation of Freeze-Stopped Material in Nonaqueous Media. Plant physiology **75,** 542-547.

Gerhardt, R., Stitt, M., and Heldt, H.W. (1987). Subcellular Metabolite Levels in Spinach Leaves : Regulation of Sucrose Synthesis during Diurnal Alterations in Photosynthetic Partitioning. Plant physiology **83,** 399-407.

Ghosh, H.P., and Preiss, J. (1966). Adenosine diphosphate glucose pyrophosphorylase. A regulatory enzyme in the biosynthesis of starch in spinach leaf chloroplasts. The Journal of biological chemistry **241,** 4491-4504.

Gibon, Y., Blasing, O.E., Palacios-Rojas, N., Pankovic, D., Hendriks, J.H., Fisahn, J., Hohne, M., Gunther, M., and Stitt, M. (2004a). Adjustment of diurnal starch turnover to short days: depletion of sugar during the night leads to a temporary inhibition of carbohydrate utilization, accumulation of sugars and post-translational activation of ADP-glucose pyrophosphorylase in the following light period. Plant J **39,** 847-862.

Gibon, Y., Blaesing, O.E., Hannemann, J., Carillo, P., Hohne, M., Hendriks, J.H., Palacios, N., Cross, J., Selbig, J., and Stitt, M. (2004b). A Robot-based platform to measure multiple enzyme activities in Arabidopsis using a set of cycling assays: comparison of changes of enzyme activities and transcript levels during diurnal cycles and in prolonged darkness. The Plant cell **16,** 3304-3325.

Giersch, C., Heber, U., Kaiser, G., Walker, D.A., and Robinson, S.P. (1980). Intracellular metabolite gradients and flow of carbon during photosynthesis of leaf protoplasts. Archives of biochemistry and biophysics **205,** 246-259.

Gout, E., Bligny, R., and Douce, R. (1992). Regulation of intracellular pH values in higher plant cells. Carbon-13 and phosphorus-31 nuclear magnetic resonance studies. The Journal of biological chemistry **267,** 13903-13909.

Haake, V., Geiger, M., and Stitt, M. (1999). Changes in aldolase activity in wild-type potato plants are important for acclimation to growth irradiance and carbon dioxide concentration, because plastid aldolase exerts control over the ambient rate of photosynthesis across a range of growth conditions. . Plant J **17,** 479-489.

Haake, V., Zrenner, R., Sonnewald, U., and Stitt, M. (1998). A moderate decrease of plastid aldolase activity inhibits photosynthesis, alters the levels of sugars and starch, and inhibits growth of potato plants. Plant J **14,** 147-157.

Harbron, S., Foyer, C., and Walker, D. (1981). The purification and properties of sucrose-phosphate synthetase from spinach leaves: the involvement of this enzyme and fructose bisphosphatase in the regulation of sucrose biosynthesis. Archives of biochemistry and biophysics **212,** 237-246.

Harrison, E.P., Olcer, H., Lloyd, J.C., Long, S.P., and Raines, C.A. (2001). Small decreases in SBPase cause a linear decline in the apparent RuBP regeneration rate, but do not affect Rubisco carboxylation capacity. Journal of experimental botany **52,** 1779-1784.

Heineke, D., Riens, B., Grosse, H., Hoferichter, P., Peter, U., Flugge, U.I., and Heldt, H.W. (1991). Redox Transfer across the Inner Chloroplast Envelope Membrane. Plant physiology **95,** 1131-1137.

Heinrich, R., and Rapoport, T.A. (1974). A linear steady-state treatment of enzymatic chains. General properties, control and effector strength. European journal of biochemistry / FEBS **42,** 89-95.

Heldt, H., and Heldt, F. (2005). Plant Biochemistry.

Heldt, H.W., Piechulla, B., and Heldt, F. (2010). Plant Biochemistry.

Heldt, H.W., Portis, A.R., Lilley, R.M., Mosbach, A., and Chon, C.J. (1980). Assay of nucleotides and other phosphate-containing compounds in isolated chloroplasts by ion exchange chromatography. Anal Biochem **101,** 278-287.

Hemschemeier, A., Fouchard, S., Cournac, L., Peltier, G., and Happe, T. (2008). Hydrogen production by Chlamydomonas reinhardtii: an elaborate interplay of electron sources and sinks. Planta **227,** 397-407.

Hendriks, J.H.M., Kolbe, A., Gibon, Y., Stitt, M., and Geigenberger, P. (2003). ADP-glucose pyrophosphorylase is activated by posttranslational redox-modification in response to light and to sugars in leaves of Arabidopsis and other plant species. Plant physiology **133,** 838-849.

Henkes, S., Sonnewald, U., Badur, R., Flachmann, R., and Stitt, M. (2001). A small decrease of plastid transketolase activity in antisense tobacco transformants has dramatic effects on photosynthesis and phenylpropanoid metabolism. The Plant cell **13,** 535-551.

Herrmann, K.M. (1995). The shikimate pathway as an entry to aromatic secondary metabolism. Plant physiology **107,** 7-12.

Herzog, B., Stitt, M., and Heldt, H.W. (1984). Control of Photosynthetic Sucrose Synthesis by Fructose 2,6-Bisphosphate : III. Properties of the Cytosolic Fructose 1,6-Bisphosphatase. Plant physiology **75,** 561-565.

Howard, T.P., Metodiev, M., Lloyd, J.C., and Raines, C.A. (2008). Thioredoxin-mediated reversible dissociation of a stromal multiprotein complex in response to changes in light availability. Proc Natl Acad Sci U S A **105,** 4056-4061.

Huber, S.C., and Huber, J.L. (1996). Role and regulation of sucrose-phosphate synthase in higher plants. Annual Review of Plant Physiology and Plant Molecular Biology **47,** 431-444.

Ishihama, Y., Oda, Y., Tabata, T., Sato, T., Nagasu, T., Rappsilber, J., and Mann, M. (2005). Exponentially modified protein abundance index (emPAI) for estimation of absolute protein amount in proteomics by the number of sequenced peptides per protein. Mol Cell Proteomics **4,** 1265-1272.

Jang, H.K., Lee, S.W., Lee, Y.H., and Hahn, T.R. (2003). Purification and characterization of a recombinant pea cytoplasmic fructose-1,6-bisphosphatase. Protein expression and purification **28,** 42-48.

Jiao, Y., Lau, O.S., and Deng, X.W. (2007). Light-regulated transcriptional networks in higher plants. Nat Rev Genet **8,** 217-230.

Kacser, H., and Burns, J.A. (1973). The control of flux. Symposia of the Society for Experimental Biology **27,** 65-104.

Kebeish, R., Niessen, M., Thiruveedhi, K., Bari, R., Hirsch, H.J., Rosenkranz, R., Stabler, N., Schonfeld, B., Kreuzaler, F., and Peterhansel, C. (2007). Chloroplastic photorespiratory bypass increases photosynthesis and biomass production in Arabidopsis thaliana. Nature biotechnology **25,** 593-599.

Keerberg, O., Ivanova, H., Keerberg, H., Parnik, T., Talts, P., and Gardestrom, P. (2011). Quantitative analysis of photosynthetic carbon metabolism in protoplasts and intact leaves of barley. Determination of carbon fluxes and pool sizes of metabolites in different cellular compartments. Biosystems **103,** 291-301.

Kierszniowska, S., Walther, D., and Schulze, W.X. (2009). Ratio-dependent significance thresholds in reciprocal 15N-labeling experiments as a robust tool in detection of candidate proteins responding to biological treatment. Proteomics **9,** 1916-1924.

Klein, U. (1986). Compartmentation of Glycolysis and of the Oxidative Pentose-Phosphate Pathway in Chlamydomonas-Reinhardii. Planta **167,** 81-86.

Klein, U. (1987). Intracellular Carbon Partitioning in Chlamydomonas-Reinhardtii. Plant physiology **85,** 892-897.

Kockenberger, W. (2001). Nuclear magnetic resonance micro-imaging in the investigation of plant cell metabolism. Journal of experimental botany **52,** 641-652.

Kolbe, A., Tiessen, A., Schluepmann, H., Paul, M., Ulrich, S., and Geigenberger, P. (2005). Trehalose 6-phosphate regulates starch synthesis via posttranslational redox activation of ADP-glucose pyrophosphorylase. Proc Natl Acad Sci U S A **102,** 11118-11123.

Konat, G.W. (2003). H2O2-induced higher order chromatin degradation: a novel mechanism of oxidative genotoxicity. Journal of biosciences **28,** 57-60.

Kopke-Secundo, E., Molnar, I., and Schnarrenberger, C. (1990). Isolation and characterization of the cytosolic and chloroplastic 3-phosphoglycerate kinase from spinach leaves. Plant physiology **93,** 40-47.

Kossmann, J., Sonnewald, U., and Willmitzer, L. (1994). Reduction of the chloroplastic fructose-1,6-bisphosphatase in transgenic potato plants impairs photosynthesis and plant growth. Plant J **6,** 637-650.

Kreim, M., and Giersch, C. (2007). Measuring in vivo elasticities of Calvin cycle enzymes: network structure and patterns of modulations. Phytochemistry **68,** 2152-2162.

Krishnan, P., Kruger, N.J., and Ratcliffe, R.G. (2005). Metabolite fingerprinting and profiling in plants using NMR. Journal of experimental botany **56,** 255-265.

Krueger, S., Niehl, A., Martin, M.C., Steinhauser, D., Donath, A., Hildebrandt, T., Romero, L.C., Hoefgen, R., Gotor, C., and Hesse, H. (2009). Analysis of cytosolic and plastidic serine acetyltransferase mutants and subcellular metabolite distributions suggests interplay of the cellular compartments for cysteine biosynthesis in Arabidopsis. Plant Cell and Environment **32,** 349-367.

Krueger, S., Giavalisco, P., Krall, L., Steinhauser, M.C., Bussis, D., Usadel, B., Flugge, U.I., Fernie, A.R., Willmitzer, L., and Steinhauser, D. (2011). A Topological Map of the Compartmentalized Arabidopsis thaliana Leaf Metabolome. PloS one **6,** e17806.

Kruger, I., and Schnarrenberger, C. (1983). Purification, subunit structure and immunological comparison of fructose-bisphosphate aldolases from spinach and corn leaves. European journal of biochemistry / FEBS **136,** 101-106.

Kruger, N.J., and von Schaewen, A. (2003). The oxidative pentose phosphate pathway: structure and organisation. Current opinion in plant biology **6,** 236-246.

Kudla, J., Batistic, O., and Hashimoto, K. (2010). Calcium signals: the lead currency of plant information processing. The Plant cell **22,** 541-563.

Kuhn, C., and Grof, C.P.L. (2010). Sucrose transporters of higher plants. Current opinion in plant biology **13,** 288-298.

Laing, W.A., Stitt, M., and Heldt, H.W. (1981). Control of Co2 Fixation - Changes in the Activity of Ribulosephosphate Kinase and Fructose-Bisphosphatase and Sedoheptulose-Bisphosphatase in Chloroplasts. Biochimica et biophysica acta **637,** 348-359.

Lawson, T., Bryant, B., Lefebvre, S., Lloyd, J.C., and Raines, C.A. (2006). Decreased SBPase activity alters growth and development in transgenic tobacco plants. Plant, cell & environment **29,** 48-58.

Lefebvre, S., Lawson, T., Zakhleniuk, O.V., Lloyd, J.C., Raines, C.A., and Fryer, M. (2005). Increased sedoheptulose-1,7-bisphosphatase activity in transgenic tobacco plants stimulates photosynthesis and growth from an early stage in development. Plant physiology **138,** 451-460.

Lilley, K.S., and Dupree, P. (2007). Plant organelle proteomics. Current opinion in plant biology **10,** 594-599.

Lilley, R.M., Chon, C.J., Mosbach, A., and Heldt, H.W. (1977). The distribution of metabolites between spinach chloroplasts and medium during photosynthesis in vitro. Biochimica et biophysica acta **460,** 259-272.

Lilley, R.M., Stitt, M., Mader, G., and Heldt, H.W. (1982). Rapid fractionation of wheat leaf protoplasts using membrane filtration : the determination of metabolite levels in the chloroplasts, cytosol, and mitochondria. Plant physiology **70,** 965-970.

Lin, T.P., Caspar, T., Somerville, C., and Preiss, J. (1988). Isolation and Characterization of a Starchless Mutant of Arabidopsis-Thaliana (L) Heynh Lacking Adpglucose Pyrophosphorylase Activity. Plant physiology **86,** 1131-1135.

Lisec, J., Schauer, N., Kopka, J., Willmitzer, L., and Fernie, A.R. (2006). Gas chromatography mass spectrometry-based metabolite profiling in plants. Nature Protocols **1,** 387-396.

Looger, L.L., Lalonde, S., and Frommer, W.B. (2005). Genetically encoded FRET sensors for visualizing metabolites with subcellular resolution in living cells. Plant physiology **138,** 555-557.

Lunn, J.E. (2007). Compartmentation in plant metabolism. Journal of experimental botany **58,** 35-47.

Lunn, J.E., and ap Rees, T. (1990). Apparent equilibrium constant and mass-action ratio for sucrose-phosphate synthase in seeds of Pisum sativum. The Biochemical journal **267,** 739-743.

Lunn, J.E., and Hatch, M.D. (1995). Primary partitioning and storage of photosynthate in sucrose and starch in leaves of C4 plants. Planta **197,** 385-391.

Lunn, J.E., and MacRae, E. (2003). New complexities in the synthesis of sucrose. Current opinion in plant biology **6,** 208-214.

Lunn, J.E., and MacRae, E. (2006). Control of sucrose synthesis. In Control of Primary Metabolism in Plants, W.C. Plaxton and M.T. McManus, eds (Blackwell Publishing Ltd), **,** pp. 408.

Lunn, J.E., Feil, R., Hendriks, J.H., Gibon, Y., Morcuende, R., Osuna, D., Scheible, W.R., Carillo, P., Hajirezaei, M.R., and Stitt, M. (2006). Sugar-induced increases in trehalose 6-phosphate are correlated with redox activation of ADPglucose pyrophosphorylase and higher rates of starch synthesis in Arabidopsis thaliana. The Biochemical journal **397,** 139-148.

Macasev, D., Newbigin, E., Whelan, J., and Lithgow, T. (2000). How do plant mitochondria avoid importing chloroplast proteins? Components of the import apparatus Tom20 and Tom22 from Arabidopsis differ from their fungal counterparts. Plant Physiol **123,** 811-816.

Margulis, L. (1971). The origin of plant and animal cells. Am Sci **59,** 230-235.

Martin, C., and Smith, A.M. (1995). Starch biosynthesis. The Plant cell **7,** 971-985.

Martin, W. (2010). Evolutionary origins of metabolic compartmentalization in eukaryotes. Philosophical Transactions of the Royal Society B-Biological Sciences **365,** 847-855.

Martinoia, E., Maeshima, M., and Neuhaus, H.E. (2007). Vacuolar transporters and their essential role in plant metabolism. Journal of experimental botany **58,** 83-102.

Mate, C.J., Hudson, G.S., von Caemmerer, S., Evans, J.R., and Andrews, T.J. (1993). Reduction of ribulose biphosphate carboxylase activase levels in tobacco (Nicotiana tabacum) by antisense RNA reduces ribulose biphosphate carboxylase carbamylation and impairs photosynthesis. Plant physiology **102,** 1119-1128.

Matt, P., Krapp, A., Haake, V., Mock, H.P., and Stitt, M. (2002). Decreased Rubisco activity leads to dramatic changes of nitrate metabolism, amino acid metabolism and the levels of phenylpropanoids and nicotine in tobacco antisense RBCS transformants. Plant J **30,** 663-677.

May, P., Christian, J.O., Kempa, S., and Walther, D. (2009). ChlamyCyc: an integrative systems biology database and web-portal for Chlamydomonas reinhardtii. BMC genomics **10,** 209.

May, P., Wienkoop, S., Kempa, S., Usadel, B., Christian, N., Rupprecht, J., Weiss, J., Recuenco-Munoz, L., Ebenhoh, O., Weckwerth, W., and Walther, D. (2008). Metabolomics- and proteomics-assisted genome annotation and analysis of the draft metabolic network of Chlamydomonas reinhardtii. Genetics **179,** 157-166.

Miflin, B.J., and Beevers, H. (1974). Isolation of intact plastids from a range of plant tissues. Plant physiology **53,** 870-874.

Miyagawa, Y., Tamoi, M., and Shigeoka, S. (2001). Overexpression of a cyanobacterial fructose-1,6-/sedoheptulose-1,7-bisphosphatase in tobacco enhances photosynthesis and growth. Nature biotechnology **19,** 965-969.

Miyawaki, A., Llopis, J., Heim, R., McCaffery, J.M., Adams, J.A., Ikura, M., and Tsien, R.Y. (1997). Fluorescent indicators for Ca2+ based on green fluorescent proteins and calmodulin. Nature **388,** 882-887.

Moore, B.D., Palmquist, D.E., and Seemann, J.R. (1997). Influence of plant growth at high CO2 concentrations on leaf content of ribulose-1,5-bisphosphate carboxylase/oxygenase and intracellular distribution of soluble carbohydrates in tobacco, snapdragon, and parsley. Plant physiology **115,** 241-248.

Moore, T.S., and Beevers, H. (1974). Isolation and characterization of organelles from soybean suspension cultures. Plant physiology **53,** 261-265.

Munoz, F.J., Baroja-Fernandez, E., Moran-Zorzano, M.T., Viale, A.M., Etxeberria, E., Alonso-Casajus, N., and Pozueta-Romero, J. (2005). Sucrose synthase controls both intracellular ADP glucose levels and transitory starch biosynthesis in source leaves. Plant Cell Physiol **46,** 1366-1376.

Nakamoto, R.K., Baylis Scanlon, J.A., and Al-Shawi, M.K. (2008). The rotary mechanism of the ATP synthase. Archives of biochemistry and biophysics **476,** 43-50.

Nelson, N. (1994). Energizing porters by proton-motive force. J Exp Biol **196,** 7-13.

Neuhaus, H.E. (2007). Transport of primary metabolites across the plant vacuolar membrane. FEBS letters **581,** 2223-2226.

Neuhaus, H.E., and Emes, M.J. (2000). Nonphotosynthetic metabolism in plastids. Annual Review of Plant Physiology and Plant Molecular Biology **51,** 111-140.

Neuhaus, H.E., Hausler, R.E., and Sonnewald, U. (2005). No need to shift the paradigm on the metabolic pathway to transitory starch in leaves. Trends in plant science **10,** 154-156; author reply 156-158.

Neuhaus, H.E., A.L., K., Feil, R., and Stitt, M. (1989). Reduced activity mutants of phosphoglucose isomerase in the cytosol and chloroplast of Clarkia xantiana. Planta **178,** 110-122.

Newsholme, E.A., and Crabtree, B. (1979). Theoretical principles in the approaches to control of metabolic pathways and their application to glycolysis in muscle. Journal of molecular and cellular cardiology **11,** 839-856.

Newsholme, E.A., and Leech, A.R. (1983). Biochemistry for the Medical Sciences**,** 448.

Niittyla, T., Messerli, G., Trevisan, M., Chen, J., Smith, A.M., and Zeeman, S.C. (2004). A previously unknown maltose transporter essential for starch degradation in leaves. Science **303,** 87-89.

Niittylä, T., Messerli, G., Trevisan, M., Chen, J., Smith, A.M., and Zeeman, S.C. (2004). A previously unknown maltose transporter essential for starch degradation in leaves. Science (New York, N.Y **303,** 87-89.

Niittylae T, C.B., Sauer U, Frommer WB. (2009). Comparison of Quantitative Metabolite Imaging Tools
and Carbon-13 Techniques for Fluxomics. Plant Systems Biology **553,** 355 - 372.

Nishimura, M., and Beevers, H. (1978). Isolation of intact plastids from protoplasts from castor bean endosperm. Plant physiology **62,** 40-43.

Nishimura, M., and Beevers, H. (1979). Subcellular distribution of gluconeogenetic enzymes in germinating castor bean endosperm. Plant physiology **64,** 31-37.

Olcer, H., Lloyd, J.C., and Raines, C.A. (2001). Photosynthetic capacity is differentially affected by reductions in sedoheptulose-1,7-bisphosphatase activity during leaf development in transgenic tobacco plants. Plant physiology **125,** 982-989.

Packer, L., Douce, R. (1987). Plant Cell Membranes. Methods in Enzymology **148**.

Paul, M. (2007). Trehallose 6-phosphate. Current opinion in plant biology **10,** 303-309.

Paul, M.J., Primavesi, L.F., Jhurreea, D., and Zhang, Y. (2008). Trehalose metabolism and signaling. Annu Rev Plant Biol **59,** 417-441.

Paul, M.J., Driscoll, S.P., Andralojc, P.J., Knight, J.S., Gray, J.C., and Lawlor, D.W. (2000). Decrease of phosphoribulokinase activity by antisense RNA in transgenic tobacco: definition of the light environment under which phosphoribulokinase is not in large excess. Planta **211,** 112-119.

Paul, M.J., Knight, J.S., Habash, D., Parry, M.A.J., Lawlor, D.W., Barnes, S.A., Loynes, A., and Gray, J.C. (1995). Reduction in phosphoribulokinase activity by antisense RNA in transgenic tobacco: effect on CO2 assimilation and growth in low irradiance. Plant J **7,** 535-542.

Pennisi, E. (2004). Evolutionary biology. The birth of the nucleus. Science **305,** 766-768.

Pettersson, G., and Ryde-Pettersson, U. (1988). A Mathematical-Model of the Calvin Photosynthesis Cycle. European Journal of Biochemistry **175,** 661-672.

Piques, M., Schulze, W.X., Hohne, M., Usadel, B., Gibon, Y., Rohwer, J., and Stitt, M. (2009). Ribosome and transcript copy numbers, polysome occupancy and enzyme dynamics in Arabidopsis. Molecular systems biology **5,** 314.

Poolman, M.G., Fell, D.A., and Thomas, S. (2000). Modelling photosynthesis and its control. Journal of experimental botany **51 Spec No,** 319-328.

Poolman, M.G., Olcer, H., Lloyd, J.C., Raines, C.A., and Fell, D.A. (2001). Computer modelling and experimental evidence for two steady states in the photosynthetic Calvin cycle. Eur J Biochem **268,** 2810-2816.

Portis, A.R., Jr., and Heldt, H.W. (1976). Light-dependent changes of the Mg2+ concentration in the stroma in relation to the Mg2+ dependency of CO2 fixation in intact chloroplasts. Biochimica et biophysica acta **449,** 434-436.

Portis, A.R., Jr., and Parry, M.A. (2007). Discoveries in Rubisco (Ribulose 1,5-bisphosphate carboxylase/oxygenase): a historical perspective. Photosynth Res **94,** 121-143.

Portis, A.R., Jr., Chon, C.J., Mosbach, A., and Heldt, H.W. (1977). Fructose-and sedoheptulosebisphosphatase. The sites of a possible control of CO2 fixation by lightdependent changes of the stromal Mg2+ concentration. Biochimica et biophysica acta **461,** 313-325.

Pozueta-Romero, J., Ardila, F., and Akazawa, T. (1991a). ADP-Glucose Transport by the Chloroplast Adenylate Translocator Is Linked to Starch Biosynthesis. Plant physiology **97,** 1565-1572.

Pozueta-Romero, J., Frehner, M., Viale, A.M., and Akazawa, T. (1991b). Direct transport of ADPglucose by an adenylate translocator is linked to starch biosynthesis in amyloplasts. Proc Natl Acad Sci U S A **88,** 5769-5773.

Pracharoenwattana, I., Cornah, J.E., and Smith, S.M. (2007). Arabidopsis peroxisomal malate dehydrogenase functions in beta-oxidation but not in the glyoxylate cycle. Plant J **50,** 381-390.

Pratt, J., Boisson, A.M., Gout, E., Bligny, R., Douce, R., and Aubert, S. (2009). Phosphate (Pi) starvation effect on the cytosolic Pi concentration and Pi exchanges across the tonoplast in plant cells: an in vivo 31P-nuclear magnetic resonance study using methylphosphonate as a Pi analog. Plant physiology **151,** 1646-1657.

Price, G.D., Evans, J.R., von Caemmerer, S., Yu, J.W., and Badger, M.R. (1995). Specific reduction of chloroplast glyceraldehyde-3-phosphate dehydrogenase activity by antisense RNA reduces CO2 assimilation via a reduction in ribulose bisphosphate regeneration in transgenic tobacco plants. Planta **195,** 369-378.

Quick, W.P. (1994). Analysis of transgenic tobacco plants containing varying amounts of ribulose-1,5-bisphosphate carboxylase/oxygenase. Biochemical Society transactions **22,** 899-903.

Raines, C.A. (2003). The Calvin cycle revisited. Photosynth Res **75,** 1-10.

Raines, C.A. (2006). Transgenic approaches to manipulate the environmental responses of the C-3 carbon fixation cycle. Plant Cell and Environment **29,** 331-339.

Rappsilber, J., Ishihama, Y., and Mann, M. (2003). Stop and go extraction tips for matrix-assisted laser desorption/ionization, nanoelectrospray, and LC/MS sample pretreatment in proteomics. Analytical chemistry **75,** 663-670.

Ratcliffe, R.G., and Shachar-Hill, Y. (2005). Revealing metabolic phenotypes in plants: inputs from NMR analysis. Biological reviews of the Cambridge Philosophical Society **80,** 27-43.

Reimholz, R., Geigenberger, P., and Stitt, M. (1994). Sucrose-phosphate synthase is regulated via metabolites and protein phosphorylation in potato tubers, in a manner analogous to the enzyme in leaves. Planta **192,** 480-488.

Riens, B., Lohaus, G., Heineke, D., and Heldt, H.W. (1991). Amino Acid and Sucrose Content Determined in the Cytosolic, Chloroplastic, and Vacuolar Compartments and in the Phloem Sap of Spinach Leaves. Plant physiology **97,** 227-233.

Riesmeier, J.W., Flugge, U.I., Schulz, B., Heineke, D., Heldt, H.W., Willmitzer, L., and Frommer, W.B. (1993). Antisense repression of the chloroplast triose phosphate translocator affects carbon partitioning in transgenic potato plants. Proceedings of the National Academy of Sciences of the United States of America **90,** 6160-6164.

Robinson, S.P., and Walker, D.A. (1979a). The control of 3-phosphoglycerate reduction in isolated chloroplasts by the concentrations of ATP, ADP and 3-phosphoglycerate. Biochimica et biophysica acta **545,** 528-536.

Robinson, S.P., and Walker, D.A. (1979b). Rapid separation of the chloroplast and cytoplasmic fractions from intact leaf protoplasts. Archives of biochemistry and biophysics **196,** 319-323.

Robinson, S.P., and Walker, D.A. (1979c). The site of sucrose synthesis in isolated leaf protoplasts. FEBS Lett **107,** 295-299.

Robinson, S.P., and Walker, D.A. (1980). Distribution of Metabolites between Chloroplast and Cytoplasm during the Induction Phase of Photosynthesis in Leaf Protoplasts. Plant physiology **65,** 902-905.

Robinson, S.P., Downton, W.J., and Millhouse, J.A. (1983). Photosynthesis and ion content of leaves and isolated chloroplasts of salt-stressed spinach. Plant physiology **73,** 238-242.

Roelfsema, M.R., and Hedrich, R. (2010). Making sense out of Ca(2+) signals: their role in regulating stomatal movements. Plant, cell & environment **33,** 305-321.

Rojo, E., and Denecke, J. (2008). What is moving in the secretory pathway of plants? Plant physiology **147,** 1493-1503.

Schnarrenberger, C., Flechner, A., and Martin, W. (1995). Enzymatic Evidence for a Complete Oxidative Pentose-Phosphate Pathway in Chloroplasts and an Incomplete Pathway in the Cytosol of Spinach Leaves. Plant physiology **108,** 609-614.

Schomburg, I., Chang, A., Hofmann, O., Ebeling, C., Ehrentreich, F., and Schomburg, D. (2002). BRENDA: a resource for enzyme data and metabolic information. Trends in biochemical sciences **27,** 54-56.

Schurmann, P., and Buchanan, B.B. (1975). Role of ferredoxin in the activation of sedoheptulose diphosphatase in isolated chloroplasts. Biochim Biophys Acta **376,** 189-192.

Schwender, J., Ohlrogge, J., and Shachar-Hill, Y. (2004). Understanding flux in plant metabolic networks. Current opinion in plant biology **7,** 309-317.

Serrato, A.J., Barajas-Lopez, J.D., Chueca, A., and Sahrawy, M. (2009). Changing sugar partitioning in FBPase-manipulated plants. Journal of experimental botany **60,** 2923-2931.

Shannon, J.C., Pien, F.M., Cao, H.P., and Liu, K.C. (1998). Brittle-1, an adenylate translocator, facilitates transfer of extraplastidial synthesized ADP-glucose into amyloplasts of maize endosperms. Plant physiology **117,** 1235-1252.

Sharkey, T.D., and Vanderveer, P.J. (1989). Stromal Phosphate Concentration Is Low during Feedback Limited Photosynthesis. Plant physiology **91,** 679-684.

Siegl, G., MacKintosh, C., and Stitt, M. (1990). Sucrose-phosphate synthase is dephosphorylated by protein phosphatase 2A in spinach leaves. Evidence from the effects of okadaic acid and microcystin. FEBS Lett **270,** 198-202.

Smith, A.M., Zeeman, S.C., and Smith, S.M. (2005). Starch degradation. Annual review of plant biology **56,** 73-98.

Smith, A.M., Zeeman, S.C., Thorneycroft, D., and Smith, S.M. (2003). Starch mobilization in leaves. Journal of experimental botany **54,** 577-583.

Smith, A.M., Coupland, G., Dolan, L., Harberd, N., Jones, J., Martin, C., Sablowski, R., and and Amey, A. (2010). Plant Biology.

Stitt, M. (1987). Fructose 2,6-Bisphosphate and Plant Carbohydrate Metabolism. Plant physiology **84,** 201-204.

Stitt, M. (1993). Control of photosynthetic carbon fixation and partitioning: How can use of genetically manipulated plants improve the nature and quality of information about regulation? Phil. Trans. Roy. Soc (London) Series B **340,** 225-233.

Stitt, M. (1996). Metabolic Regulation of Photosynthesis. Photosynthesis and the Environment**,** 151-190.

Stitt, M. (1999). The first will be last and the last will be first: non-regulated enzymes call the tune? . In Plant Carbohydrate Biochemistry, ed. J.A. Burrell, M.M. Bryant and N.J. Kruger, BIOS Scientific Publ., Oxford**,** 1-16.

Stitt, M., and Heldt, H.W. (1985). Control of Photosynthetic Sucrose Synthesis by Fructose-2,6-Bisphosphate - Intercellular Metabolite Distribution and Properties of the Cytosolic Fructosebisphosphatase in Leaves of Zea-Mays-L. Planta **164,** 179-188.

Stitt, M., and Quick, P. (1989). Photosynthetic Carbon Partitioning - Its Regulation and Possibilities for Manipulation. Physiologia Plantarum **77,** 633-641.

Stitt, M., and Sonnewald, U. (1995). Regulation of Metabolism in Transgenic Plants. Annual Review of Plant Physiology and Plant Molecular Biology **46,** 341-368.

Stitt, M., Wirtz, W., and Heldt, H.W. (1980). Metabolite levels during induction in the chloroplast and extrachloroplast compartments of spinach protoplasts. Biochimica et biophysica acta **593,** 85-102.

Stitt, M., Lilley, R.M., and Heldt, H.W. (1982). Adenine nucleotide levels in the cytosol, chloroplasts, and mitochondria of wheat leaf protoplasts. Plant physiology **70,** 971-977.

Stitt, M., Sulpice, R., and Keurentjes, J. (2010a). Metabolic Networks: How to Identify Key Components in the Regulation of Metabolism and Growth. Plant physiology **152,** 428-444.

Stitt, M., Lunn, J., and Usadel, B. (2010b). Arabidopsis and primary photosynthetic metabolism - more than the icing on the cake. Plant Journal **61,** 1067-1091.

Stitt, M., Quick, W.P., Schurr, U., Schulze, E.D., Rodermel, S.R., and Bogorad, L. (1991). Decreased Ribulose-1,5-Bisphosphate Carboxylase-Oxygenase in Transgenic Tobacco Transformed with Antisense Rbcs .2. Flux-Control Coefficients for Photosynthesis in Varying Light, Co2, and Air Humidity. Planta **183,** 555-566.

Streb, S., Egli, B., Eicke, S., and Zeeman, S.C. (2009). The debate on the pathway of starch synthesis: a closer look at low-starch mutants lacking plastidial phosphoglucomutase supports the chloroplast-localised pathway. Plant physiology.

Stryer, L. (2002). Biochemistry.

Sulpice, R., Pyl, E.T., Ishihara, H., Trenkamp, S., Steinfath, M., Witucka-Wall, H., Gibon, Y., Usadel, B., Poree, F., Piques, M.C., Von Korff, M., Steinhauser, M.C., Keurentjes, J.J., Guenther, M., Hoehne, M., Selbig, J., Fernie, A.R., Altmann, T., and Stitt, M. (2009). Starch as a major integrator in the regulation of plant growth. Proc Natl Acad Sci U S A **106,** 10348-10353.

Suss, K.H., Prokhorenko, I., and Adler, K. (1995). In-Situ Association of Calvin Cycle Enzymes, Ribulose-1,5-Bisphosphate Carboxylase Oxygenase Activase, Ferredoxin-Nadp(+) Reductase, and Nitrite Reductase with Thylakoid and Pyrenoid Membranes of Chlamydomonas-Reinhardtii Chloroplasts as Revealed by Immunoelectron Microscopy. Plant physiology **107,** 1387-1397.

Terashima, I., Hanba, Y.T., Tazoe, Y., Vyas, P., and Yano, S. (2006). Irradiance and phenotype: comparative eco-development of sun and shade leaves in relation to photosynthetic CO2 diffusion. Journal of experimental botany **57,** 343-354.

Tian, G.W., Mohanty, A., Chary, S.N., Li, S., Paap, B., Drakakaki, G., Kopec, C.D., Li, J., Ehrhardt, D., Jackson, D., Rhee, S.Y., Raikhel, N.V., and Citovsky, V. (2004). High-throughput fluorescent tagging of full-length Arabidopsis gene products in planta. Plant physiology **135,** 25-38.

Tiessen, A., Hendriks, J.H., Stitt, M., Branscheid, A., Gibon, Y., Farre, E.M., and Geigenberger, P. (2002). Starch synthesis in potato tubers is regulated by post-translational redox modification of ADP-glucose pyrophosphorylase: a novel regulatory mechanism linking starch synthesis to the sucrose supply. The Plant cell **14,** 2191-2213.

Tobin, A.K., and Yamaya, T. (2001). Cellular compartmentation of ammonium assimilation in rice and barley. Journal of experimental botany **52,** 591-604.

Toroser, D., and Huber, S.C. (1997). Protein phosphorylation as a mechanism for osmotic-stress activation of sucrose-phosphate synthase in spinach leaves. Plant physiology **114,** 947-955.

Toroser, D., Athwal, G.S., and Huber, S.C. (1998). Site-specific regulatory interaction between spinach leaf sucrose-phosphate synthase and 14-3-3 proteins. FEBS Lett **435,** 110-114.

Toroser, D., McMichael, R., Jr., Krause, K.P., Kurreck, J., Sonnewald, U., Stitt, M., and Huber, S.C. (1999). Site-directed mutagenesis of serine 158 demonstrates its role in spinach leaf sucrose-phosphate synthase modulation. Plant J **17,** 407-413.

United Nations, D.o.E.a.S.A. (2004). World Population to 2300.

Verkerk, R., Schreiner, M., Krumbein, A., Ciska, E., Holst, B., Rowland, I., De Schrijver, R., Hansen, M., Gerhauser, C., Mithen, R., and Dekker, M. (2009). Glucosinolates in Brassica vegetables: the influence of the food supply chain on intake, bioavailability and human health. Mol Nutr Food Res **53 Suppl 2,** S219.

Weiner, H., and Heldt, H.W. (1992). Intercellular and Intracellular-Distribution of Amino-Acids and Other Metabolites in Maize (Zea-Mays L) Leaves. Planta **187,** 242-246.

Weiner, H., Stitt, M., and Heldt, H.W. (1987). Subcellular Compartmentation of Pyrophosphate and Alkaline Pyrophosphatase in Leaves. Biochimica et biophysica acta **893,** 13-21.

Weise, S.E., Weber, A.P., and Sharkey, T.D. (2004). Maltose is the major form of carbon exported from the chloroplast at night. Planta **218,** 474-482.

Wellman, C.H., and Gray, J. (2000). The microfossil record of early land plants. Philosophical transactions of the Royal Society of London **355,** 717-731; discussion 731-712.

Whitney, S.M., and Andrews, T.J. (2001). Plastome-encoded bacterial ribulose-1,5-bisphosphate carboxylase/oxygenase (RubisCO) supports photosynthesis and growth in tobacco. Proceedings of the National Academy of Sciences of the United States of America **98,** 14738-14743.

Whitney, S.M., and Andrews, T.J. (2003). Photosynthesis and growth of tobacco with a substituted bacterial Rubisco mirror the properties of the introduced enzyme. Plant physiology **133,** 287-294.

Wienkoop, S., Baginsky, S., and Weckwerth, W. (2010). Arabidopsis thaliana as a model organism for plant proteome research. J Proteomics **73,** 2239-2248.

Winter, H., and Huber, S.C. (2000). Regulation of sucrose metabolism in higher plants: localization and regulation of activity of key enzymes. Crit Rev Biochem Mol Biol **35,** 253-289.

Winter, H., Lohaus, G., and Heldt, H.W. (1992). Phloem Transport of Amino-Acids in Relation to Their Cytosolic Levels in Barley Leaves. Plant physiology **99,** 996-1004.

Winter, H., Robinson, D.G., and Heldt, H.W. (1993). Subcellular Volumes and Metabolite Concentrations in Barley Leaves. Planta **191,** 180-190.

Winter, H., Robinson, D.G., and Heldt, H.W. (1994). Subcellular Volumes and Metabolite Concentrations in Spinach Leaves. Planta **193,** 530-535.

Wirtz, W., Stitt, M., and Heldt, H.W. (1980). Enzymic Determination of Metabolites in the Subcellular Compartments of Spinach Protoplasts. Plant physiology **66,** 187-193.

Wolosiuk, R.A., and Buchanan, B.B. (1976). Studies on the regulation of chloroplast NADP-linked glyceraldehyde-3-phosphate dehydrogenase. The Journal of biological chemistry **251,** 6456-6461.

Wolosiuk, R.A., and Buchanan, B.B. (1978a). Activation of Chloroplast NADP-linked Glyceraldehyde-3-Phosphate Dehydrogenase by the Ferredoxin/Thioredoxin System. Plant physiology **61,** 669-671.

Wolosiuk, R.A., and Buchanan, B.B. (1978b). Regulation of chloroplast phosphoribulokinase by the ferredoxin/thioredoxin system. Archives of biochemistry and biophysics **189,** 97-101.

Wolosiuk, R.A., Ballicora, M.A., and Hagelin, K. (1993). The reductive pentose phosphate cycle for photosynthetic CO2 assimilation: enzyme modulation. Faseb J **7,** 622-637.

Woodrow, I.E., Murphy, D.J., and Walker, D.A. (1983). Regulation of photosynthetic carbon metabolism. The effect of inorganic phosphate on stromal sedoheptulose-1,7-bisphosphatase. Eur J Biochem **132,** 121-123.

Woodrow, I.E., Murphy, D.J., and Latzko, E. (1984). Regulation of stromal sedoheptulose 1,7-bisphosphatase activity by pH and Mg2+ concentration. The Journal of biological chemistry **259,** 3791-3795.

Yamano, T., and Fukuzawa, H. (2009). Carbon-concentrating mechanism in a green alga, Chlamydomonas reinhardtii, revealed by transcriptome analyses. Journal of Basic Microbiology **49,** 42-51.

Yano, T., Oku, M., Akeyama, N., Itoyama, A., Yurimoto, H., Kuge, S., Fujiki, Y., and Sakai, Y. (2010). A novel fluorescent sensor protein for visualization of redox states in the cytoplasm and in peroxisomes. Mol Cell Biol **30,** 3758-3766.

Yu, T.S., Lue, W.L., Wang, S.M., and Chen, J. (2000). Mutation of Arabidopsis plastid phosphoglucose isomerase affects leaf starch synthesis and floral initiation. Plant physiology **123,** 319-326.

Zeeman, S.C., Smith, S.M., and Smith, A.M. (2007). The diurnal metabolism of leaf starch. The Biochemical journal **401,** 13-28.

Zeeman, S.C., Tiessen, A., Pilling, E., Kato, K.L., Donald, A.M., and Smith, A.M. (2002). Starch synthesis in Arabidopsis. Granule synthesis, composition, and structure. Plant physiology **129,** 516-529.

Zhu, X.G., de Sturler, E., and Long, S.P. (2007). Optimizing the distribution of resources between enzymes of carbon metabolism can dramatically increase photosynthetic rate: A numerical simulation using an evolutionary algorithm. Plant physiology **145,** 513-526.

Zrenner, R., Krause, K.P., Apel, P., and Sonnewald, U. (1996). Reduction of the cytosolic fructose-1,6-bisphosphatase in transgenic potato plants limits photosynthetic sucrose biosynthesis with no impact on plant growth and tuber yield. Plant J **9,** 671-681.